Neural coding of different visual cues in the monarch butterfly sun compass

Neuronale Kodierung verschiedener visueller Signale im Sonnenkompass des Monarchfalters

Doctoral thesis for a doctoral degree
at the Graduate School of Life Sciences
Julius-Maximilians-Universität Würzburg

Section Integrative Biology

submitted by

Tu Anh Thi Nguyen

from

Erfurt

Würzburg 2022

Submitted on:

……..……..

Office stamp

Members of the Thesis Committee

Chairperson: Prof. Dr. Christian Wegener

Primary Supervisor: Prof. Dr. Basil el Jundi

Supervisor (Second): Prof. Dr. Wolfgang Rössler

Supervisor (Third): Prof. Dr. Eric Warrant

Supervisor (Fourth): Prof. Dr. Keram Pfeiffer

Date of Public Defence: ……..……..

Date of Receipt of Certificates: ……...

Summary

Monarch butterflies are famous for their annual long-distance migration. Decreasing temperatures and reduced daylight induce the migratory state in the autumn generation of monarch butterflies. Not only are they in a reproductive diapause, they also produce fat deposits to be prepared for the upcoming journey: Driven by their instinct to migrate, they depart from their eclosion grounds in the northern regions of the North American continent and start their southern journey to their hibernation spots in Central Mexico. The butterflies cover a distance of up to 4000 km across the United States. In the next spring, the same butterflies invert their preferred heading direction due to seasonal changes and start their northward spring migration. The spring migration is continued by three consecutive butterfly generations, until the animals repopulate the northern regions in North America as non-migratory monarch butterflies. The monarch butterflies' migratory state is genetically and epigenetically regulated, including the directed flight behavior. Therefore, the insect's internal compass system does not only have to encode the butterflies preferred, but also its current heading direction. However, the butterfly's internal heading representation has to be matched to external cues, to avoid departing from its initial flight path and increasing its risk of missing its desired destination. During the migratory flight, visual cues provide the butterflies with reliable orientation information. The butterflies refer to the sun as their main orientation cue. In addition to the sun, the butterflies likely use the polarization pattern of the sky for orientation. The sky compass signals are processed within a region in the brain, termed the central complex (CX). Previous research on the CX neural circuitry of the monarch butterflies demonstrated that tangential central complex neurons (TL) carry the visual input information into the CX and respond to a simulated sun and polarized light. However, whether these cells process additional visual cues like the panoramic skyline is still unknown. Furthermore, little is known about how the migratory state affects visual cue processing. In addition to this, most experiments studying the monarch butterfly CX focused on how neurons process single visual cues. However, how combined visual stimuli are processed in the CX is still unknown.

This thesis is investigating the following questions:

1) How does the migratory state affect visual cue processing in the TL cells within the monarch butterfly brain?
2) How are multiple visual cues integrated in the TL cells?
3) How is compass information modulated in the CX?

To study these questions, TL neurons from both animal groups (migratory and non-migratory) were electrophysiologically characterized using intracellular recordings while presenting different simulated celestial cues and visual sceneries. I showed that the TL neurons of migratory butterflies are more narrowly tuned to the sun, possibly helping them in keeping a directed flight course during migration. Furthermore, I found that TL cells encode a panoramic skyline, suggesting that the CX network combines celestial and terrestrial information. Experiments with combined celestial stimuli revealed that the TL cells combine both cue information linearly. However, if exposing the animals to a simulated visual scenery containing a panoramic skyline and a simulated sun, the single visual cues are weighted differently. These results indicate that the CX's input region can flexibly adapt to different visual cue conditions. Furthermore, I characterize a previously unknown neuron in the monarch butterfly CX which responds to celestial stimuli and connects the CX with other brain neuropiles. How this cell type affects heading direction encoding has yet to be determined.

Zusammenfassung

Monarchfalter sind berühmt für ihre jährlichen Migrationsflüge. Sinkende Temperaturen und die verkürzte Tageslichtbestrahlung induzieren die Migration in einer Herbstgeneration der Monarchfalter. Sie sind nicht nur in reproduktiver Diapause, sondern produzieren Fettreserven für die bevorstehende Reise: Getrieben von ihrem Migrationsinstinkt verlassen sie ihre Schlüpfstätten in den nördlichen Regionen des Nordamerikanischen Kontinents und starten ihre südliche Wanderung zu ihren Überwinterunsgstätten in Zentralmexiko. Dabei legen die Schmetterlinge Strecken von bis zu 4000 km durch die Vereinigten Staaten zurück. Im nächsten Frühling kehren die gleichen Schmetterlinge ihre Vorzugsrichtung durch die jahreszeitlich bedingten Veränderungen um und die Tiere bewegen sich nordwärts. Die Frühlingsgeneration wird insgesamt über drei Schmetterlingsgeneration durchgeführt, bis die Tiere die nördlichen Regionen in Nordamerika wieder als nicht-migrierende Monarchfalter besiedeln. Der Migrationsstatus der Monarchfalter ist genetisch und epigenetisch reguliert, was auch das gerichtete Flugverhalten einschließt. Demnach muss das interne Kompasssystem der Falter nicht nur die bevorzugte, sondern auch die aktuelle Flugrichtung prozessieren. Die interne Repräsentation der Flugrichtung des Falters muss jedoch mit der Umwelt abgeglichen werden, ansonsten droht das Tier von der ursprünglichen Flugrichtung abzuweichen und erhöht das Risiko den Wunschort nicht zu erreichen. Während des Migrationsfluges bieten visuelle Signale verlässliche Orientierungsinformationen. Dabei ist die Sonne ihre Hauptorientierungsreferenz. Zusätzlich zur Sonne nutzen die Schmetterlinge vermutlich noch das Polarisationsmuster des Himmels zur Orientierung. Diese Himmelskompasssignale werden im Gehirn in einer Gehirnregion, den Zentralkomplex, integriert. Vergangene Forschungsprojekte am Zentralkomplex haben gezeigt, dass tangentiale Zentralkomplex-Neurone (TL) die visuellen Signale in den Zentralkomplex leiten und auf eine simulierte Sonne und polarisiertes Licht sensitiv sind. Ob diese Zellen noch weitere visuelle Signale verarbeiten, wie zum Beispiel den Horizont eines Panoramas, ist nicht bekannt. Auch ist der Einfluss des Migrationsstatus auf die visuelle Signalverarbeitung im Zentralkomplex bisher unerforscht. Des Weiteren haben die meisten Experimente am Zentralkomplex des Monarchfalters den Fokus auf die Verarbeitung einzelner simulierter visueller Reize gelegt. Wie aber Kombinationen aus Stimuli im Zentralkomplex verarbeitet werden, ist nicht bekannt.

Diese Dissertation beschäftigt sich mit folgenden Fragen:

1) Wie beeinflusst der Migrationsstatus die visuelle Reizverarbeitung in TL-Zellen im Monarchfaltergehirn?
2) Wie werden mehrere visuelle Reize in TL-Zellen miteinander kombiniert?
3) Wie wird Kompassinformation im Zentralkomplex moduliert?

In diesem Zusammenhang wurden TL-Neurone aus beiden Gruppen (migrierende und nichtmigrierende Monarchfalter) elektrophysiologisch mittels intrazellulärer Aufnahmen charakterisiert, während den Tieren unterschiedliche simulierte Himmelkompasssignale und visuelle Szenerien präsentiert wurden. Hierbei konnte ich zeigen dass die TL-Neuronen in migrierenden Tieren ein engeres Tuning zur Sonne aufwiesen, was den Tieren helfen könnte, eine gerichtete Flugrichtung zu halten. Außerdem antworten die TL-Neurone auf ein Panorama, womit der Zentralkomplex in der Lage wäre, Himmelskompasssignale mit terrestrischer Information zu kombinieren. In Experimenten mit zwei kombinierten simulierten Himmelskompasssignalen konnte ich zeigen, dass die TL-Zellen beide Signalinformationen linear miteinander verrechnen. Wenn die TL-Zellen jedoch mit einer visuellen Szenerie stimuliert werden, welche eine simulierte Sonne und ein Panorama beinhaltet, werden die einzelnen visuellen Signale unterschiedlich gewichtet. Die Ergebnisse sind ein Hinweis darauf, dass die Eingangsregion im Zentralkomplex sich flexibel an die visuellen Signalbedingungen anpassen können. Außerdem habe ich ein bis dahin unbekanntes Neuron während meiner Studien charakterisieren können, welches auf simulierte Himmelskompasssignale antwortet und den Zentralkomplex mit anderen Neuropilen im Gehirn verbindet. Wie dieser Neuronentyp Einfluss auf die Kodierung der Flugrichtung nimmt, muss in der Zukunft weiter erforscht werden.

Contents

1. General Introduction

1.1 Spatial orientation and visual cue integration in insects

Foraging (Brines and Gould, 1979), homing (Fleischmann et al., 2018) or searching for conspecifics (Obara, 1979) - to successfully perform these behaviors insects have to efficiently orient themselves in their environment (reviewed by Honkanen et al., 2018 and Grob et al., 2021). To reach their destination or object of desire, insects determine their heading direction with the help of idiothetic cue information (reviewed by Grob et al., 2021 and Heinze et al., 2018). These self-motion based cues includes the travelled distance derived from an internal step integrator (Wittlinger et al., 2006), rotational (Varga, and Ritzmann, 2016) or translational optic flow information (Srinivasan et al., 2000; Stone et al., 2017). However, exclusively relying on self-motion cues is insufficient to keep a directed course: Insects will accumulate movement errors and diverge from their desired direction, if they cannot perceive the external cues from their environment (Cheung et al. 2007; Heinze et al., 2018; Stuchlik and Bures, 2002). External cue information like olfactory (reviewed by Steck 2012), geomagnetic (Dreyer et al, 2018; Fleischmann et al., 2018), wind (Dacke et al., 2019; Müller and Wehner, 2007; Okubo et al., 2020) and visual information (Brines and Gould, 1979; Legge et al., 2014; Ugolini et al., 1999b) are therefore crucial to correct the insect's internal representation of their heading direction.

In contrast to olfactory cue information, which disperses in the air over time (reviewed by Riffel et al., 2008) and possibly dilutes beyond recognition, visual cues are comparably more stable and reliably detectable over longer distances (Stone et al., 2018). Visual cues can be subcategorized into terrestrial and celestial cues **(Fig. 1A and B)**. The first group of visual cues are earthbound and includes the panoramic skyline (Graham and Cheng, 2009; Towne et al., 2018) and visual landmark information (reviewed by Collett, 1996). The panoramic skyline consists of distant terrestrial objects, visible to the insects as an unevenly shaped silhouette on the horizon (Graham and Cheng, 2009; Towne et al., 2018). In contrast to the panoramic skyline, the term "landmark" was not clearly defined in the literature and was used to describe a diverse group of orientation cues with different sensory modalities (reviewed by Kheradmand and Nieh, 2019). For this dissertation, a visual landmark is defined as a terrestrial object or object group within the environment that is salient to the insect and is used as an orientation reference (Kheradmand and Nieh, 2019). Previous research concentrated on understanding the

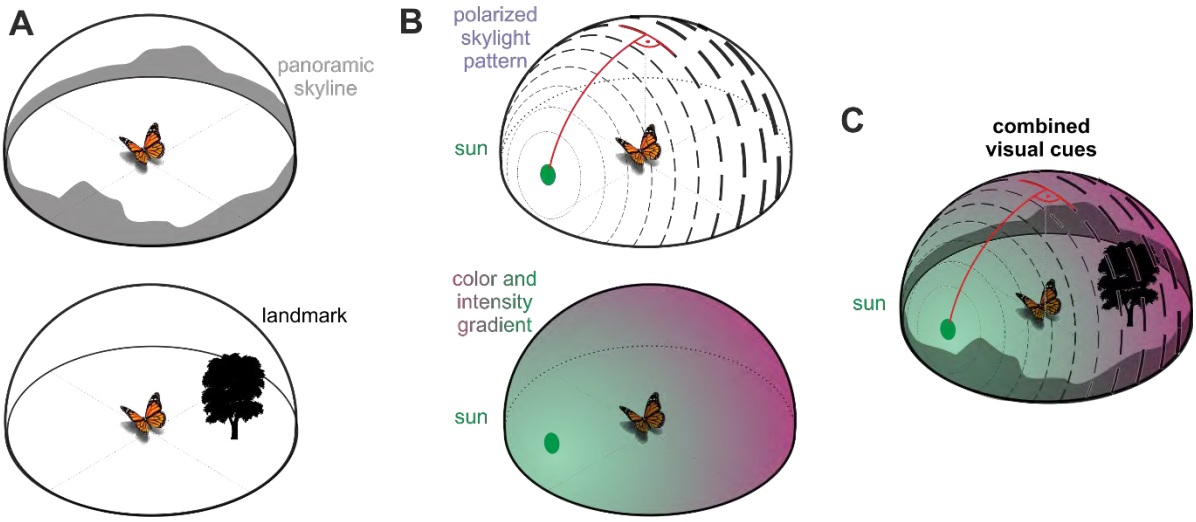

Figure 1: Schemes of the visual cues integrated during orientation. (A) Terrestrial cues, including the panoramic skyline (above) and visual landmark information (below). **(B)** Diurnal skylight cues influenced by the sun. Above: Polarized light pattern. Solar azimuth and angle of polarization are in an orthogonal relationship (see red arc). Below: Color gradient, where the visible light decreases in intensity and wavelength the further the animal moves into the antisolar hemisphere. **(C)** Combined presentation of both terrestrial and celestial cues illustrating a more naturalistic environment an insect may encounter.

orientation strategies involving terrestrial landmarks (reviewed by Collett, 1996). Furthermore, behavioral experiments identified how different properties of a visual landmark like the height (Collett, 1995) its position in the environment (Collett and Collett, 2002) and richness of the visual scenery a landmark is located in (Schultheiss et al., 2016) affects the insect's orientation behavior.

The second group summarizes the astronomic bodies and other sky-related cue information like the stars (Dacke et al. 2013; Foster et al., 2017), the moon (Dacke et al., 2004; Klotz and Reid, 1993; Ugolini et al., 1999b; Ugolini and Chiussi, 1996) and the sun (Giraldo et al., 2018; el Jundi et al., 2014; Kennedy and Wigglesworth, 1951; Ugolini et al., 1999a; Ugolini et al., 2002). However, external cues are rarely static: Depending on the animal's location, weather conditions or the time of the day, the same visual cue can change its properties and therefore affecting the animal's orientation capacities (Dreyer et al., 2018). For instance, on cloudy days neither the sun nor the moon are available as orientation cues. However, they both shape the polarized skylight cue, which is detectable under overcast conditions (Gál et al., 2001; Hegedüs et al., 2007; Foster et al., 2019). Based on the Rayleigh model (Coulson, 1959; Heinze, 2014), tiny particles in the sky scatter the light and create a polarization pattern arranged in concentric circles around the celestial body **(Fig. 1B, upper graph)**. Both the percentage of polarized light and the angle of polarization is linked to the positon of the celestial body (Coulson, 1959; Heinze, 2014). Changing the celestial body's positon in the sky influences the polarized light

pattern, but the azimuth of the celestial body and the angle of polarization in the animal's zenith will always be 90° apart (Coulson, 1959). Honey bees (Brines and Gould, 1979), desert ants (Wehner and Müller, 2006) and two night active dung beetle species (Dacke et al., 2004; el Jundi et al., 2015) have been demonstrated to prefer the more robust polarized skylight cue over the celestial body cue if determining a heading direction. Furthermore, the orthogonal relationship between the celestial body and polarized light is integrated in the internal compass of desert ants (Lebhardt and Ronacher, 2014) and is encoded in the internal matched polarized light filter in desert locusts (Zitrell et al., 2020). Other skylight cues linked to a celestial body are the skylight intensity and color gradient, which are both connected to the sun **(Fig. 1B, lower graph)**. The solar hemisphere is bright and contains a high amount of green wavelength light, while the antisolar hemisphere is dimmer and high on UV light (Coemans et al., 1994). Past experiments have demonstrated that insects are capable of using the skylight intensity gradient (el Jundi et al., 2014; Haberkern et al., 2022) and the spectral sky gradient (Brines and Gould, 1979; Ciogini et al., 2021) for orientation. For instance, bees can determine the sun's position based on the UV content of the antisolar hemisphere in the sky (Brines and Gould, 1979; Rossel and Wehner, 1984).

Insects use different types of visual cues to orient themselves. Under naturalistic conditions, however, the visual scenery of an environment is composed of multiple visual cues **(Fig.1C)**. Insects therefore have to identify the relevant cue information in a noisy environment. While determining a heading direction, some insects prioritize visual cues based on an internal hierarchy (Brines and Gould, 1979; el Jundi et al., 2014; Legge et al., 2014; Wehner and Müller, 2006). In the absence of the dominant orientation cue, insects can resort to a lower-hierarchy visual cue as a backup (Ciogini et al., 2021; el Jundi et al., 2014). For instance, the celestial cue hierarchy of the diurnal dung beetle *Scarabaeus lamarcki* is dominated by the sun, but it can switch to using polarized light or the skylight intensity gradient whenever the sun is not visible (el Jundi et al., 2014). Within a hierarchical framework, insects tend to disregard the sensory information of the lower ranked cues in the presence of the dominant cue in an "all-or-nothing" manner (Lebhardt and Ronacher, 2014). However, some insects can calculate a directional course by integrating the sensory information of multiple visual cues. In this case the available cue information is weighted in relation to each other (Lebhardt and Ronacher, 2014). Two ambiguous visual cues may provide reliable orientation information if integrated together. By including multiple and even redundant cue information the precision and robustness of the animals' internal compass can increase (Cheng et al., 2007; Honkanen et al.,

2018). For example, experiments on ants revealed that if presenting celestial cue information in conflict to each other, they will determine an intermediate vector direction (Lebhardt and Ronacher, 2014; Wystrach et al., 2014). Furthermore, bees and ants can combine the panoramic skyline with the celestial cue information (Legge et al., 2014; Reid et al., 2011; Towne et al., 2008). Visual cues can also be integrated with other sensory cue information (reviewed in Buehlmann et al., 2020). As observed for visual cues, multimodal cue integration can operate on a hierarchical or a weighted cue modality. For instance, the dung beetle switches from its internal sun compass to a wind compass, once the celestial body reaches higher elevations during noon and does no longer provide reliable directional information (Dacke et al., 2019). In the bogong moth, however, the steering behavior changes if both visual landmarks and the geomagnetic field are put in conflict to each other, possibly hinting to a weighted cue integration (Dreyer et al., 2018).

Apart from a hierarchical or weighted cue context, insects can switch between different orientation strategies based on the animal's behavioral context (Collet et al.1998; Schwartz et al. 2017). Desert ants of the species *Cataglyphis velox* mainly refer to terrestrial cues when walking forwards; but if walking backwards while carrying heavy forage, they integrate celestial cues (Schwartz et al. 2017). While insects can adapt to changing cue conditions, not every visual cue provides unambiguous directional information. Collett and Collett (2002) have demonstrated that honeybees interpret the isolated landmark within the animal's visual field in the context of the presented panoramic background. Furthermore if the panoramic context is no longer available to the bee, they discard the provided landmark information (Collett and Collett, 2002). In this case, the bees use the landmark as a local orientation cue, which provides reliable cue information for the learned context (Grob et al., 2021). How insects subjectively learn the context of the available visual cues can be illustrated with the Australian desert ant: During their foraging trips, they refer to their memory of the visual scenery at the nest entrance and the landmark information along a foraging route (Narendra, 2007; Narendra et al., 2013). Both visual cues can be classified as a local cues, because they contain enough directional information for beaconing or route trailing (Collett, 1996; Grob et al., 2021). However, they are only viable in the orientation context of the individual ant; these two visual information do not provide a universal reference if they were to be displaced (Grob et al., 2021). If the animal is moving within a familiar area around a stationary nest, relying on local cues is sufficient to consistently forage and return home (Narendra, 2007). However, what happens if an insect has to pass through unfamiliar areas, for instance to reach a yet unknown mating spot (Lohmann

and Lohmann, 1996)? Instead of relying on the more ambiguous local cues, switching to global cues is more effective. Global cues, like the geomagnetic field, provide unambiguous spatial information regardless of the time point or the animal's location on Earth (Grob et al., 2021). True navigators, like experienced migratory birds, can infer their geographic coordinates on Earth using global orientation cues and can correct their flight direction when displaced (Grob et al., 2021; Mouritsen et al. 2013). If animals keep a directed course using global orientation cues in the absence of their exact ego- or geocentric positional information, they perform compass orientation (Grob et al., 2021; Mouritsen et al. 2013). Though insects seem to respond similarly to the same orientation cue, they may interpret the visual cue differently in their internal compass system. One example for how the same cue can elicit different orientation strategies in insects is the sun. If insects continuously move towards the sun during menotactic behavior, the celestial body is used as a non-compass related directional cue (el Jundi et al., 2015; Giraldo et al, 2018). If insects adapt their heading direction to the time-of-day information, however, the sun is used as an unambiguous compass cue (Dyer and Dickinson, 1994; Wehner and Lanfranconi, 1981). Compass orientation is therefore a suitable orientation strategy for insects that have to move to an unfamiliar destination and keep a directed course over a prolonged time period– thus helpful for insects performing migratory behavior.

1.2 Ecology of monarch butterfly migration and migratory state

Migration refers to the periodic displacement of animals from one geographic location to another to avoid predation or parasitic infection, to escape to more favorable climate conditions and eventually to increase reproductive success (Chapman et al., 2015; Honkanen et al., 2019). While vertebrates like sea turtles (Lohmann and Lohmann, 1996) and birds (Wiltschkwo and Wiltschko, 1972) are usually associated with migratory behavior, insects like the desert locust (reviewed by Homberg et al., 2015), the bogong moth (reviewed by Warrant et al., 2016) and the painted lady (Nesbit et al., 2009; Stefanescu et al., 2007) are capable of long distance migration as well. However, one of the most prominent long-distance migratory insects still remains to be the monarch butterfly (*Danaus plexippus*) since its beauty and its annual migratory flight **(Fig. 2A)** captures the attention of scientist and the general population alike (reviewed by Merlin and Liedvogel, 2019, Reppert et al., 2018 and Reppert et al., 2016). Since the 1960s both the scientific community and general public investigated the migratory movements of the North American population of monarch butterflies (reviewed by Brower, 1995; Reppert et al., 2016). Abiotic factors play a central role in the transition from the non-migratory to the migratory generation. In late August, the decreasing photoperiod length,

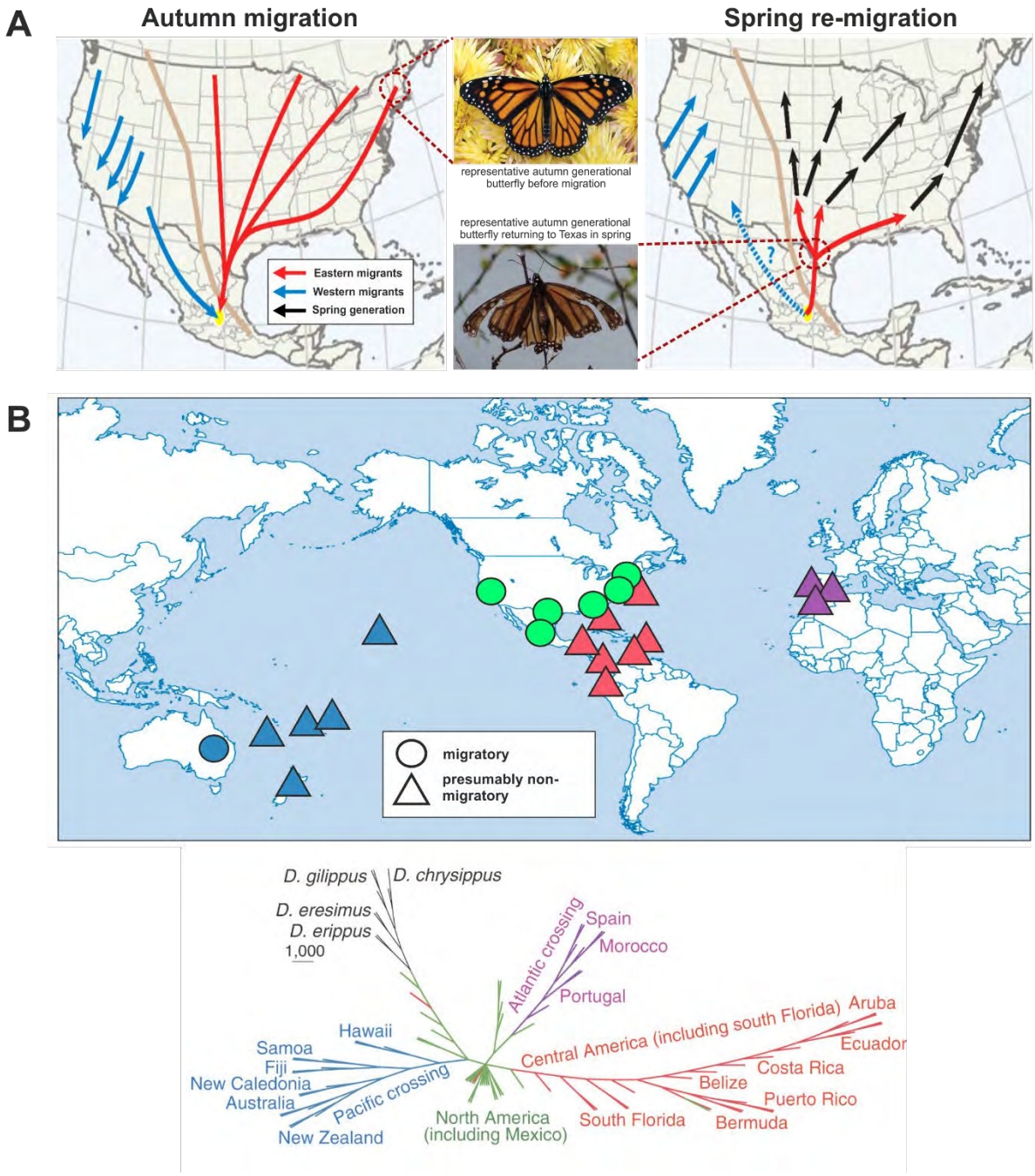

Figure 2: The migratory state of the monarch butterfly. **(A)** The migratory cycle of the North American monarch butterfly. Maps displaying the autumnal (outer left column) and spring seasonal (outer right column) migratory routes. Pictures of representative butterflies illustrating the physiological shape of the autumn generation at the beginning of their migratory flight (center upper panel) and after returning from their hibernation in spring (center lower panel). Modified after Reppert et al. (2016). **(B)** Global populations of monarch butterflies. Upper panel: Sampled monarch butterfly colonies. Lower panel: Phylogenetic tree based on the collected samples as color coded above. Modified after Reppert et al. (2018) and Merlin and Liedvogel (2019).

fluctuating temperatures over the day and the aging milkweed plants (*Asclepias* spp.) - the monarch butterfly larvae's main feeding plant - epigenetically induce the migratory state within the late-summer born butterfly larvae and/ or pupae (Goering and Oberhauser, 2002; Merlin and Liedvogel, 2019; Reppert et al., 2018). The resulting autumn generation of adult butterflies decrease juvenile hormone (JH) production, which subsequently shrinks their reproductive

glands (Herman, 1981) doubling the animals' life span compared to the previous butterfly generation (Herman and Tatar, 2001). Apart from the reproductive diapause and reduced mating behavior (Brower et al., 1977), the migratory animals produce extensive fat reserves (Beall, 1948; Masters et al., 1988), are more resistant to decreased temperatures (Masters et al., 1988) and are internally driven to fly in a southwestern direction (Urquhart and Urquhart, 1977; Zhu et al., 2009). Starting in their northern breeding ranges on the North American continent **(Fig. 2A, left map)**, the butterflies' flight path either leads them across the West Coast of the North American continent over Arizona (Urquhart and Urquhart, 1977) or along the East Coast over Texas (Urquhart and Urquhart, 1978) to their hibernation spots in Central Mexico (Urquhart and Urquhart, 1977). While it is still unclear how the transition from long distance behavior to local pinpointing and landing behavior occurs in monarch butterflies, it is likely that the odor emitted from the trees at their overwintering spots acts as a stop signal terminating the butterflies' migratory behavior (Mouritsen, 2018; Mourtisen et al., 2013). In spring, the animals awaken from their resting state and adopt a northern flight direction **(Fig. 2A, right map)**, induced by the cold temperatures at their overwintering sites (Guerra and Reppert, 2013; Urquhart and Urquhart, 1979). After re-entering the USA, the wings of the migratory butterflies are torn from last year's southwards migration. Rather than continuing to fly to their starting place from last year, most of the butterflies stop in the south of the USA and reproduce. **(Fig. 2A, right map)**. The subsequent generation keeps on migrating to the north, possibly guided by the regrowth of the *Asclepias* plants across the country (Reppert et al., 2018; Reppert et al., 2016), but covering a smaller distance compared to their predecessors (Malcom et al., 1993). Therefore, to cross the remaining distance and to reach their predecessor's breeding grounds in the north, two or three spring generations cycle though the pattern of northern migratory flight and reproduction (Malcom et al., 1993). In the end, instead of one generation, a subset of three to four generational cycles have covered the distance across the USA (Malcom et al., 1993), until one spring generation reaches South Canada. The offspring in this area, the summer generation, maintain a stationary lifestyle and are reproductively active (Calvert, 2001). In autumn, once a new generation of migratory adults emerge, the migratory cycle starts anew.

In contrast to songbirds, who repeat their migratory journey multiple times in their lives (Merlin and Liedvogel, 2019), the monarch butterfly's life span in its migratory state ranges between 4-5 months (Herman and Tatar, 2001), limiting them to only one migratory flight. Without the guidance of the previous autumn generation or any experiences from past flights, the newly emerged butterflies need to find a yet unfamiliar destination. To consistently maintain the

migratory behavior over several generations, the migratory traits like the directed flight behavior need to be encoded in the monarch butterfly's genome (reviewed by Reppert et al., 2016) and epigenetically regulated by environmental factors (Merlin and Liedvogel, 2019). That seasonal conditions may affect which genes are expressed or not has been revealed in a study comparing the gene expression profile of brain tissue from both butterfly generations. In the autumn generation, gene loci linked to cytoskeletal organization and immune response are upregulated, while in the summer generation the ones related to steroid and cholesterol metabolism, lipid metabolism and circadian control are highly expressed (Zhu et al., 2009). By rearing the offspring of summer generational monarch butterflies indoors under autumn-like conditions, the emerging adults are more efficient with their flight metabolic rate (Schroeder et al., 2019) compared to their parents. Surprisingly, treating migratory animals with JH and reversing their reproductive diapause did not affect their directed flight behavior, indicating that JH deficiency is not needed to maintain the animal's orientation behavior (Zhu et al., 2009).

While the North American monarch butterfly population can occur in a migratory and non-migratory form, there are different monarch butterfly subpopulations distributed in different parts of the world **(Fig. 2B, upper graph)**. Some of them can migrate shorter distances, like the Australian subpopulation (Dingle et al., 1999), but others remain completely stationary without going on a migratory journey like the Puerto Rican, Costa-Rican or Hawaiian subpopulations (Altizer and Davis, 2010). A phylogenetic tree analysis **(Fig. 2B, lower graph)** revealed that the ancestor of the North American monarch butterfly population was migratory and dispersal events in combination with natural selection led to the development of exclusively non-migratory butterfly colonies (Zhan et al., 2018). Furthermore, the different butterfly subgroups do not only differ in their genomes (Zhan et al., 2018), but also on a physiological level. Migratory monarch butterflies are well adapted to survive a long distant flight: they develop larger and more elongated forewings (Altizer and Davis, 2010), their flight metabolic rate is lower (Zhan et al., 2018) and they fly more efficiently (Gibo and Pallet, 1979; Schroeder et al., 2019) compared to their non-migratory counterparts.

1.3 Compass orientation in monarch butterflies

Strategies to keep a directed course differ between insects (reviewed by Chapman et al., 2015 and Grob et al., 2021). In contrast to insects that display spatial orientation over a short distance like the dung beetle (reviewed by el Jundi et al., 2019) or the sand hopper (Ugolini et al., 2022; Ugolini et al., 1999b), a monarch butterfly can cover several thousands of kilometers during its migratory flight (Reppert et al., 2018). However, similar to the diurnal dung beetle (el Jundi et

al., 2014) and the sand hopper (Ugolini et al., 2022), the monarch butterfly refers to the sun as its main orientation cue regardless of its migratory state (Franzke et al., 2020; Stalleicken et al. 2005). While representing the brightest visual cue on clear days, the sun on its own does not provide unambiguous directional information. During the day, the sun changes elevation and azimuthal positon along its trajectory in the sky. The monarch butterfly needs to continuously adjust its flight direction to compensate for the different sun positon over the day. Indeed, shifting the internal clock of migratory butterflies by six hours changed their heading direction compared to the non-shifted control group (Frost and Mouristen, 2002; Merlin et al., 2009; Guerra and Reppert, 2013). Further investigations revealed that covering the butterfly's antennae with black paint disrupts its oriented flight behavior completely (Merlin et al., 2009) and that the time information is encoded in the animal's antenna (Merlin et al., 2009) and brain (Sauman, 2006). Therefore, in combination with its internal clock information, the monarch butterflies can use the sun as a reliable compass cue (Merlin et al., 2009). While capable of compass orientation, monarch butterflies do not belong to the group of true navigators. This was proven by displacement experiments conducted by Mouritsen et al. (2013). The butterflies did not align their body axis to their destination in Central Mexico, but rather kept their south western heading direction (Mouritsen et al., 2013). Therefore, monarch butterflies need to update their internal sun compass to external cues, otherwise they will be displaced. As suggested by Calvert (2001) and Mouritsen et al. (2013), monarch butterflies may adjust their flight path by integrating geographic features like the Rock Mountains, possibly visible to the animals as a panoramic skyline. Indeed, flight simulator experiments revealed that the butterflies use the panoramic skyline for flight stabilization (Franzke et al., 2020). While demonstrated in other insects (Brines and Gould, 1979; Wehner and Müler, 2006), it is still under debate whether monarch butterflies use the polarized skylight pattern as an orientation cue (Reppert et al, 2004; Stalleicken et al. 2007). Similarly, while monarch butterflies may sense the magnetic field (Guerra et al., 2014; Wan et al., 2021) not much is known about how they use this cue to determine a heading. However, a weighted cue integration as demonstrated for the bogong moth (Dreyer et al., 2018) is conceivable.

1.4 Visual cue processing in the monarch butterfly brain

While it has yet to be determined whether monarch butterflies use polarized light an orientation cue, they are capable of polarized light perception (Heinze and Reppert, 2011; Stalleicken et al., 2006). Like other celestial cue information, the polarized light cue is processed over the anterior visual pathway (reviewed in Heinze 2014). As observed for other insects (Hardcastle et al., 2021; Labhardt et al, 1984; Schmeling et al., 2014), the compound eye of the monarch butterfly is compartmentalized **(Fig. 3A)**. Most photoreceptors of the butterfly's compound eye are sensitive to light in the green wavelength range, thus adapted to detect the sun (Stalleicken et al., 2006). Polarized light vision, however, is mediated by a small segment termed the dorsal rim area (DRA). One ommatidium within the DRA is composed of eight monochromatic UV sensitive photoreceptors (Stalleicken et al., 2006; Sauman et al., 2005). Polarized light detection is mediated by a region within the ommatidium called the rhabdom **(Fig. 3B)**. The microvilli arrangement within the rhabdom determines the ommatidium's preference for a certain angle of polarization of the incoming light. (Heinze 2014; Labhart et al., 2009). While microvilli organization is consistent across the DRA, the ommatidia on the DRA are arranged in a fan-shaped manner **(Fig. 3B)**: ommatidia with predominantly horizontal microvilli arrangement are located on the frontal and caudal site, while the remaining ommatidia with predominantly vertical microvilli arrangement are parallel to the eye border (Labhart et al., 2009). Compared to the desert locust, the receptive field for polarized light is predicted to be smaller and more narrow in monarch butterflies **(Fig. 3C)**, because the acceptance angle of the polarization

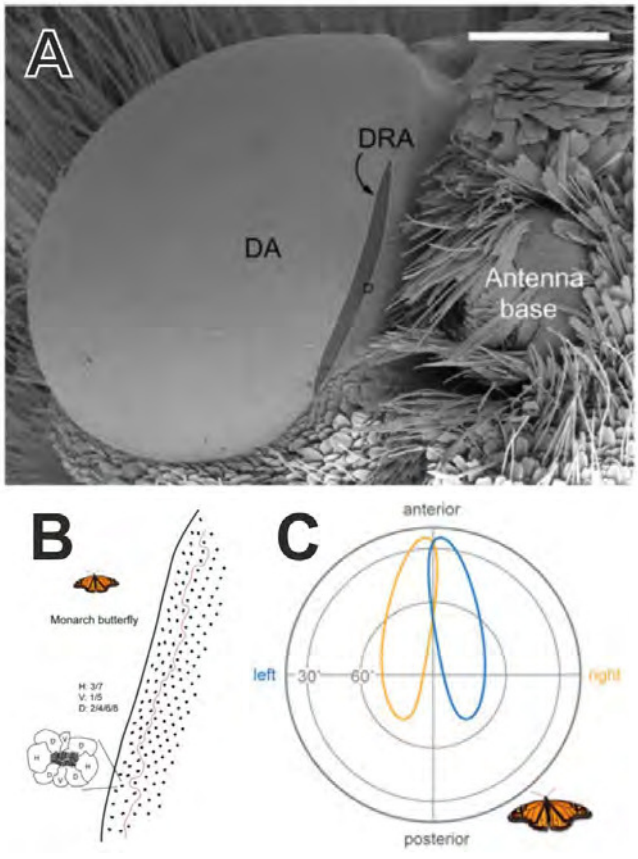

Figure 3: Compound eye of the monarch butterfly. (A) Compound eye of the monarch butterfly. Abbreviations: DA, dorsal area; DRA, dorsal rim area. Reproduced from Labhardt et al., (2009) **(B)** Arrangement of ommatidiae in the DRA of the monarch butterfly's compound eye. As an inset: representative scheme of a rhabdom of one ommatidium. Highlighted are the microvilli arranged inside the rhabdom. Abbreviations: D, dorsal; H, horizontal; V, ventral. Reproduced from Heinze (2014) **(C)** Reconstructed visual field of the DRA in the monarch butterfly. Reproduced from Heinze (2014).

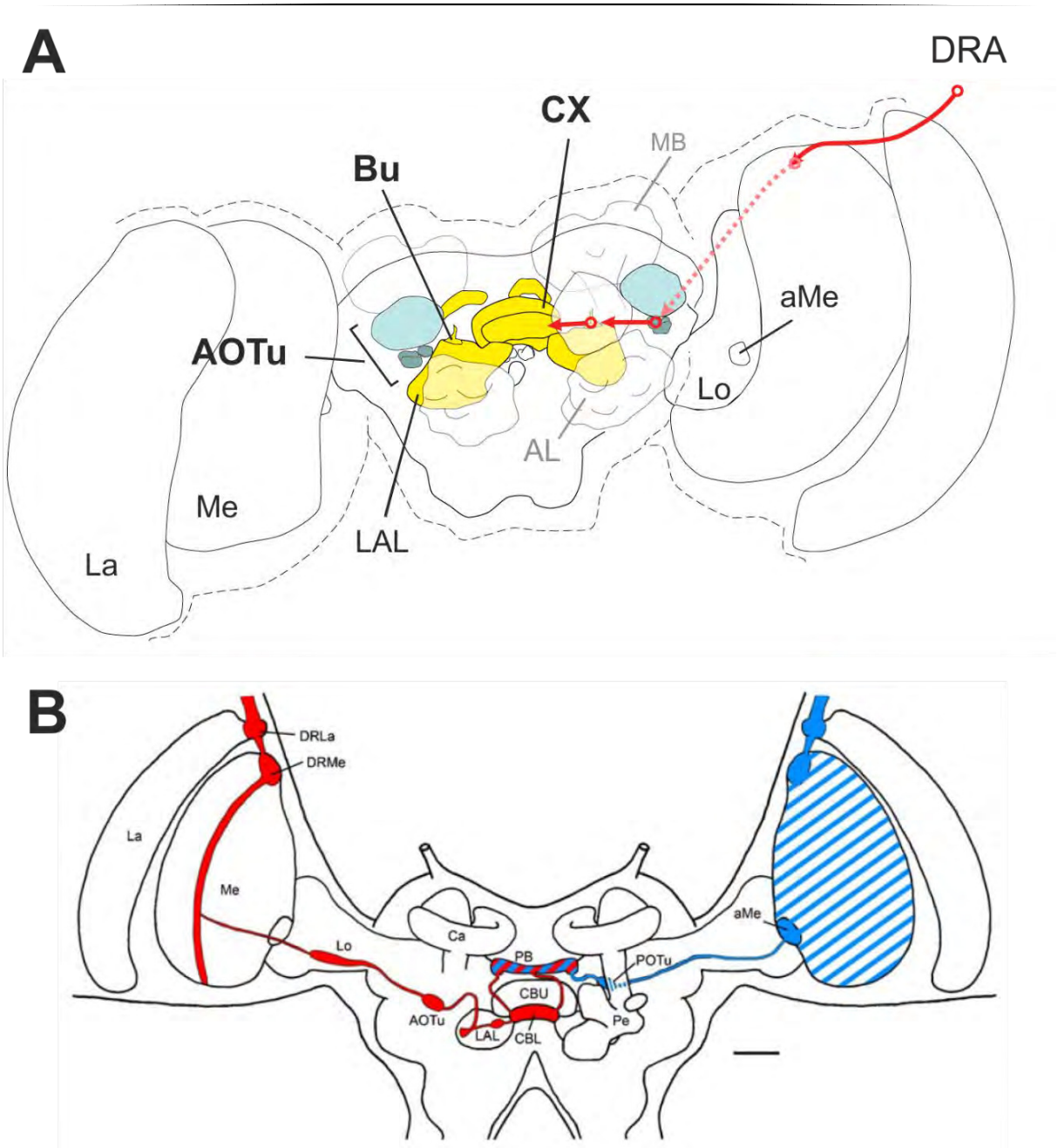

Figure 4: Anterior visual pathway in insects. (A) Scheme of the anterior visual pathway in the monarch butterfly. Solid lines indicates confirmed and dotted red lines presumed neural connection. Circles mark neuropiles involved in the anterior visual pathway. Modified after Reppert et al. (2018) **(B)** Anterior visual pathway as characterized in the desert locust. Scale bar: 200 mm µm. Reproduced from el Jundi and Homberg (2010). Abbreviations: aMe, accessory medulla; AOTu, anterior optic tubercle; AL, antennal lobe; Ca, calyx; CBL, lower division of the central body; CBU, upper division of the central body; DRLa, dorsal rim area of the lamina; DRMe, dorsal rim area ofthe medulla; La, lamina; LAL, lateral accessory lobe; Lo, lobula; MB, mushroom body; Me, medulla; PB, protocerebral bridge; Pe, pedunculus; POTu, posterior optic tubercle.

sensitive photoreceptors is higher in the desert locust (33°; Schmeling et al., 2014) than in the monarch butterfly (4°; Stalleicken et al., 2006).

Neurons connected to the photoreceptors transfer the visual cue information past the medulla (Me), lobula (Lo) and the lower subunit of the anterior optic tubercle (AOTu), which has been

associated with time compensation (Heinze and Reppert 2011; Pfeiffer et al., 2005) and color cue processing (Kinoshita et al., 2007; Pfeiffer and Homberg, 2007). A neuron that is sensitive to visual stimuli connects the AOTu with a small region of the lateral complex (Lx): Based on the pre-existing literature it is termed as TuLAL in monarch butterflies and equivalent to the *Drosophila*'s TuBu-cells (Pfeiffer et al., 2005; Hardcaste et al. 2021). The neuropile containing the presynaptic innervation of the TuLAL cells is known as bulb (Bu). In the monarch butterfly and dung beetle the Bu is unsegmented (el Jundi et al., 2019; Heinze et al. 2013), while in the desert locust the same neuropile is organized into smaller subunits (Träger et al., 2008). Contrastingly to other regions of the Lx, the Bu does not process motor, but visual cue information (Hardcastle et al., 2021; Heinze and Reppert 2011; Pfeiffer et al., 2005). It has been suggested that different areas of the Bu process different visual cue information (Shiozaki and Kazama 2017; Hardcastle et al., 2021). For instance, for in the fruit fly, the superior Bu processes unpolarized small receptive field stimuli like the sun, the anterior bulb processes polarized light, and the inferior Bu is involved in perceiving unpolarized wide-field visual information (Hardcastle et al., 2021). Furthermore, the Bu is composed of microglomeruli which are enlarged synaptic connections of a TuLAL and an input neurons of the sun compass neuropiles (Held et al., 2016), allowing for a more efficient transfer of visual information. In *Cataglyphis* ants, light exposure of nursing ants increased the number of microglomeruli, indicating that the Bu and the synaptic connections innervating the Bu are highly plastic (Schmitt et al., 2016). Visual cue information from the Bu is then transmitted to the sun compass encoding central complex (CX).

1.5 Central complex and heading direction encoding

As demonstrated in other insect (reviewed by Heinze, 2014 and Honkanen et al., 2018), the central complex is associated with encoding spatial memory (Ofstadt et al., 2011), locomotor control (Ritzmann et al., 2012) and spatial orientation (Homberg et al., 2011). Since the CX neuropiles and underlying neural circuitry are conserved across insects (el Jundi et al., 2018; Hanesch et al., 1989; Kaiser et al., 2022; Kurylas et al., 2008; Rother et al., 2021), the monarch butterfly's CX is also divided into the central body lower unit (CBL), central body upper unit (CBU), a pair of noduli (NO) and the protocerebral bridge (PB). Consistent with the observations made in other insects (Hanesch et al., 1989; Heinze and Homberg, 2008), all CX subunits except the NO are organized in 16 columns, while the CBL, CBU and NO are divided into four horizontal layers each (Heinze et al. 2013; Heinze et al., 2012).

Depending on their arborization pattern, CX neurons can be classified as tangential or columnar neurons (Heinze et al. 2013). The CX receives input information by the tangential neurons innervating the CBL (TL), which are subdivided based on their arborization patterns. TL cells projecting to the lateral accessory lobe (LAL) receive wind information (Okuba et al. 2020) and TL cells innervating the bulb process visual information (Heinze and Reppert, 2011). Regardless of subtype, all TL cells are GABAergic and terminate in a horizontal layer of the CBL (Heinze et al., 2013; Heinze and Reppert 2011). Since TL cells are also synaptically coupled to each other (Phillips-Portillio and Strausfeld, 2012; Turner-Evans et al., 2020), they postsynaptically inhibit other TL neurons as well (Turner-Evans et al., 2020) and the heading direction encoding columnar cells innervating the CBL (CL). CL cells receive input from the CBL and project their output synapses in the PB and the LAL.

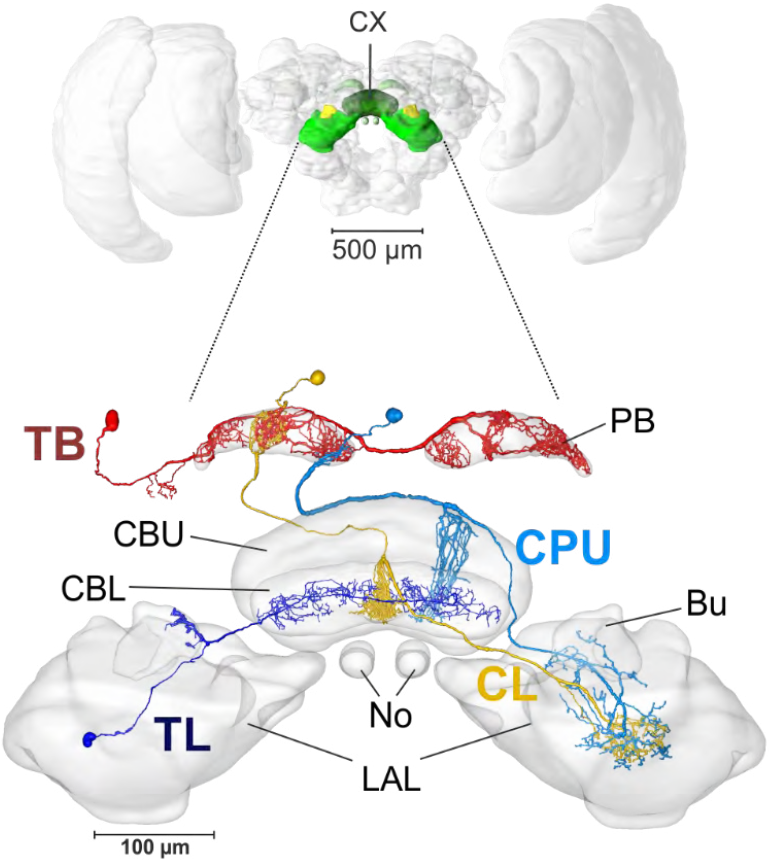

Figure 5: Sun compass neurons of the monarch butterflies. Shown above is the reconstructed monarch butterfly brain with the CX and LX being colorized. Inset displays the LX and CX innervated by the main sun compass encoding neurons. Modified after Heinze et al. (2013). Abbreviations: Bu, bulb; CBL, central body lower unit; CBU, central body upper unit; No, noduli; LAL, lateral accessory lobe; PB, protocerebral bridge.

While the exact details of heading direction encoding are not known for the monarch butterfly, due to the conserved nature of the CX across insects it is very likely that the butterfly shares similarities with the ring attractor circuitry in the fruit fly (Kim et al., 2017; Turner-Evans et al., 2020). Based on the ring attractor framework, the internal heading direction is represented by a single active CL cell within the CBL, while the remaining CL cells are inhibited by the TL cells (Fisher et al., 2019). By integrating external cue information the heading direction representation can shift to a neighboring CL cell

(Seelig and Jayaraman, 2015). Since the synapse connecting the TL and CL cells is highly plastic (Fisher et al., 2019), the internal heading representation can be flexibly adapted based on the visual scenery (Kim et al., 2019). Apart from integrating visual (Kim et al., 2019) and mechanosensory (Okuba et al. 2020) information, the CBL also receives the angular velocity information processed in the NO (Turner-Evans et al., 2017).

The heading direction information is then transferred to the protocerebral bridge (PB). The columns within the PB topographically represent the angle of polarizations in the desert locust (Heinze and Homberg, 2007). Cue processing continues in the PB innervating tangential cell (TB), which connects a PB column from the ipsi- and contralateral brain hemisphere (Heinze et al., 2013). The TB cells are involved in stabilizing the heading direction representation (Turner-Evans et al., 2020) and possibly transforming the heading direction information for further downstream processing (Hulse et al., 2022). In the CBU the idiothetic heading direction is translated into a world-centric direction (Lu et al., 2022). Furthermore, as suggested by Stone et al. (2017), the CBU might be innervated by the monarch butterfly's memory cells hypothesized to encode the animal's vector direction. The columnar neuron type that innervates the CBU (CPU), however, has yet to be characterized on an electrophysiological level. Most of the known CPU subtypes contain smooth synapses in the CBU and PB, while arborizing with varicose endings in the LAL (Heinze et al., 2013). Based on the cell's neuroanatomy, the CPU cells may provide the input information for the Lx to regulate steering or other motorsensory behavior (Heinze and Homberg, 2009; Steinbeck et al., 2019).

While the existence of heading direction memory has yet to be investigated in detail, it has been shown that the migratory state does affect brain morphology: The brains in migratory monarch butterflies are 20%-40% larger in CX volume than in non-migratory animals (Heinze et al., 2013). However, the higher volume of the PB in CX of migratory butterflies cannot be explained with their increased lifespan and is very likely linked to their migratory behavior (Heinze et al., 2013). This opens up the possibility that the monarch butterfly's migratory state affects the physiology of sun compass neurons. However, it is unclear which neurons would be affected and how they change the sun compass tuning.

1.5 Outline of the thesis

As shown above, the monarch butterfly is a suitable model organism to study the neural ethology of the long distance migration in insects. Past studies concentrated on investigating the ecology behind the monarch butterfly migration (reviewed by Brower, 1995) and examining the factors contributing to the declining migratory populations over the last decade (Malcom, 2018; Saunders et al., 2019; Wilcox et al., 2020). Furthermore, since the molecular mechanisms behind the induction of the migratory state is still unknown, other studies investigated underlying genetic (reviewed in Reppert et al., 2018 and Merlin and Liedvogel, 2019) and physiological (Altizer and Davis, 2010; Schroeder et al., 2019; Zhan et al., 2018) features connected to the monarch butterfly migratory behavior. Related to the migratory state, flight simulator experiments tested the animal's directed flight behavior and their response to natural (Mouritsen et al., 2013; Mouritsen and Frost, 2002; Stalleicken et al. 2007) and simulated (Franzke et al., 2020; Franzke et al., 2022) orientation cues.

On a neurological level, apart from creating a brain atlas (Heinze and Reppert, 2012), compass cue encoding in monarch butterflies was characterized by investigating the animal's anterior visual pathway (Heinze and Reppert, 2011) and anatomically characterizing the CX and its underlying circuitry (Heinze et al, 2013). However, since the last neurophysiology study focused on the neurons innervating the AOTu (Heinze and Reppert, 2011), the observed CX neurons where investigated in conjuncture with other visual cue processing neurons. Furthermore, since there are differences in CX-neuropile volume between migratory and non-migratory monarch butterflies (Heinze et al., 2013), the migratory state may affect the physiology of the CX circuitry and how visual cues are encoded. While the monarch butterfly is capable of time compensating its flight direction (Merlin et al., 2009; Guerra and Reppert, 2013), alternate encoding mechanisms like sun elevation based cue compensation have been analyzed (Heinze and Reppert, 2011).

The main goal of my thesis was to investigating visual cue processed in the monarch butterfly's sun compass. To allow for the identification of CX neurons and the observed physiology, I did single cell recordings with a sharp electrode. The input TL neurons were targeted since these neurons are being the least affected by the immobilization of the animals (Rosner et al., 2019). Summarized are the main questions:

- How does the migratory state affect sun compass tuning in monarch butterflies?
- How do CX neurons encode multiple visual inputs?
- How might the time information in monarch butterflies be transferred to the CX?

The thesis is organize in three chapters:

1. How does the migratory state affect the monarch butterfly's sun compass?

In the first part of the thesis, the main question was whether migratory and non-migratory monarch butterflies perceive celestial stimuli differently and whether differences in their behavioral state affects sun compass tuning. I used single cell recordings and the subsequent analysis of TL neuron physiology in response to different celestial stimuli as employed in other insects (el Jundi et al., 2015, Heinze et al., 2009; Pegel et al., 2018, Sakura et al., 2008). The parameters of TL cells derived from migratory and non-migratory butterflies were compared to each other to further understand celestial cue encoding in the monarch butterfly.

2. How does the internal sun compass of the monarch butterfly integrate multiple visual cues?

Since visual cues do not exist in singularity, the single cue conditions tested in the first project do not reflect the natural cue conditions. Therefore, the next project identified how the input cells of the CX process multimodal visual cues. For the first part of the project, combined celestial stimuli were presented to the animal during single-cell recordings to understand which celestial cue may dominate the TL encoding. For the second part of the project, we investigated whether the internal sun compass is capable of integrating the panoramic skyline information. We used the same wide field stimulus as described in Franzke et al., (2020) and identified how the TL neurons respond to the panoramic skyline and the combined presentation of skyline and sun stimulus.

3. How is the heading direction information modulated in the CBL of the CX?

Apart from the aforementioned time and elevation compensation methods (see above) the CX may receive additional visual input from the POTu. During my experiments, I observed a possible neural candidate which may modulate the heading direction representation in the CBL.

2. Manuscript I: How does the migratory state affect the monarch butterfly's sun compass?

Modified after Reppert et al. (2016)

© Basil el Jundi

© Myriam Franzke

Manuscript was originally published in: Nguyen, T. A. T., Beetz, M. J., Merlin, C. and el Jundi, B. (2021). Sun compass neurons are tuned to migratory orientation in monarch butterflies. Proceedings of the Royal Society B: Biological Sciences 288, 20202988.

Sun compass neurons are tuned to migratory orientation in monarch butterflies

Tu Anh Thi Nguyen[1], M. Jerome Beetz[1], Christine Merlin[2], Basil el Jundi[1]*

Affiliations:

[1] University of Wuerzburg, Biocenter, Zoology II, Würzburg, Germany

[2]Department of Biology and Center for Biological Clocks Research, Texas A&M University, College Station, TX, USA

*Corresponding authors: basil.el-jundi@uni-wuerzburg.de

Keywords: insect, central complex, navigation, orientation, lepidoptera

Abstract

Every autumn, monarch butterflies migrate from North America to their overwintering sites in Central Mexico. To maintain their southward direction, these butterflies rely on celestial cues as orientation references. The position of the sun combined with additional skylight cues are integrated in the central complex, a region in the butterfly's brain that acts as an internal compass. However, the central complex does not solely guide the butterflies on their migration but also helps monarchs in their non-migratory form manoeuvre on foraging trips through their habitat. By comparing the activity of input neurons of the central complex between migratory and non-migratory butterflies, we investigated how a different lifestyle affects the coding of orientation information in the brain. During recording, we presented the animals with different simulated celestial cues and found that the encoding of the sun was narrower in migratory compared to non-migratory butterflies. This feature might reflect the need of the migratory monarchs to rely on a precise sun compass to keep their direction during their journey. Taken together, our study sheds light on the neural coding of celestial cues and provides insights into how a compass is adapted in migratory animals to successfully steer them to their destination.

1. Introduction

Migration requires the use of a sophisticated form of orientation exhibited widely across taxa, from birds and sea turtles to insects [1]. One of the most well-known insect migration is accomplished by monarch butterflies *(Danaus plexippus*), which travel every fall from North America to overwintering locations in Central Mexico [2, 3]. To maintain their migratory direction, these butterflies rely on the sun as their main orientation reference [4]. In addition, they integrate time of day information from circadian clocks in the antennae [5, 6] and perhaps also in the brain [7] into the compass network. This guarantees that the butterflies can maintain a constant southerly direction even though the azimuthal position of the sun changes over the course of a day [4, 8]. When the sun is occluded on overcast days, the butterflies can rely on other orientation cues, such as the polarized skylight [9], and/or the earth's magnetic-field [10] to maintain their course. In addition, the spectral gradient present in the sky [11] could also serve as an orientation signal, as demonstrated in other insects [12].

The neural network that processes sky compass information in monarch butterflies has previously been described in detail [13, 14]. While photoreceptors of the butterfly's dorsal rim area (DRA) detect the polarized skylight, the remaining photoreceptors on the compound eye detect unpolarized light [7, 15]. The polarized and unpolarized signals converge in the same compass network and are transferred to a region of the central brain, called the bulb [16]. There, tangential (TL) neurons have their synaptic input and transmit the information to the central body lower division of the central complex (figure 1*a*). Recent studies have shown that the central complex plays a key role in processing skylight information in insects [13, 17-19] and is involved in a variety of orientation tasks [20, 21]. While not explicitly demonstrated in monarchs, the central complex likely functions as the internal compass during the migration by matching the actual heading direction with the desired southward direction [22].

While monarchs are best known for their autumn long-distance migration, completion of the migratory cycle is achieved by several generations. After overwintering in Central Mexico, migratory monarchs return north in the spring to southern states of the United States [23, 24]. Recolonization of the breeding sites is not completed by the overwintered butterflies, but requires at least two spring generations that continue traveling north until they reach their summer habitat and produce non-migratory summer generations [14, 25]. Thus, North American monarch butterflies occur in either a migratory or non-migratory form [26]. While migratory butterflies are physiologically adapted to effectively perform their long journey, non-

migratory butterflies spend their time foraging in more restricted areas [27]. The transition from a generation of non-migratory to migratory butterflies significantly affects the volumes of compass neuropils within the central complex [16]. While these changes might be correlated with adaptations to the migration of these butterflies, their physiological consequence on the network remains unclear. To study this, we recorded the activity of the TL neurons intracellularly, while simultaneously presenting different simulated skylight cues to migratory and non-migratory butterflies. We found that the tuning width of the TL neurons to a green light spot representing the sun was narrower in migratory butterflies. In addition, the neurons in migratory butterflies exhibited a higher angular sensitivity to the sun in their frontal visual field, which matches the sun's position during their southward migration. Taken together, this supports the idea that the compass of migratory butterflies is adapted for their long-distance migration by allowing them to keep their flight direction with high precision over the course of the day.

2. Methods

(a) Animals

Recordings from the non-migratory monarch butterflies (*Danaus plexippus*) were performed from April to September 2018, 2019 in Würzburg (Germany). The butterflies were obtained as pupae from the Costa Rica Entomology Supply. After eclosion, the adult butterflies were kept in an incubator (I-30VL, Percival Scientific) at 12:12 light/dark condition, 25 °C and at 50 % relative humidity. The animals' diet consisted of 15 % sugar water solution ad libitum. Migratory animals were collected in College Station, TX, USA from October to November in 2018, 2019 and recordings were performed at this location. Wild-caught animals were kept in glassine envelopes and the incubator (I-30VL, Percival Scientific) was adjusted to an 11:13 light-dark cycle with 23 °C set during light and 12 °C during dark phases to simulate the conditions during fall season. Animals were fed every other day with a 20 % honey solution.

(b) Electrophysiology

Although the recordings were performed on two different electrophysiology setups (one at the University of Wuerzburg and one at Texas A&M University), both the equipment used and procedures for recordings from migratory and non-migratory animals were similar. To ensure stable recordings, the legs and wings were clipped off and the animals were fixed on a metal holder. After opening the head capsule, the neural sheath was removed using fine tweezers to

expose the brain. At least one of the antennae remained intact to prevent the loss of time compensation [6]. During recording, the head capsule was filled with ringer solution (150 mM NaCl, 3 mM KCl, 10 mM TES, 25 mM sucrose, 3 mM $CaCl_2$). Electrodes (50-200MΩ) were drawn from borosilicate glass (inner/outer diameter: 0.75/1.5 mm, inner filament diameter: 0.2 mm; Hilgenberg) using a Flaming/Brown puller (P-97, Sutter Instruments) and were filled with 1M KCl and loaded with 4% Neurobiotin (Vector Laboratories). In addition, a silver wire was immersed in the head capsule as a reference. A micromanipulator (Leica Microsystems) was used to position the electrode in the brain. Action potentials of single neurons were amplified using an intracellular amplifier (BA-03X, npi Elelctronic). The signals were digitized (Power1401, CED) with a resolution of 1-20 kHz and recorded using the Spike2.9 software (CED). After recording, the Neurobiotin was iontophoretically injected with 1-3.5 nA into the neuron for about 3-5 min and the brain was dissected out of the head. To identify the recorded neuron, we followed the immunohistochemical protocol described in [17] (for details, see supplementary methods, Histology and imaging). During cell injections, we often co-labeled several TL subtypes (figure S1*a*). We were therefore not able to define from which TL subtype (TL2a/b or TL3, [16]) exactly our recordings were obtained. The similarity in the general tuning characteristic between migratory and non-migratory TL neurons suggests that, even if different TL subtypes may have different functional roles in monarch butterflies, this did not affect our comparisons between migratory and non-migratory TL neurons.

(c) Visual stimulus

To stimulate the butterflies with simulated skylight cues during recording, UV (365 nm, OSRAM) and green (520 nm, OSRAM) LEDs were mounted on a rotation stage (DT-50, PI miCos). The rotation stage was positioned dorsally to the animal. As the butterfly's dorsal rim area is sensitive to UV light [7, 15], a UV-LED was mounted at the centre of the rotation stage. The light of the LED was passed through a diffuser (quarter white diffusion, LEE Filters) and a UV permeable polarizer (Bolder Vision Optik). Additionally, four arms were attached perpendicular to each other to the rotation stage. One arm was equipped with a green and the arm opposite, with a UV LED at the head of the arms. The stimulus was positioned in such a way that both LEDs were set at an elevation of 30° to the animal. All LEDs (unpolarized and polarized light) were adjusted to the same photon flux of about 1.4×10^{14} photons/cm^2/s using a spectrometer (Maya200 Pro, Ocean Optics) and measured in the position in which the animals would be facing the stimuli during the experiments. The angular extent of the polarization stimulus at the butterfly eye was 10.42° in non-migratory and 9.55° in migratory butterflies

due to slight differences in the setups. The angular size of the unpolarized light spots were 1.44° in non-migratory and 1.32° in migratory butterflies. The motions of the rotation stage were controlled via a custom-written MATLAB script (Version R2019b, MathWorks). Similar to previous experiments [13], the polarizer orientation was changed with an angular velocity of 60°/s. Likewise, the unpolarized light spots were moved on a circular path around the animal at a velocity of 60°/s. The rotation stage was turned clockwise and counterclockwise while the tested cue (either the polarized or unpolarized light) was turned on.

(d) Data analysis

Neurons were included in the analysis if they fulfilled the following criteria: *i)* stable baseline throughout the whole recordings, *ii)* consistency in shape of action potentials, *iii)* spiking amplitude above the noise ratio, *iv)* neuron identifiable based on the tracer injection. The data were exported from Spike2 for further evaluation in MATLAB using a custom-written script that included the CircStat toolbox [28] and the CircHist function [29].

Action potentials were detected using a manually set threshold. Background activity was evaluated based on a 3-6 sec section of the recording prior to light stimulation. As the recording quality can affect the observed background activity (a lower electrode resistance can lead to more spikes/s), we ensured that the background activity did not correlate with the electrode resistance (figure S1*b*). The same segment as for the background activity was used to determine the background variability [30]. Sliding averages of the responses were obtained by applying a low-pass filter to the inter-spike-intervals. The maximum spike rate during stimulation was calculated by defining the highest action potential rate for each rotation and averaging it across all rotations. To calculate the neuron's preferred directions (φ_{max}) for each light stimulus, each action potential was assigned to a degree according to the stimulus position. The preferred direction was then determined based on a circular unimodal (unpolarized light) or bimodal (polarized light) distribution. The modulation strength of each neuron, which contains information about the response strength to a light cue (a higher modulation value indicates a stronger response), was calculated in 20° bins according to [17]. To obtain the tuning curves, spike frequencies were calculated in 5° bins and the preferred direction (φ_{max}) of each rotation was shifted to 0°. The firing rates from all rotations were averaged to obtain mean tuning curves for each neuron. The resulting curves were then normalized by the area below the curve. The tuning width for each cell was determined by calculating the full width at half maximum. The angular sensitivity (change of firing rate) of the neurons was calculated by determining the difference in the spike rate between adjacent bins. To analyse the distribution and compare the

data statistically, we used linear and circular statistics (for details, see supplementary methods, Statistics). All data are reported as mean ± standard deviation (SD).

3. Results

(a) General tuning characteristics of TL neurons

We recorded from 34 TL neurons: 17 from migratory and 17 from non-migratory monarch butterflies. In many insects, a green light spot is interpreted as the sun's direction [17, 31, 32]. During recordings, a green light spot was therefore moved on a circular path around the butterfly to simulate a rotation of the animal under the sun (figure 1*b*). To test if the neurons encode the celestial spectral gradient, we observed the neural response to a moving UV light spot. A rotation of the butterfly under the polarization pattern was simulated through a full rotation of a zenithal polarizer. TL neurons typically exhibited a bimodal response to the polarizer (figure 1*c*, left) and a unimodal response to the unpolarized light spots (figure 1*c*; middle, right). However, not every neuron showed a significant modulation to the tested stimuli. 33 of the 34 recorded neurons showed a significant response to the polarization stimulus (figure 1*d*; $p < 0.05$; Rayleigh test). Out of the 34 tested neurons, 13 (38.23%) TL cells responded to the green light spot (figure 1*d*; $p < 0.05$; Rayleigh test). Interestingly, the neurons' responsiveness to the UV light was much higher (79.41%). Ten of the tested TL neurons responded to all three stimuli with a significant modulation of the firing rate (figure 1*e*). In these cells, the modulation strength was higher to the polarization (105.22 ± 49.65, mean ± SD) and the UV stimulus (133.37 ± 67.08) than to the green light (76.26 ± 39.53). Hereby, the modulation strength increased with the background activity when the neurons were stimulated with the polarization or the green light (figures 1*f*; S2). A similar trend towards higher modulation strengths at higher background activities was also observed for the UV light spot. Taken together, our results show that TL neurons code for different skylight cues in monarch butterflies.

(b) Comparison of the responses in migratory and non-migratory butterflies

Next, we compared the TL-neuron responses of migratory and non-migratory butterflies. The responsiveness of the TL neurons to the presented stimuli did not differ between migratory and non-migratory monarchs (figure 2*a*), suggesting that skylight cues are equally relevant for the functioning of TL neurons in both forms. The stimulus position that evokes the strongest average response of a neuron is referred to as the preferred direction (φ_{max}; figure 1*c*). In

general, the preferred directions of the TL neurons to polarized light and the UV light covered all possible directions, while the preferred directions to the green light were clustered around 0° (figure S3*a*). The preferred directions of the TL neurons to polarized light did not differ significantly between the forms (figure 2*b*, left plots). We could also not detect any obvious difference in the preferred direction to the green light between the migratory and non-migratory TL neurons (figure 2*b*, middle plots). However, the distribution of the UV preferred directions differed significantly between the two forms (figure 2*b*, right plots) because there were more migratory ones tuned to the left and more non-migratory ones tuned to the right visual field of the animals. We also calculated the angular differences between the preferred directions ($\Delta\varphi_{max}$; figure S3*b*). The spatial relationship between the polarized light and the green/UV light spot deviated from the natural 90°-relationship in TL neurons of both forms. In most of the TL cells, the relationship between the green and UV light was clustered between 0-90°, irrespective of the butterflies' form (figure S3*b*). Taken together, the preferred directions did not show any obvious differences between migratory and non-migratory butterflies to polarized light and the green light, suggesting that the recorded neurons were representing a wide range of the classical TL neuron population.

(c) Comparison of general physiological properties

We next compared the basic physiological properties of the TL neurons between the forms. On average, the background activity of the TL neurons in migratory butterflies was 9.25 ± 5.8 spikes/s; n = 15), which was not different from the background activity observed in non-migratory TL neurons (11.61 ± 6.75 spikes/s; n = 17; figure 2*c*, left plot). Similarly, the background variability (*Cv*) did not differ either between groups (figure 2*c*, right plot). In addition, we investigated if the butterflies' form could influence the neurons' response to the tested skylight cues by comparing their maximum spike rate during stimulation (figure 2*d*). The maximum spike rate of the migrants TL neurons to polarized light was on average 19.67 ± 8.08 spikes/s (n = 17) and was comparable to the TL neurons of non-migratory butterflies (19.61 ± 11.29 spikes/s; n = 16). Similarly, the responses to the green (max. spike $rate_{migratory}$= 20.00 ± 10.78 spikes/s; n = 8; max. spike $rate_{non\text{-}migratory}$= 24.26 ± 14.4 spikes/s; n = 5) or UV light (max. spike $rate_{migratory}$= 20.92 ± 9.53 spikes/s; n = 14; max. spike $rate_{non\text{-}migratory}$= 24.77 ± 21.57 spikes/s; n = 13) did not differ between the two monarch forms (figure 2*d*). Together with our findings that TL neurons display similar background activity/variability in migratory and non-migratory monarchs, these data suggest that the butterfly's form does not influence the general physiological properties of TL neurons.

(d) Comparison of functional tuning characteristics

We next compared the tuning curves of the responses to the presented stimuli between the migratory and non-migratory TL neurons (figure 3*a*). For each TL cell, we generated individual tuning curves and shifted the preferred direction to 0° (figure S4). The average tuning width of migratory TL neurons to polarized light (82.94 ± 19.93°) was similar to the tuning width observed in non-migratory butterflies (88.13 ± 15.04°; figure 3*a*,*b*). Similarly, the tuning width of the TL neurons to the UV light spot did not differ between migratory (140.71 ± 44.41°) and non-migratory (159.62 ± 61.56°) butterflies (figure 3*a*,*b*). In contrast, while the tuning curve in migratory butterflies was relatively narrow (106.88 ± 67.61°), the tuning curve in response to the green light in non-migratory butterflies was consistently broader (222.00 ± 19.87°; figures 3*a*+*b,* S4). To exclude the possibility that the narrower tuning curves could result from stronger responses to the green light in TL neurons of migratory monarchs, we also compared the modulation strength of the responses. Neither the modulation strength to polarized light ($M_{migratory}$ = 89.68 ± 45.72, n=17; $M_{non\text{-}migratory}$ = 88.64 ± 42.72, n=16), to the UV light ($M_{migratory}$ = 107.94 ± 55.01, n=14; $M_{non\text{-}migratory}$ = 103.31 ± 64.49, n=13), or to the green light ($M_{migratory}$ = 72.12 ± 42.94, n=8; $M_{non\text{-}migratory}$= 93.20 ± 25.81, n=5) differed between migratory and non-migratory butterflies (figure 3*c*) suggesting that the narrower tuning to the green light in migrants does not arise from differences in response strength.

The precision of a compass increases by a high alteration of the neurons' spiking rate as the animal rotates around its body axis [12]. To test if the different tuning widths affect the rotational sensitivity of the TL network, we also compared the angular sensitivity, i.e. the change of firing rate, of the neurons between migratory and non-migratory butterflies (figure 4*a*). Interestingly, the angle relative to the preferred direction at which the neurons exhibited the highest sensitivity differed between the forms: while the angular sensitivity to the green light was significantly higher in the sector around the preferred direction in the migratory TL cells, the angular sensitivity of the non-migratory cells was higher in the sectors that were about 120° away from the preferred direction (figure 4*b*). As expected, these differences in the angular sensitivity were not observed when stimulating with polarized light or the UV light (figure S5). Thus, although the tuning curves in response to the green light were broader in non-migratory butterflies, the TL neurons in both forms have the angular sensitivity to code for the sun. To investigate how the spatial difference in the angular sensitivity affects the precision of the compass, we analysed the angular sensitivity of each TL cell with respect to the position of the green light stimulus (figure 4*c*). In contrast to the TL neurons in non-

migratory butterflies ($p=0.91$; V-test, $n=5$), in migratory TL neurons the highest angular sensitivities were significantly centred in the animals' anterior visual fields ($p<0.001$; V-test, $n=8$). Interestingly, this increased sensitivity in the front of the animals correlated with the sun azimuth during their southward migration (figure 4*c*). In summary, the TL neurons in migrants are well suited to maintain the sun in front of the animal and might help the butterflies to keep their southerly direction with a high precision during their long-distance migration.

4. Discussion

(a) General characteristics of TL neurons

We showed that monarch TL neurons encode different skylight cues, which is in line with previous findings [13]. Each TL neuron is tuned to a specific polarization angle as observed in TL-neurons in locusts, crickets, beetles [17, 19, 33], and butterflies [13], and may additionally encode the sun. Interestingly, the TL neurons preferred directions to the green light were directed towards the animal's frontal visual field. Currently, we do not know what causes this bias or if it has any functional implication. The observed differences in the cells' responsiveness to polarized light/UV light vs. green light is most likely a bias in the way of detecting the neurons during experiments. The polarization response helped in identifying a compass neuron and this was then tested using the green and UV light spot. Interestingly, the neurons showed higher responsiveness and modulation strength to the UV light than to the green light. This indicates that the UV photoreceptors in the butterflies' eye are either more sensitive than the green photoreceptors or that the UV light information is integrated over a larger array of ommatidia than the green light information.

Heinze et al. [16] divided the monarch TL neurons anatomically into three subtypes that innervate different layers in the central body lower division. We were not able to find any physiological differences between TL subtypes and, as we often co-labelled several TL subtypes (figure S1*a*), were not always able to define from which subtypes our recordings were obtained. All three subtypes of monarch TL neuron are GABA-ergic [34] and inhibit the downstream heading-direction network, termed CL1 (E-PG in fruit flies) neurons, in the central body lower division (ellipsoid body in fruit flies [35]). Our results here show that the background activity of the TL neurons correlates with the modulation strength to polarized light and the green light spot. Thus, the sensitivity could be altered by changing the background activity of individual TL cells and with it, the inhibitory input on the CL1 network.

Interestingly, TL neurons also receive circadian [36] and self-motion signals [37] in fruit flies. These inputs could modify the background activity of individual TL neurons in monarch butterflies and change the sensitivity for coding heading-direction information in a time-of-day or context-dependent (walking vs. flying) manner.

(b) Integration of different celestial cues

The skylight polarization angles vibrate at 90° to the sun's position in nature. This spatial relationship, however, is not reflected in the TL cells in our study, in line with previous results from TL neurons in monarch butterflies [13]. This deviation originates in the dorsal rim area, which is not centred in the zenith in monarchs [15]. Compass neurons in the brain need to match the relationship between polarized light and the sun in a time-of-day dependent manner due to the change of the sun's elevation over the course of the day [38]. Although such a time-dependent "elevation-compensation" has previously been reported in the monarch TL neurons [13], our TL recordings were too limited in terms of number of cells tuned to the simulated sun, to fully re-evaluate this.

Most of the TL cells' preferred direction was not affected by the spectral content of the light spot which is in line with previous reports in monarchs [13]. We found one migratory TL neuron that exhibited a 180° relationship between the green and UV light (figure S2*b*). Such a neuron would help monarchs distinguish between solar and antisolar hemisphere based on spectral information. However, responses of compass neurons to spectral cues strongly depend on the light intensity [39]. Thus, more TL neurons might be detected that encode the celestial spectral information if tested at the correct light intensities.

(c) Behavioural context and neural plasticity

The volume of brain regions differs dramatically between the non-migratory and migratory forms in monarch butterflies and desert locusts [16, 40]. In both species, this does not affect the general tuning properties of compass neurons [41, this study]. We here observed that the tuning width of the TL neurons in response to the simulated sun was narrower in migratory monarchs than in non-migrants, which led to a higher angular sensitivity in the frontal visual field. While the detailed neural mechanisms are unclear, this higher sensitivity may allow the migratory butterflies to precisely maintain the sun in their frontal visual field during their southward migration. This is essential during their long journeys in which an accumulation of even small deviations from the optimal course could lead to energetically costly detours. Despite being able to maintain a constant direction using a sun stimulus indoors [42], non-

migratory butterflies do not show a group orientation to the south [26]. In line with this, we did not find any obvious bias in the spatial distribution of the TL neurons' angular sensitivity in non-migratory butterflies.

The TL neurons' input regions, the bulb, is highly conserved amongst insects and consists of large synapses [37,43-45]. This region has been shown to be highly plastic in *Cataglyphis* ants with the number of large synapses increasing in ants that change from workers to foragers [44]. Thus, the bulb represents an attractive candidate site where the differences in the tuning width might be established in the butterfly's brain. Future anatomical experiments comparing the large synapses of migratory and non-migratory butterflies may reveal differences depending on the behavioural context of the butterflies. Combined with a behavioural assay in which the butterflies maintain constant headings to a simulated sun [42], we will next be able to quantify the narrower tuning in migratory TL neurons on the precision of the butterflies compass.

Data accessibility. Raw data and analyses scripts are available on Dryad (https://doi.org/10.5061/dryad.dv41ns1wr)

Acknowledgments. We thank Samantha Iiams, Aldrin Lugena, Guijun Wan and Ying Zhang for helping capture migratory monarchs in College Station TX and for checking them for *Ophryocystis elektroscirrha*. We would like to thank Anna Stoeckl, Emily Baird, and James Foster for their helpful comments on the manuscript and Johannes Spaethe for providing us a spectrometer. In addition, we would like to thank Sergio Siles (butterflyfarm.co.cr) and Marie Gerlinde Blaese for providing us with monarch butterfly pupae in Würzburg.

Authors' contributions. Study design: TATN, CM, BeJ. Conducting experiments: TATN. Analysis of data: TATN, MJB, BeJ. Interpretation of data: TATN, MJB, CM, BeJ. Drafting of the manuscript: TATN, BeJ. Critical review of the manuscript: MJB, CM. Acquired Funding: BeJ. All authors approved of the final version of the manuscript.

Funding. This work was supported by the Emmy Noether program of the Deutsche Forschungsgemeinschaft granted to BeJ (GZ: EL784/1-1).

Competing interests. The authors declare no competing interests.

References

1. Mouritsen H. 2018 Long-distance navigation and magnetoreception in migratory animals. Nature 558, 50-59. (doi:10.1038/s41586-018-0176-1).

2. Reppert S.M., de Roode J.C. 2018 Demystifying Monarch Butterfly Migration. Curr Biol 28, R1009-R1022. (doi:10.1016/j.cub.2018.02.067).

3. Merlin C., Iiams S.E., Lugena A.B. 2020 Monarch Butterfly Migration Moving into the Genetic Era. Trends Genet 36, 689-701. (doi:10.1016/j.tig.2020.06.011).

4. Mouritsen H., Frost B.J. 2002 Virtual migration in tethered flying monarch butterflies reveals their orientation mechanisms. Proc Natl Acad Sci U S A 99, 10162-10166. (doi:10.1073/pnas.152137299).

5. Merlin C., Gegear R.J., Reppert S.M. 2009 Antennal circadian clocks coordinate sun compass orientation in migratory monarch butterflies. Science 325, 1700-1704. (doi:10.1126/science.1176221).

6. Guerra P.A., Merlin C., Gegear R.J., Reppert S.M. 2012 Discordant timing between antennae disrupts sun compass orientation in migratory monarch butterflies. Nat Commun 3, 958. (doi:10.1038/ncomms1965).

7. Sauman I., Briscoe A.D., Zhu H., Shi D., Froy O., Stalleicken J., Yuan Q., Casselman A., Reppert S.M. 2005 Connecting the navigational clock to sun compass input in monarch butterfly brain. Neuron 46, 457-467. (doi:10.1016/j.neuron.2005.03.014).

8. Froy O., Gotter A.L., Casselman A.L., Reppert S.M. 2003 Illuminating the circadian clock in monarch butterfly migration. Science 300, 1303-1305. (doi:10.1126/science.1084874).

9. Reppert S.M., Zhu H., White R.H. 2004 Polarized Light Helps Monarch Butterflies Navigate. Curr Biol 14, 155-158. (doi:10.1016/j.cub.2003.12.034).

10. Guerra P.A., Gegear R.J., Reppert S.M. 2014 A magnetic compass aids monarch butterfly migration. Nat Commun 5, 4164. (doi:10.1038/ncomms5164).

11. Coemans M.A., Vos Hzn J.J., Nuboer J.F. 1994 The relation between celestial colour gradients and the position of the sun, with regard to the sun compass. Vision Res 34, 1461-1470. (doi:10.1016/0042-6989(94)90148-1).

12. el Jundi B., Pfeiffer K., Heinze S., Homberg U. 2014 Integration of polarization and chromatic cues in the insect sky compass. J Comp Physiol A 200, 575-589. (doi:10.1007/s00359-014-0890-6).

13. Heinze S., Reppert S.M. 2011 Sun compass integration of skylight cues in migratory monarch butterflies. Neuron 69, 345-358. (doi:10.1016/j.neuron.2010.12.025).

14. Reppert S.M., Guerra P.A., Merlin C. 2016 Neurobiology of Monarch Butterfly Migration. Annu Rev Entomol 61, 25-42. (doi:10.1146/annurev-ento-010814-020855).

15. Stalleicken J., Labhart T., Mouritsen H. 2006 Physiological characterization of the compound eye in monarch butterflies with focus on the dorsal rim area. J Comp Physiol A 192, 321-331. (doi:10.1007/s00359-005-0073-6).

16. Heinze S., Florman J., Asokaraj S., el Jundi B., Reppert S.M. 2013 Anatomical basis of sun compass navigation II: the neuronal composition of the central complex of the monarch butterfly. J Comp Neurol 521, 267-298. (doi:10.1002/cne.23214).

17. el Jundi B., Warrant E.J., Byrne M.J., Khaldy L., Baird E., Smolka J., Dacke M. 2015 Neural coding underlying the cue preference for celestial orientation. Proc Natl Acad Sci U S A 112, 11395-11400. (doi:10.1073/pnas.1501272112).

18. Giraldo Y.M., Leitch K.J., Ros I.G., Warren T.L., Weir P.T., Dickinson M.H. 2018 Sun Navigation Requires Compass Neurons in Drosophila. Curr Biol 28, 2845-2852. (doi:10.1016/j.cub.2018.07.002).

19. Pegel U., Pfeiffer K., Homberg U. 2018 Integration of celestial compass cues in the central complex of the locust brain. J Exp Biol 221, 1-15. (doi:10.1242/jeb.171207).

20. Neuser K., Triphan T., Mronz M., Poeck B., Strauss R. 2008 Analysis of a spatial orientation memory in Drosophila. Nature 453, 1244-1247. (doi:10.1038/nature07003).

21. Ofstad T.A., Zuker C.S., Reiser M.B. 2011 Visual place learning in Drosophila melanogaster. Nature 474, 204-207. (doi:10.1038/nature10131).

22. Heinze S. 2017 Unraveling the neural basis of insect navigation. Curr Opin Insect Sci 24, 58-67. (doi:10.1016/j.cois.2017.09.001).

23. Urquhart F.A. 1964 Monarch Butterfly (Danaus plexippus) Migration Studies: Autumnal Movement. Proc Entomol Soc Ont 95, 23-33.

24. Urquhart F.A., Urquhart N.R. 1979 Vernal Migration of the Monarch Butterfly (Danaus P. plexippus, Lepidoptera: Danaidae) in North-America from the Overwintering Site in the Neo-Volcanic Plateau of Mexico. Can Entomol 111, 15-18. (doi:10.4039/Ent11115-1).

25. Brower L.P. 1995 Understanding and misunderstanding the migration of the monarch butterfly (Nymphalidae) in North America: 1857-1995. J Lepid Soc 49, 304-385.

26. Zhu H., Gegear R.J., Casselman A., Kanginakudru S., Reppert S.M. 2009 Defining behavioral and molecular differences between summer and migratory monarch butterflies. BMC Biol 7, 1-14. (doi:10.1186/1741-7007-7-14).

27. Calvert W.H. 2001 Monarch butterfly (Danaus plexippus L., nymphalidae) fall migration: Flight behavior and direction in relation to celestial and physiographic cues. J Lepid Soc 55, 162-168.

28. Berens P. 2009 CircStat: A MATLAB Toolbox for Circular Statistics. J Stat Softw 31, 1-21. (doi:10.18637/jss.v031.i10).

29. Zittrell F., Pfeiffer K., Homberg U. 2020 Matched-filter coding of sky polarization results in an internal sun compass in the brain of the desert locust. Proc Natl Acad Sci U S A 117, 25810-25817. (doi:10.1073/pnas.2005192117).

30. Kuebler E., Thivierge J.-P. 2014 Spiking variability: Theory, measures and implementation in MATLAB. Quant Meth Psych 10, 131-142. (doi:10.20982/tqmp.10.2.p131).

31. Edrich W., Neumeyer C., von Heiversen O. 1979 “Anti-sun orientation” of bees with regard to a field of ultraviolet light. J Comp Physiol 134, 151-157. (doi:10.1007/BF00610473).

32. Rossel S., Wehner R. 1984 Celestial orientation in bees: the use of spectral cues. J Comp Physiol A 155, 605-613. (doi:10.1007/BF00610846).

33. Sakura M., Lambrinos D., Labhart T. 2008 Polarized skylight navigation in insects: model and electrophysiology of e-vector coding by neurons in the central complex. J Neurophysiol 99, 667-682. (doi:10.1152/jn.00784.2007).

34. Homberg U., Humberg T.H., Seyfarth J., Bode K., Perez M.Q. 2018 GABA immunostaining in the central complex of dicondylian insects. J Comp Neurol 526, 2301-2318. (doi:10.1002/cne.24497).

35. Fisher Y.E., Lu J., D'Alessandro I., Wilson R.I. 2019 Sensorimotor experience remaps visual input to a heading-direction network. Nature 576, 121-125. (doi:10.1038/s41586-019-1772-4).

36. Lamaze A., Kratschmer P., Chen K.F., Lowe S., Jepson J.E.C. 2018 A Wake-Promoting Circadian Output Circuit in Drosophila. Curr Biol 28, 3098-3105. (doi:10.1016/j.cub.2018.07.024).

37. Seelig J.D., Jayaraman V. 2013 Feature detection and orientation tuning in the Drosophila central complex. Nature 503, 262-266. (doi:10.1038/nature12601).

38. Pfeiffer K., Homberg U. 2007 Coding of azimuthal directions via time-compensated combination of celestial compass cues. Curr Biol 17, 960-965. (doi:10.1016/j.cub.2007.04.059).

39. Kinoshita M., Pfeiffer K., Homberg U. 2007 Spectral properties of identified polarized-light sensitive interneurons in the brain of the desert locust Schistocerca gregaria. J Exp Biol 210, 1350-1361. (doi:10.1242/jeb.02744).

40. Ott S.R., Rogers S.M. 2010 Gregarious desert locusts have substantially larger brains with altered proportions compared with the solitarious phase. Proc R Soc B 277, 3087-3096. (doi:10.1098/rspb.2010.0694).

41. el Jundi B., Homberg U. 2012 Receptive field properties and intensity-response functions of polarization-sensitive neurons of the optic tubercle in gregarious and solitarious locusts. J Neurophysiol 108, 1695-1710. (doi:10.1152/jn.01023.2011).

42. Franzke M., Kraus C., Dreyer D., Pfeiffer K., Beetz M.J., Stöckl A.L., Foster J.J., Warrant E.J., el Jundi B. 2020 Spatial orientation based on multiple visual cues in non-migratory monarch butterflies. J Exp Biol 223, 1-12. (doi:10.1242/jeb.223800).

43. Held M., Berz A., Hensgen R., Muenz T.S., Scholl C., Rossler W., Homberg U., Pfeiffer K. 2016 Microglomerular Synaptic Complexes in the Sky-Compass Network of the Honeybee Connect Parallel Pathways from the Anterior Optic Tubercle to the Central Complex. Front Behav Neurosci 10, 91-105. (doi:10.3389/fnbeh.2016.00186).

44. Schmitt F., Stieb S.M., Wehner R., Rossler W. 2016 Experience-related reorganization of giant synapses in the lateral complex: Potential role in plasticity of the sky-compass pathway in the desert ant Cataglyphis fortis. Dev Neurobiol 76, 390-404. (doi:10.1002/dneu.22322).

45. Träger U., Wagner R., Bausenwein B., Homberg U. 2008 A novel type of microglomerular synaptic complex in the polarization vision pathway of the locust brain. J Comp Neurol 506, 288-300. (doi:10.1002/cne.21512).

Figures

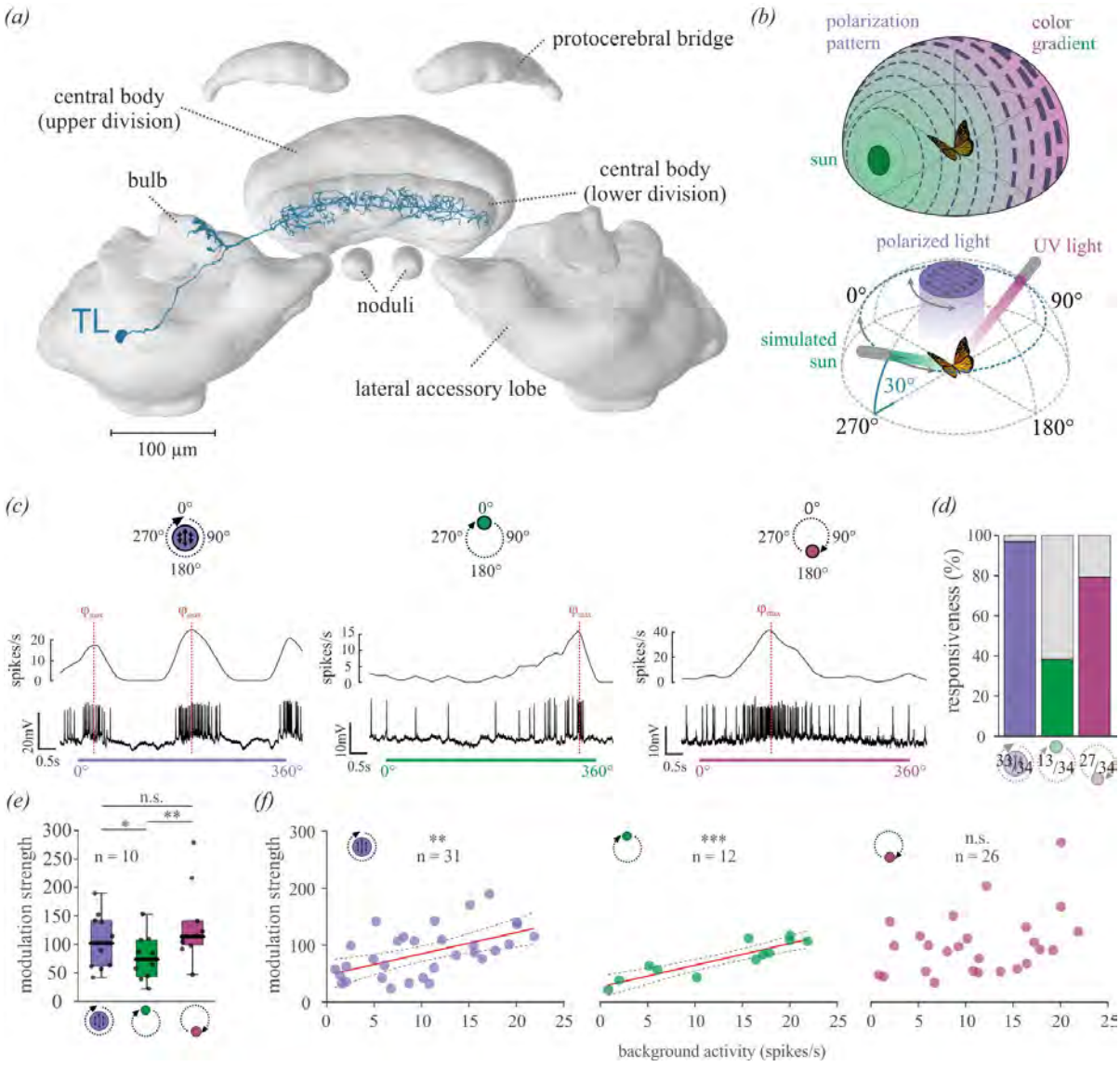

Figure 1. Neural responses of TL neurons to simulated celestial cues. *(a)* TL neuron (blue) visualized in the monarch butterfly central complex. Modified from [16]. *(b)* Top: schematic drawing of the celestial cues in nature. Concentric circles illustrate the polarization pattern around the sun (green), with the line thickness denoting the degree of polarization. The colour gradient between the solar (green) and antisolar (magenta) hemisphere is shown. Bottom: schematic of the stimuli used during recordings. The polarization stimulus was presented in the animal's dorsal visual field (with the 0°-polarization angle aligned in parallel to the antero-posterior body axis). The green/UV light spot (set 180° apart) were moved on a circular path (both at an elevation of 30°) around the animal. *(c)* Intracellular recordings from different TL neurons show the responses to polarized light (left), the green (middle) and the UV light spot

(right). The schematic drawing (top) indicates the initial positions of each stimulus. The preferred directions (φ_{max}) of the neuron are shown as red lines. *(d)* The responsiveness of the neurons to the different light cues [polarized light (left), green light (middle), UV light (right)]. Coloured bars indicate the percentage of responsive neurons. *(e)* Modulation strengths of the TL neurons that responded significantly to all tested light stimuli (n = 10). These neurons showed a higher modulation to UV and polarized light compared to the green light ($p_{POL\ vs.\ GREEN} = 0.01$, sign rank = 52; $p_{UV\ vs.\ GREEN} = 0.002$, sign rank = 0, n = 10; Wilcoxon signed rank test). Individual data points are shown as black dots. Boxes indicate interquartile range. Whiskers extend to the 2.5th and 97.5th percentiles. Black horizontal lines show the median. *(f)* The modulation strength of the TL neurons to polarized and the green light correlated linearly with the background activity ($p_{polarized\ light} = 0.002$, $F = 12.32$, $R^2_{adj.} = 0.27$; $p_{green\ light} < 0.001$, $F = 41.97$, $R^2_{adj.} = 0.79$), which was not the case for the UV light ($p = 0.072$, $\rho_{Spearman} = 0.35$). The linear regressions are shown as solid red lines and the 95% confidence intervals are shown as dashed lines. Error bars indicate the standard deviations. n.s., not significant *(e, f)*; *: p <0.05 *(e)*, **: p <0.01 *(e, f)*; ***: p <0.001 *(e, f)*.

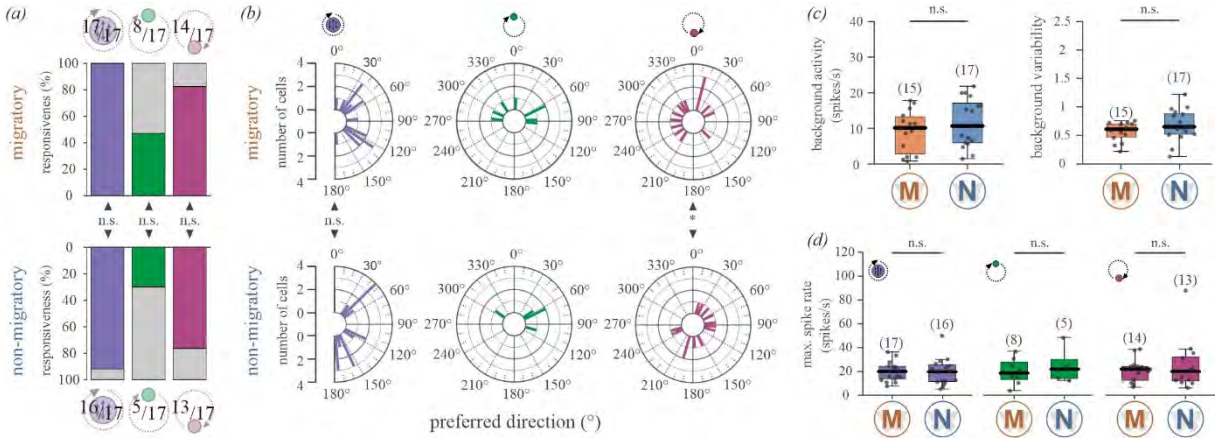

Figure 2. Comparison of the general tuning characteristics of TL neurons in migratory and non-migratory butterflies. *(a)* Responsiveness to the different light stimuli [polarized light (left); green light (middle); UV light (right)] did not differ between the migratory and non-migratory TL neurons ($p_{polarized\ light} = 1.00$, $\chi2 = 0.00$; $p_{green\ light} = 0.48$, $\chi2 = 0.50$; $p_{uv\ light} = 1.00$, $\chi2 = 0.00$; Chi-square test). *(b)* The preferred directions to polarized light (left), the green light (middle), and the UV light (right) in migratory (top; n = 17) and non-migratory (bottom; n = 17) TL neurons. The preferred directions did not differ between the forms for the polarized light ($p = 0.57$, $W = 1.13$, Mardia-Watson-Wheeler test), but for the UV light ($p = 0.01$, $W = 8.62$, Mardia-Watson-Wheeler test). Due to the low sample size, a statistical analysis of the distributions was not performed for the preferred directions to the green light. *(c)* Background

activity (left, p = 0.35, Z =-0.94, Wilcoxon rank-sum test) and background variability (right, p = 0.21, Z = -1.25, Wilcoxon rank-sum test) did not differ between migratory (M) and non-migratory (N) neurons. *(d)* Maximum spiking rates did not differ between the forms ($p_{polarized\ light}$ = 0.73, Z = 0.34; $p_{green\ light}$ = 0.83, rank sum = 54.00; $p_{UV\ light}$ = 0.87, Z = 0.17; Wilcoxon rank-sum test). The number of neurons is shown in brackets. Individual data points are shown as black dots. Boxes indicate interquartile range. Whiskers extend to the 2.5th and 97.5th percentiles. Black horizontal lines show the median. n.s.: not significant *(a-d)*, *: p <0.05 *(b)*.

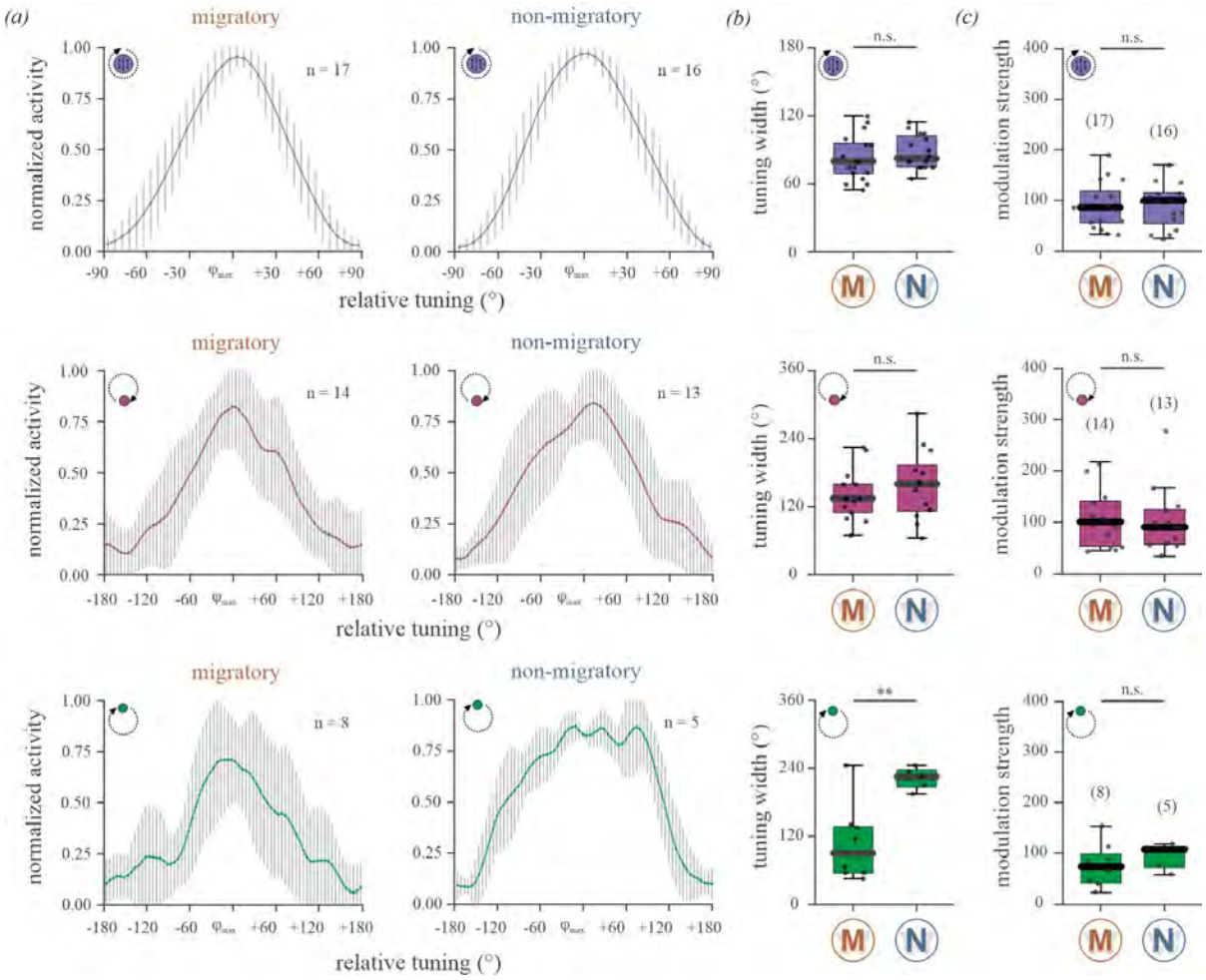

Figure 3. Comparison of the tuning shapes between migratory (M) and non-migratory (N) animals to polarized light (top), UV light (middle) and the green light (bottom). *(a)* Averaged tuning curves (bin size 5°) of the TL cells in migratory (left) and non-migratory animals (right). The n-size refers to the number of analysed cells. The error bars indicate the standard deviations. *(b)* While the tuning widths (full width at half maximum) of the responses to polarized light (p = 0.41, t-distribution = -0.84) and the UV light (p = 0.37, t-distribution = -0.92, unpaired t-test) were similar between the forms, a difference was found for the green light (p = 0.004, t-distribution = -3.66, unpaired t-test). *(c)* The modulation strengths to polarized

light (p = 0.99, Z = 0.02), the UV light (p = 0.79, Z = 0.27) and the green light (p = 0.44, rank sum = 50.00) did not differ between migratory and non-migratory butterflies. Individual data points are represented by black dots. Boxes of the box plots display the interquartile ranges. Whiskers extend to the 2.5th and 97.5th percentiles. Black horizontal lines indicate the median. Sample size is marked in brackets. n.s.: not significant *(b, c)*., **: p <0.01 *(b)*.

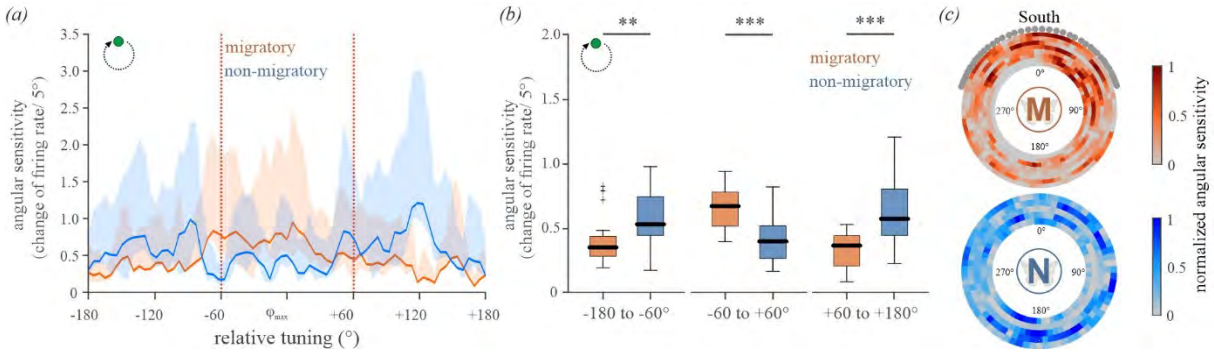

Figure 4. Comparison of the angular sensitivity to a moving green light spot. *(a)* The change of firing rate (bin size: 5°) to the green light stimulus with respect to the preferred direction of the cells (φ_{max}) is shown for migratory (orange) and non-migratory (blue) TL neurons. Shaded areas indicate the 25-75% quantiles. Red vertical dashed lines separate the sectors that are statistically analysed in (b). *(b)* The mean angular sensitivity of the neurons to the green light. The TL neurons in migratory butterflies were more sensitive around the φ_{max} (-60° to 60°(middle); p < 0.001, Z = 4.46, Wilcoxon rank sum test), while the non-migratory neurons were more sensitive at an angular distance of about 120° away from the φ_{max} (-180° to -60° (left); p < 0.022, Z = -3.06; +180° to +60° (right); p < 0.001, Z = -4.42, Wilcoxon rank sum test). *(c)* The circular plots show the normalized angular sensitivity in relation to the position of the green light for migratory (M, n =8) and non-migratory (N, n=5) TL neurons. Each row shows the angular sensitivity of one TL neuron. Grey dots at the perimeter of the upper plot indicate the sun azimuth over the course of a day (with respect to South) during the migration (November 1st, College Station, TX). **p <0.01 *(b)*; ***p <0.001 *(b)*.

Supplementary Material

Sun compass neurons are tuned to migratory orientation in monarch butterflies

Tu Anh Thi Nguyen[1], M. Jerome Beetz[1], Christine Merlin[2], Basil el Jundi[1]

[1] University of Wuerzburg, Biocenter, Zoology II, Würzburg, Germany
[2]Department of Biology and Center for Biological Clocks Research, Texas A&M University, College Station, TX, USA

Experimental Procedures

Histology and imaging

After recording, a tracer was iontophoretically injected with 1-3.5 nA into the recorded neuron for about 3-5 minutes and the brain was dissected out of the head capsule. The brains were first immersed in a fixative solution (4% paraformaldehyde, 1.3% picric acid, 10% glutaraldehyde in sodium-phosphate buffer) for 18-24h. After rinsing the brain samples in 0.1 M phosphate buffered saline (PBS) for 4x15 minutes, they were incubated in a solution containing either Alexa568-conjugated to streptavidin (Molecular Probes, 1:1000) or Cy3-conjugated to streptavidin (*Thermo Fisher Scientific*, 1:1000), dissolved in 0.1M PBS with 0.3 % Triton X-100 detergent (PBT) for 3 days at 4 °C in the dark. Afterwards, the brains were washed with PBT (2x20 minutes) and PBS (3x20 minutes). Samples were then dehydrated in an ascending ethanol series (30 %-100 %, 15min each). To clear the brain tissues, the samples were immersed with a 1:1 ethanol-methyl salicylate solution for 20 minutes, followed by a clearing step in 100 % methyl salicylate for about 1 hour at room temperature. Samples were then embedded in Permount (Fisher Scientific) between two cover slips. Ten reinforcement rings (Avery) were used as spacers to prevent compression of the brains.

To identify the recorded neuron, samples were imaged using a confocal microscope (TCS SP8, Leica) with either a 10x air (HCX PL-Apo 10x/0.4 CS, Leica) or a 25x oil-immersion objective (HC PL-Apo CS2 10x/0.75 Imm Corr, Leica). The brain samples were scanned with a resolution of 1024x1024 pixels and a distance of 1.5 µm in z-direction using a HeNa-laser.

Statistics

The Rayleigh test was used to determine if the occurrence of action potentials deviated from a uniform distribution (α=0.05). The V-test was applied to test if the data were clustered around 0°. Differences in the neurons' responsiveness to different light stimuli were determined using the Chi-square test for proportions. The Shapiro-Wilk test and the Levene test were applied to determine whether the data were distributed normally and if there was a difference in the variance. If there was no difference, parametric tests and calculated coefficients were employed (including the paired or unpaired Student's t-test and the Pearson correlation coefficient). Otherwise, non-parametric tests were implemented (Wilcoxon rank-sum test for unpaired and Wilcoxon signed rank test for paired data, Spearman correlation coefficient). If the data were normally distributed and showed a homogenous variance, a regression analysis was performed. The background activity was chosen as predictor parameter and the modulation strength as dependent variable. Before migratory and non-migratory TL neurons were pooled, a difference in the slopes was tested using an ANCOVA analysis, treating the migratory form as a covariate.

Figures

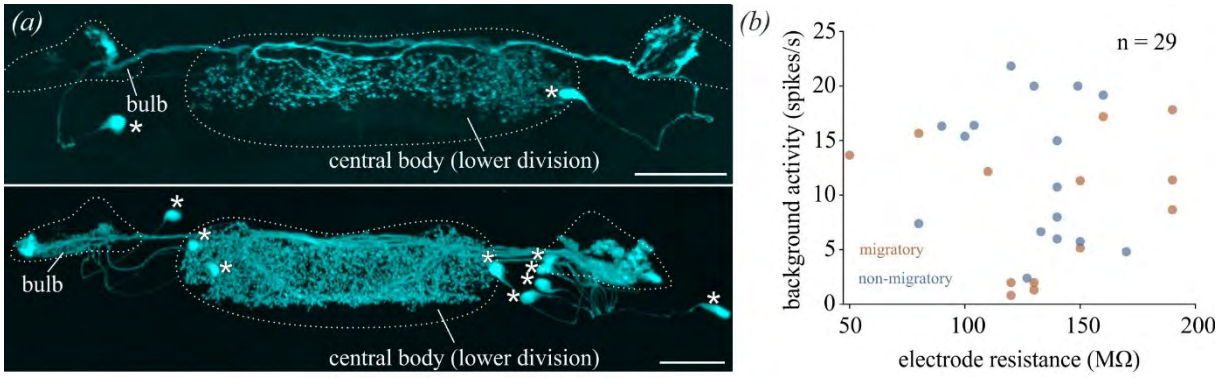

Figure S1. *(a)* Two examples of TL neuron tracings (anterior views) during electrophysiological recordings (maximum intensity projection views). In most experiments, several subtypes of TL neurons were stained. Asterisks mark the position of the cell bodies. Dotted lines outline the innervated neuropils. Scale bars: 50 µm. *(b)* Electrode resistance did not influence the background activity. There is no correlation between the observed background activity and electrode resistance ($p = 0.997$, $\rho = 4.17e^{-05}$, Spearman-coefficient).

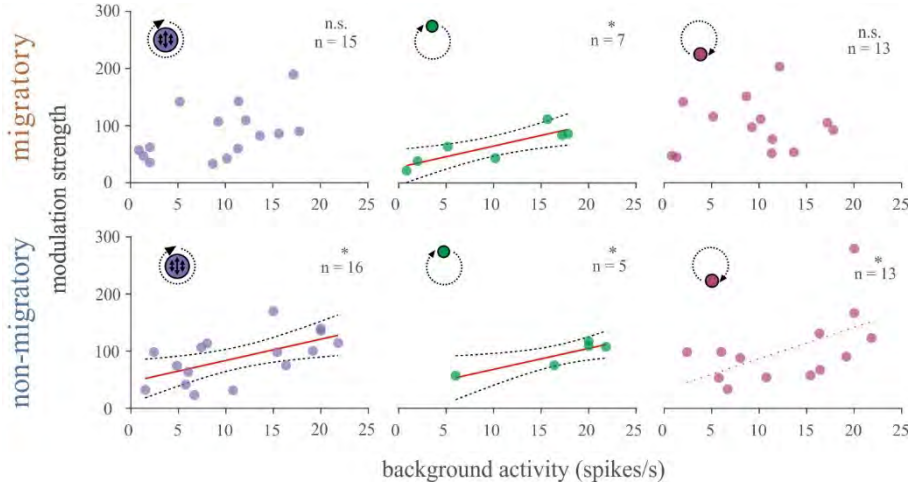

Figure S2. The relationship between background activity and modulation strength in migratory and non-migratory TL neurons. The data are the same as shown in figure 1*e* but separated into migratory (left) and non-migratory (right) TL neurons. Modulation strengths of the responses to the polarized light (upper plots), the green light (middle plots) and the UV light spot (lower plots) plotted against the background activity (individual data points are shown as dots). Linear regressions are shown if the data showed a significant ($p<0.05$) linear correlation. For polarized light: $p_{migratory} = 0.06$, $F= 4.26$, $R^2_{adj.}= 0.19$; $p_{non\text{-}migratory} = 0.01$, $F= 7.79$, $R^2_{adj.}= 0.31$. For the green light spot: $p_{migratory} = 0.02$, $F= 13.23$, $R^2_{adj.}= 0.67$; $p_{non\text{-}migratory} = 0.02$, $F= 13.94$, $R^2_{adj.} = 0.76$. For the UV light spot: $p_{migratory} = 0.70$, $\rho = 0.12$, Spearman-coefficient; $p_{non\text{-}migratory} = 0.04$, $\rho = 0.56$, Spearman-coefficient). Solid red lines show the fitted linear functions and dashed black lines illustrate the 95% confidence intervals. Dotted red lines show linear graphs calculated with the Spearman coefficient. n.s., not significant; *$p<0.05$

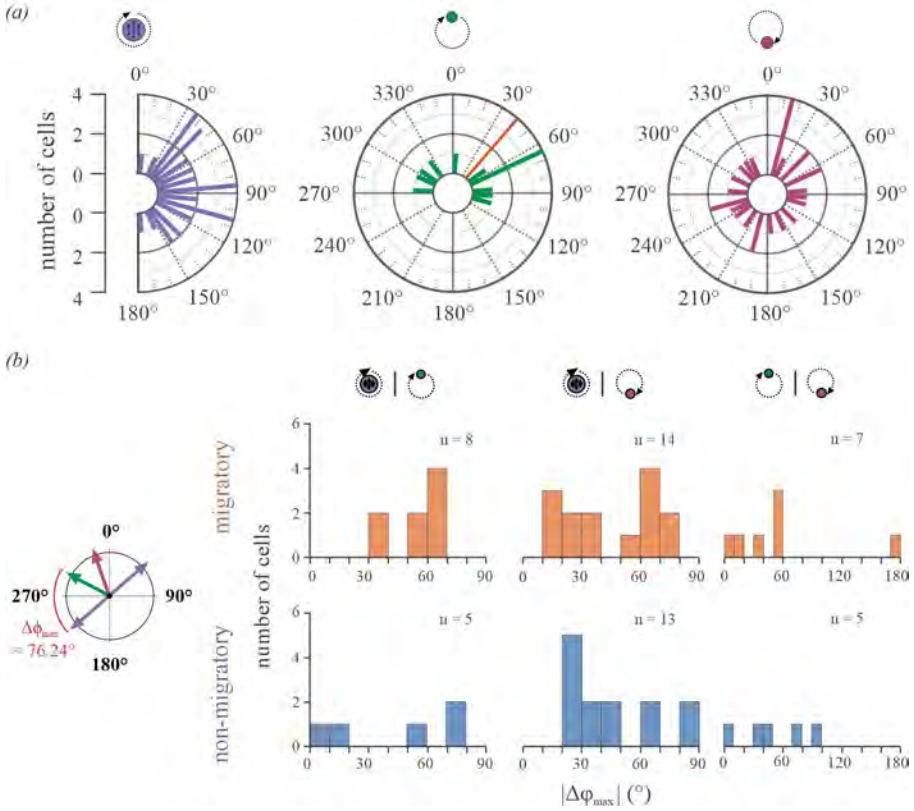

Figure S3. Preferred directions of the TL neurons. *(a)* The preferred directions (φ_{max}) to polarized light (violet, left plot, n = 33), the green light (green, middle plot, n = 13), and the UV light spot (magenta, right plot, n = 27) are shown. The observed preferred directions did not differ significantly from a uniform distribution in response to the polarized (p = 0.58, Z = 0.54, Rayleigh test) and the UV light (p = 0.76, Z = 0.28, Rayleigh test) but differed for the green light spot (p = 0.04, Z = 3.20, Rayleigh test). The symbols above the plots indicates the tested visual stimulus, while the red line shows the mean preferred direction of the neurons. *(b)* The angular differences between the preferred directions ($\Delta\varphi_{max}$). The schematic drawing (left) shows an example of how the $\Delta\varphi_{max}$ was calculated. The preferred directions of the neurons are shown as arrows (green, green light; magenta, UV light) and double-headed arrow (violet, polarized light). The red sector indicates the calculated $\Delta\varphi_{max}$ between the green light and polarized light. The histograms (right) illustrate the $\Delta\varphi_{max}$-distributions. Results from migratory animals are shown in the upper plots, while the data from non-migratory animals are shown in the lower plots. The $\Delta\varphi_{max}$ were calculated for polarized light and the green light (left), polarized light and the UV light cue (middle), and the green and UV light (right).

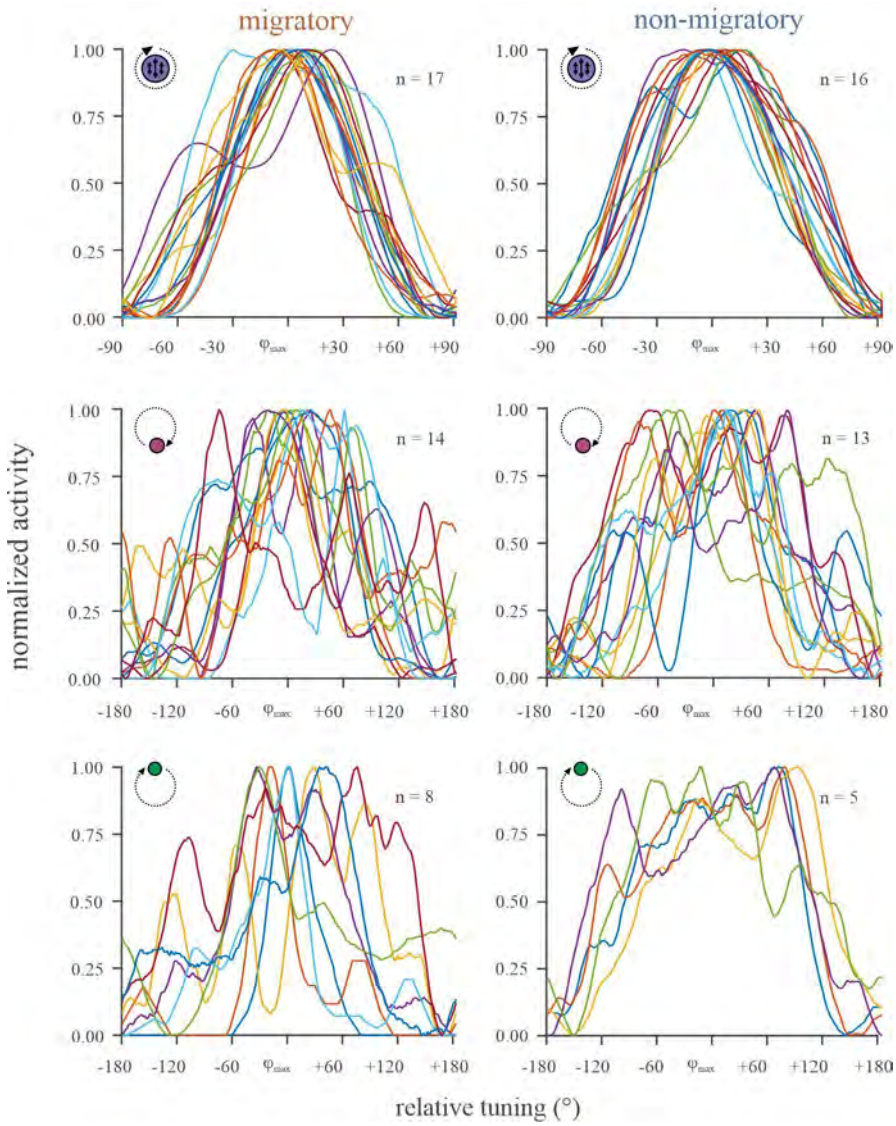

Figure S4. Single tuning curves used for the calculation of average tuning curves. Individual tuning curves of the responses of the TL cells in migratory (left panels) and non-migratory (right panels) animals to polarized light (upper plots), the UV light (middle plots) and the green light (lower plots). The data are the same as in figure 3*a*.

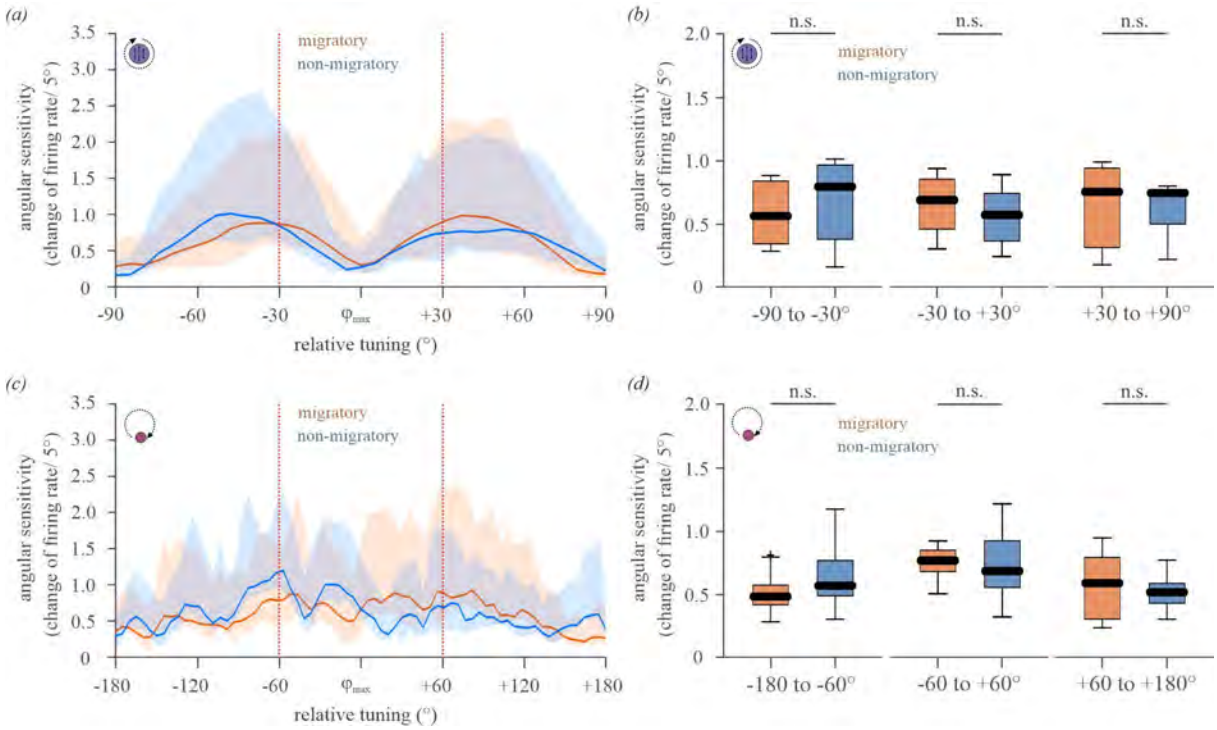

Figure S5. Angular sensitivity of the TL neurons to polarized light and the UV light. *(a,c)* The angular sensitivity (change of firing rate/5°) to the polarization stimulus *(a)* and the UV light spot *(c)*. Solid line shows the mean angular sensitivity in migratory (orange) and non-migratory (blue) TL neurons. Shaded areas indicate the 25-75% quantiles. Red vertical dashed lines separate the sectors that are statistically analyzed in (b) and (d), respectively. *(b,d)* The mean angular sensitivity of the response of the TL neurons to the polarization stimulus (*b*, same data as in *a*) and UV light (*d*, same data as in *c*) in migratory (orange) and non-migratory (blue) animals. TL neurons reveal the same angular sensitivity to polarized light in migratory and non-migratory butterflies (*b*, left plot, $p = 0.37$, $Z = -0.89$; middle plot, $p = 0.26$, $Z = 1.13$; right plot, $p = 0.51$, $Z = -0.66$, Wilcoxon rank sum test). The same was the true for the UV light spot (*d*, left plot, $p = 0.08$, $Z = -1.74$; middle plot, $p = 0.35$, $Z = 0.93$; right plot, $p = 0.56$, $Z = 0.59$, Wilcoxon rank sum test). Boxes of the box plots indicate the interquartile ranges and whiskers extend to the 2.5th and 97.5th percentiles. Black horizontal lines show the medians. n.s., not significant (b, d).

3. Manuscript II: How does the internal sun compass of the monarch butterfly integrate multiple visual cues?

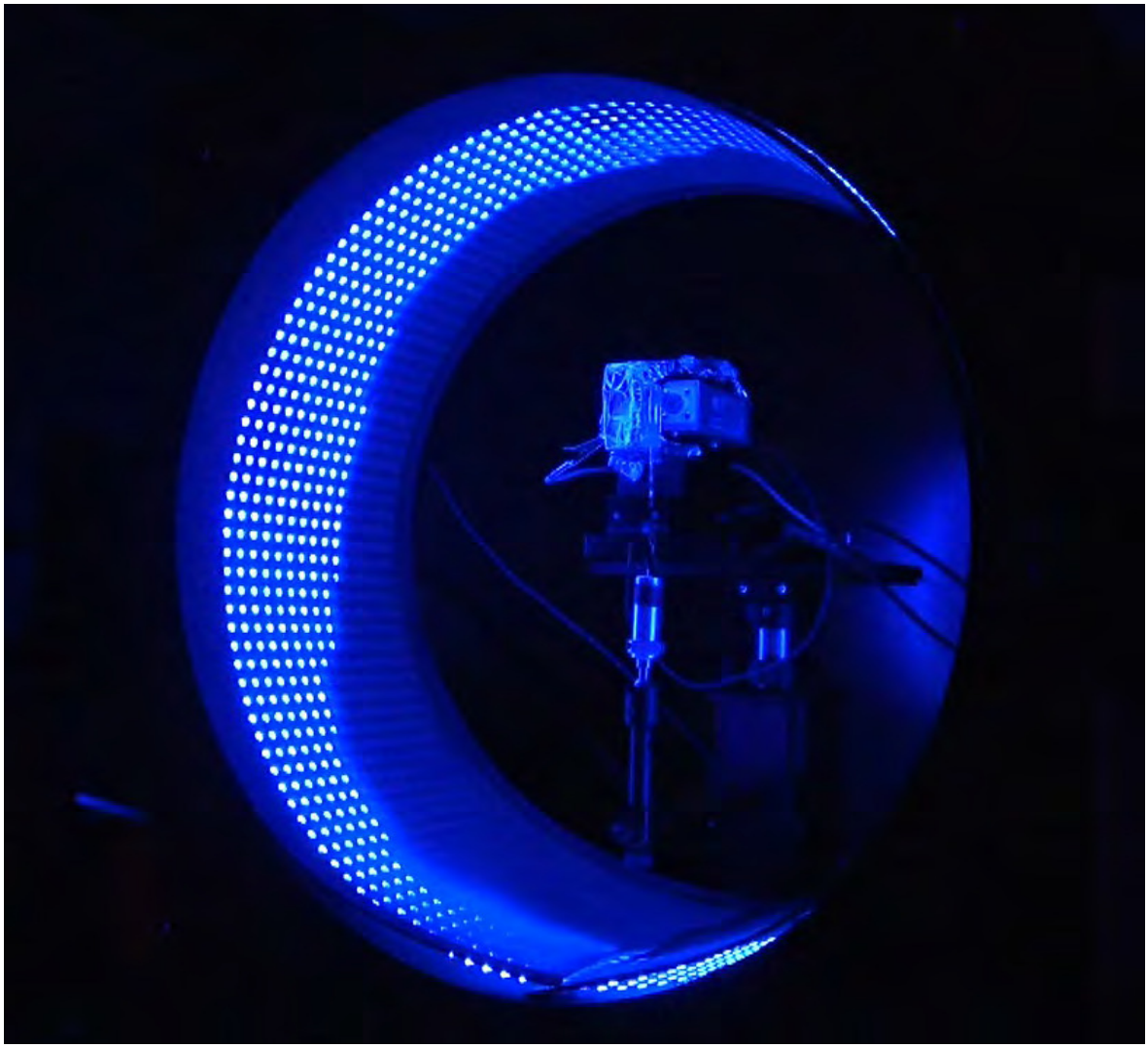

Manuscript was originally published in: Nguyen, T. A. T., Beetz, M. J., Merlin, C., Pfeiffer, K. and el Jundi, B. (2022). Weighting of Celestial and Terrestrial Cues in the Monarch Butterfly Central Complex. Frontiers in Neural Circuits 16.

Weighting of celestial and terrestrial cues in the monarch butterfly central complex

Tu Anh Thi Nguyen[1], M. Jerome Beetz[1], Christine Merlin[2], Keram Pfeiffer[1], Basil el Jundi[1,3]*

Affiliations:

[1] University of Wuerzburg, Biocenter, Zoology II, Würzburg, Germany

[2]Department of Biology and Center for Biological Clocks Research, Texas A&M University, College Station, TX, USA

[3]Department of Biology, Animal Physiology, Norwegian University of Science and Technology, Trondheim, Norway

*Corresponding author: basil.el.jundi@ntnu.no

Keywords: insect, central complex, navigation, orientation, landmark, migration, panorama, lepidoptera

Running Title:

Compass coding in monarch butterflies

Abstract

Monarch butterflies rely on external cues for orientation during their annual long-distance migration from Northern US and Canada to Central Mexico. These external cues can be celestial cues, such as the sun or polarized light, which are processed in a brain region termed the central complex (CX). Previous research typically focused on how individual simulated celestial cues are encoded in the butterfly's CX. However, in nature, the butterflies perceive several celestial cues at the same time and need to integrate them to effectively use the compound of all cues for orientation. In addition, a recent behavioral study revealed that monarch butterflies can rely on terrestrial cues, such as the panoramic skyline, for orientation and use them in combination with the sun to maintain a directed flight course. How the CX encodes a combination of celestial and terrestrial cues and how they are weighted in the butterfly's CX is still unknown. Here, we examined how input neurons of the CX, termed TL neurons, combine celestial and terrestrial information. While recording intracellularly from the neurons, we presented a sun stimulus and polarized light to the butterflies as well as a simulated sun and a panoramic scene simultaneously. Our results show that celestial cues are integrated linearly in these cells, while the combination of the sun and a panoramic skyline did not always follow a linear integration of action potential rates. Interestingly, while the sun and polarized light were invariantly weighted between individual neurons, the sun stimulus and panoramic skyline were dynamically weighted when both stimuli were simultaneously presented. Taken together, this dynamic weighting between celestial and terrestrial cues may allow the butterflies to flexibly set their cue preference during navigation.

Introduction

Spatial orientation has been investigated behaviorally in many insects, ranging from desert ants (Wehner, 2003; Wehner and Müller, 2006), honeybees (Rossel and Wehner, 1984; Edrich et al., 1979; Brines and Gould, 1979), dung beetles (el Jundi et al., 2019; Dacke et al., 2021), and locusts (Homberg, 2015), to moths (Dreyer et al., 2018a; Dreyer et al., 2018b). This also includes the monarch butterfly *(Danaus plexippus)*, which covers a distance of about 4,000 kilometers on its annual migration to its overwintering spots in Central Mexico (Merlin and Liedvogel, 2019). During this long-distance migration, the butterflies use the sun as their main orientation reference (Stalleicken et al., 2005). To successfully maintain their southerly direction over the course of a day, the butterflies integrate time information from the antennae (Merlin et al., 2009; Guerra et al., 2012) and the brain (Sauman et al., 2005) into their sun compass. In addition to the sun, monarch butterflies may also rely on the polarization pattern of the sky for orientation (Reppert et al., 2004). While the pattern of polarized light is perceived by a specialized dorsal region of the monarch butterfly eye, termed the dorsal rim area, the sun is detected by eye regions outside of the dorsal rim area (Sauman et al., 2005; Stalleicken et al., 2006). Celestial information is then transferred via the optic lobe and anterior optic tubercle to input neurons of the central complex (CX), termed tangential (TL) neurons (Heinze and Reppert, 2011; Nguyen et al., 2021). These neurons transfer celestial information from the bulb of the lateral complex to the central complex lower division in many insects (Held et al., 2015; el Jundi et al., 2018; Hensgen et al. 2020), including monarch butterflies (Fig. 1A,B). As shown for other insects (Stone et al., 2017; Hardcastle et al., 2021), TL cells (in fruit flies termed ring neurons) synapse onto a network of heading-direction cells that flexibly encode the actual flight direction of an animal based on sensory-motor information (Seelig and Jayaraman, 2015; Turner-Evans et al., 2017; Green et al., 2017; Fisher et al., 2019; Kim et al., 2019; Okubo et al., 2020, Hulse et al. 2021). While previous research focused on how the CX processes single celestial stimuli in the monarch butterfly brain (Heinze and Reppert, 2011; Nguyen et al., 2021; Beetz et al., 2022), the controlled single cue conditions in the lab rarely reflect the compound cue conditions found in nature. Thus, to obtain a highly robust compass network, multiple visual cues, such as the sun and polarized light are integrated simultaneously in nature (el Jundi et al., 2014; Lebhardt and Ronacher, 2014). Moreover, experiments on tethered flying monarch butterflies suggest that the butterflies combine a sun stimulus and a panoramic skyline to keep a directed flight heading (Franzke et al., 2020), similar to what has been reported for Australian bull ants (Reid et al., 2011) and honeybees (Towne and Moscrip, 2008; Towne et al., 2017).

But how visual sceneries composed of multiple stimuli, such as the sun and polarized light or the sun and a panoramic scene, are combined and how each of the cues is weighted neuronally has not been investigated in the monarch butterfly brain so far. To study this, we recorded intracellularly from TL cells in the monarch butterfly brain and analyzed how they respond to simultaneously presented stimuli, such as a simulated sun and polarized-light stimulus as well as a sun and panoramic-skyline stimulus.

Materials and Methods

Animals

Adult monarch butterflies (*Danaus plexippus*) of both sexes were kept in an incubator (I-30VL, Percival Scientific, Perry, IA, USA) with a 12:12 hours light-dark cycle at 25°C in Würzburg (Germany). They were provided with 15% sugar solution *ad libitum*. Some animals were caught at College Station, TX, USA during their annual southward migration. These animals were kept in the incubator at an 11:13 hours light-dark cycle at 23°C during light and 12°C during dark phases. They were fed with 20% honey solution every second day.

Preparation and electrophysiology

After clipping off wings and legs, the butterflies were attached to a custom-built holder using dental wax (Omnident, Rodgau Nieder-Roden, Germany). The head capsule was opened frontally and muscle and fat tissue above the brain were removed. At least one of the antennae remained intact to avoid a disruption of circadian inputs to the compass network (Guerra et al., 2012; Merlin et al., 2009). To access the central brain with the electrode, the neural sheath was removed using fine tweezers. Throughout preparation and subsequent neuronal recording, the brain was immersed in monarch ringer (150 mM NaCl, 3 mM KCl, 10 mM TES, 25 mM sucrose, 3 mM $CaCl_2$).

To record intracellularly from individual TL neurons, micropipettes were drawn from borosilicate glass capillaries (inner diameter: 0.75 mm and outer diameter: 1.5 mm, Hilgenberg, Malsfeld, Germany) using a Flaming/Brown horizontal puller (P-97, Sutter Instrument Company, Novato, CA, USA). After loading the micropipette with 4% Neurobiotin (Vector Laboratories, Burlingame, UK, dissolved in 1 M KCl), it was filled with a 1 M KCl solution. The micropipette was connected to an electrode holder with a chloridized silver wire, which was attached to a micromanipulator (Leica Microsystems, Wetzlar, Germany). Another chloridized silver wire served as reference electrode and was inserted into the opened head

capsule close the butterfly's mouthparts. Detected signals were amplified 10x using a BA-03X bridge amplifier (npi Elelctronic GmbH, Tamm, Germany). The signal was digitized with sampling rates between 1-20 kHz using a digitizer (Power1401, Cambridge Electronic Design, Cambridge, UK). The neuronal activity was observed on a computer using the software Spike 2 (version 9.00, Cambridge Electronic Design). To obtain recordings from TL neurons, we targeted their output regions in the central complex. All recordings were thus likely obtained from the neurons' axons that enter the central body lower division anteriorly (Fig. 1A).

Celestial stimuli

To simulate celestial cues, the same stimulus was used as described in Nguyen et al. (2021). A rotation stage (DT-50, PI miCos GmbH, Karlsruhe, Germany) was dorsally positioned to the animals. For the polarized UV light stimulus, a polarizer was mounted on top of the rotation stage. Because monarch butterflies detect polarized light in the UV range (Stalleicken et al., 2005; Sauman et al., 2005) a UV-LED with an emission peak at 365 nm (LZ1-10UV00-0000, OSRAM Sylvania Inc., Wilmington, MA, US) and a quarter white diffuser (Nr. 251, LEE filters, Hampshire, UK) were placed behind a UV permeable linear polarizer (BVO UV, Bolder Vision Optik Inc., Boulder, CO, USA) in the center of the rotation stage. This allowed us to present equally illuminated polarized UV light to the butterflies. The sun stimulus was presented using an unpolarized green LED with an emission peak at 517 nm (LZ1-10G102-0000, OSRAM, Munich, Germany). This LED was mounted on one of four arms extending from the rotation stage. To control for the influence of wavelength information, a UV LED was attached to the arm opposite to the green LED. Both light spots were adjusted to an elevation of 30° relative to the animal's head and provided unpolarized light. The angle of the zenithal polarization filter was aligned perpendicular to the two LED arms, which allowed to present the celestial cues in the spatial relationship found in nature. All light stimuli (unpolarized green/UV light, polarized UV light) were adjusted to a photon flux of about 1.4×10^{14} photons/cm^2/s, measured with a spectrometer (Maya2000 Pro, Ocean Optics) at the position where the animal faced the stimuli during recordings. Since the recordings were obtained via two setups with identical equipment, the angular positioning of the stimulus varied slightly. The polarization stimulus had an angular extent between 9.6°-10.4° at the butterfly's eye. The angular size of the unpolarized light spots was 1.3-1.4°. The movements of the rotation stage were controlled via a custom-written script for the software MATLAB (Version R2019b, MathWorks, Natick, MA, USA). During the experiments, the rotation stage was turned by 360° in clock- and counterclockwise direction at a constant velocity of 60°/s while testing the

response of the TL cells to a single stimulus (sun stimulus *or* polarized light) or a combination of the stimuli (sun stimulus *and* polarized light). As five of the TL neurons were obtained from migratory butterflies, we first tested if they differed in their general tuning characteristics from the recordings obtained in non-migratory butterflies. However, we did not find any differences in the relevant response characteristics tested here between both groups and decided to pool the data. As we often co-labeled several TL neurons from both brain hemispheres, we were unable to define for each recording from which brain hemisphere it was obtained. However, in six out of the ten celestial-cue experiments, TL neurons with synaptic input in the right bulb were either solely stained or showed a stronger staining (Fig. 1B). In the remaining four experiments, TL neurons with inputs in the left bulb were either stained stronger (two experiments) or showed the same staining strength to TL neurons in the right brain hemisphere (two experiments).

Panoramic skyline and sun stimuli

The panoramic skyline was simulated via an LED arena consisting of a circular array of 128x16 RGB-LEDs (M160256CA3SA1, iPixel LED Light Co., Ltd, Baoan Shenzhen, China). The arena covered a visual field of 360° along the horizontal and 43° along the vertical plane around the animal. The LEDs were controlled via a Raspberry Pi (Model 3B, Raspberry Pi Foundation, Cambridge, UK). We presented the same panoramic skyline to the butterflies that has been used in recent behavioral experiments on monarch butterflies (Franzke et al., 2020). Each LED above the horizon was adjusted to a photon flux of about 6.68×10^{10} photons/cm^2/s in the blue range (emission peak: 458 nm). LEDs below the horizon were turned off. The panoramic scene was uploaded as an RGB image 8bits/channel) to the Raspberry Pi and a custom-written program written in Go controlled the rotation movements of the stimulus. To avoid any dark adaption of the animals' eyes or history-dependent effects, a panorama with a flat horizon (*flat panorama*) was presented to the animals while searching for TL neurons. As soon as a TL neuron was successfully targeted, the panoramic scenery with the variable height profile (*panoramic skyline*) was used as a test stimulus. Light intensity differences between the panoramic scenery and the flat panorama were minimized by turning on a similar number of LEDs in both panoramas. To find TL neurons during our experiments, we first stimulated the animal with zenithal polarized light. Once a neuron responded to polarized light, the polarization stimulus was turned off and the panoramic skyline was presented and rotated by 360° around the animal in clock- and counterclockwise direction (at a constant velocity of 60°/s). To combine the panoramic scene with a sun stimulus, one LED above the horizon at an

angular elevation of 18.9° was switched to a wavelength emission peak of about 516 nm and an intensity of about 6.14×10^{12} photons/cm^2/s. We combined the sun stimulus either with the flat panorama or with the panoramic skyline. For the former, we moved the sun stimulus around the animal, while the flat panorama stayed stationary. For the latter, we rotated both stimuli around the animal.

Histology and imaging

To evaluate anatomically the neuron type from which we recorded, Neurobiotin was iontophoretically injected into the cells (1-3.5 nA) for 3-5 min at the end of each experiment. After allowing the Neurobiotin to distribute for 20 min, the brains were dissected out of the head capsule and fixated for 18-24 h at 4°C in a sodium-phosphate buffer containing 4% paraformaldehyde, 0.2% picric acid, and 0.25% glutaraldehyde. They were then rinsed 4 x 15 min in 0.1 M phosphate buffered saline (PBS) and, afterwards, incubated with either Cy3-conjugated to streptavidin (Thermo Fisher Scientific, Waltham, MA USA, 1:1000) or Alexa568-conjugated to streptavidin (Molecular Probes, Eugene, OR, USA, 1:1000) diluted in PBS containing 0.3% Triton-X 100 (PBT) for 3 days at 4°C. The brains were then rinsed with PBT (3 x 20min) and afterwards with PBS (2 x 20min), before they were dehydrated through an ascending ethanol series (30, 50, 70, 90, 95, and 100%; 15 min each). Afterwards, the brains were immersed in a 1:1-mixture of ethanol and methyl salicylate (Fisher Scientific GmbH, Schwerte, Germany) for 20 min and then in 100% methyl salicylate for about 1 h at room temperature. The brains were then mounted in Permount (Fisher Scientific) between two cover slips with ten reinforcement rings (Avery, Toronto, Canada) as spacers. Finally, they were imaged using a confocal microscope (Leica TCS SP8, Wetzlar, Germany) with a 10x air objective (HCX PL-Apo 10x/0.4 CS, Leica).

Data analysis

To consider a neuron for analysis, the following criteria had to be fulfilled: *i.* stable baseline during stimulus presentation, *ii.* spike amplitudes clearly above noise level and *iii.* distinct immunolabeling of the recorded neuron. If a neuron passed these criteria, the recorded file was imported into MATLAB for further analysis via custom-written scripts that included the CircStat toolbox (Berens, 2009). Events during stimulation were detected based on a manually set threshold and were assigned to a particular polarization angle during the polarizer rotation or to a corresponding azimuthal angle during circling of a light spot. Neuronal spiking rates were estimated by low-pass filtering the instantaneous firing rate of the action potentials and illustrated as sliding window averages (Gaussian filtered, window size: 0.5 s) in the results.

The preferred angles in response to the stimuli were determined as the mean vector of the bimodal (polarized light) or unimodal (sun stimulus) distribution of stimulus angles at the times of action potentials. The degree, to which the action potentials were clustered at this angular position, was defined as the vector strength. This value ranges from 0 to 1, with higher values indicating more directed responses

In addition to the aforementioned parameters, responses of each trial were binned into 18 bins and spike rate in each bin was calculated. This was used to obtain the modulation strength as described by Labhart (1996) using the following equation:

$$M = \sum_{i=1}^{18} |n_i - \bar{n}|$$

where n is the spiking rate (in spikes/s) and $\overline{n}$ is the average spiking rate over the whole stimulation period. The higher the modulation strength, the stronger is the response of a neuron to a certain stimulus.

To predict the neuronal response to a combination of stimuli and to define the relevance of each cue on the neuronal coding, a weighted linear model was applied. This was based on the responses of the same neuron to the individual stimuli using the following equation:

$$y = r_1 \cdot w + r_2 \cdot (1 - w)$$

where r_1 and r_2 describe the actual response of a neuron to an individual stimulus (e.g., sun stimulus and polarized light for the combined celestial stimuli condition), respectively and w indicates the weighting of them. If $w < 0.5$, the response of r_2 is weighted higher, while $w < 0.5$ indicates that the neuronal response of r_1 dominates the response. To identify the weighting that matches best the actual neuronal response to the combination of both stimuli, we calculated the correlation between the actual neuronal response and the modeled neuronal responses based on different linear weightings. The weighting that exhibited the highest correlation coefficient, was then considered for further analysis.

As we did not have any prediction of whether and how the TL neurons respond to the panoramic skyline, we used the inter-trial difference between single stimulus presentations as reference. Inter-trial differences were determined by treating clock- and counterclockwise responses separately. At first neuronal responses were grouped based on the stimulus rotation. Then, for both rotation directions, we calculated the mean neuronal response and correlated them with the response from each trial. Finally, the correlation coefficients were averaged

within and then across rotation groups. The closer the correlation were to unity, the more similar were the neuronal responses across trials. To quantify the neuronal response to the panoramic skyline further, the averaged neuronal response for clock- and counterclockwise rotations was compared with the response to the flat panorama during a 6 s time frame. Both correlation values were averaged across rotation groups again. If the neurons encoded parts of the panoramic skyline, we expected that the neuronal response to the panoramic skyline and the response to the flat panorama correlate less with each other than the neuronal responses across trials.

To further characterize the response of the TL cells to the panoramic skyline, we applied an intensity-based model for different elevations. Circular, excitatory TL neurons' receptive fields were modeled by a Gaussian Kernel (11.5° width ± 2.9° standard deviation, corresponding to 5 pixels width and 2 pixels standard deviation of the arena) in MATLAB. This receptive field size is in a similar range as the excitatory component of measured locust TL neuron receptive fields (Takahashi et al. 2022). When the scene is rotated around the animal, this evokes changes in brightness in the modeled receptive field that are correlated with the silhouette of the panorama. Thus, if a bright sector of the panorama moves through the receptive field, it increases the spiking activity. In turn, if a dark sector of the panorama is moved through the receptive field, it will decrease the spiking activity. However, this change in spiking activity depends on the elevation of the receptive fields (Fig. 3E), which may vary in monarch butterfly TL neurons, as shown for the homologous neurons in fruit flies (Seelig and Jayaraman, 2013). To reliably test if the TL neurons respond to the panoramic skyline, we defined each row of the LED arena between -16.1° and 16.1° as the center of a possible receptive field and modeled curves of the predicted neuronal modulation at different elevations when the panorama was rotated. To find the best match between the modeled response and the recorded neuronal response at different elevations, we calculated for the modeled responses at each elevation the cross correlation with the measured neuronal response. The modeled curve that exhibited the best match to the recorded neuronal response curve was included for further analysis.

Statistics

To identify whether action potentials in response to the simulated celestial cues are non-uniformly distributed, we applied the Rayleigh-test (significance level <0.05). To test whether the preferred directions are significantly clustered around the 0°-180° axis (polarized light) and around 90° (sun stimulus), we used the V-test (significance level <0.05). To test for normal distribution and similar variances of the modulation strengths, the Shapiro-Wilk test and the Levene-test were employed, respectively. If data were normally distributed and exhibited the same variance, parametric hypothesis tests were applied (unpaired t-test and paired t-test, respectively). Otherwise, non-parametric tests were used (Wilcoxon-rank-sum-test for unpaired and the Wilcoxon signed rank test for paired mean values). For partially paired data, like the observed weighting factors, a mixed linear model was used to test if the mean values differed significantly between the two test groups. Averaged parameters are shown as mean ± standard deviation if not mentioned otherwise.

Results

To understand how the monarch butterfly compass integrates multiple visual stimuli, we presented different visual stimuli in isolation and in combination to the animals while recording intracellularly from TL neurons of the central complex (Fig. 1A,B). We successfully obtained recordings from 34 TL-neurons. 15 TL-neurons were tested with a combination of different celestial stimuli and 19 TL-neurons with a combination of celestial and terrestrial wide field stimuli. Of the latter group, all TL cells were tested with the panoramic skyline, 15 of them were exposed long enough to the flat panorama to be included in the inter-trial response analyses and 13 of them were presented the combined sun stimulus and panoramic skyline.

Celestial cue integration in TL neurons

We first tested the neuronal tuning to simulated celestial cues. Similar to previous experiments (Heinze and Reppert, 2011; Nguyen et al., 2021; Beetz et al., 2022), a moving green light spot served as a sun stimulus while a rotating polarizer illuminated by UV light from the zenith was used to examine polarization sensitivity (Fig. 1C). To simulate the natural spatial relationship between the sun and polarized light, we oriented the polarization angle perpendicular to the sun-stimulus direction (Fig. 1C). As expected from previous experiments (Heinze and Reppert, 2011; Nguyen et al., 2021), TL neurons responded to both the sun stimulus and polarized light (Fig. 1D, left and middle graph). Interestingly, the highest action potential rates (preferred

directions, ϕ_{max}) of the TL neuron to the sun stimulus and the polarization stimulus matched the 90°-relationship of the cues in nature. To investigate if this was true for all recorded TL cells, we analyzed the spatial distribution of the preferred directions (ϕ_{max}) in response to the sun stimulus. The preferred directions to the sun stimulus were clustered around 90° in response to the sun stimulus ($p = 0.008$, $v = 5.43$; V-test; $n = 10$; Fig. 1E, left) and along the 0° - 180° axis in response to polarized light ($p = 0.03$, $v = 4.37$; V-test; $n = 10$; V-test; Fig. 1E, right). Taken together, the spatial relationship between the mean preferred directions of the recorded TL neurons when presenting sun and polarization stimulus in isolation matched the natural spatial relationship between both celestial cues.

When we presented both stimuli simultaneously, the neuronal tuning resembled a mixed response (Fig. 1D, right graph), suggesting that TL neurons integrate both stimuli in a weighted manner. To quantify which of the two stimuli dominated the neuronal response, we compared the modulation strengths in response to the single stimuli (sun stimulus *or* polarized light) with the modulation strengths of the same neurons in response to the combined stimulus (sun stimulus *and* polarized light). The modulation strength in response to the sun stimulus (62.48 ± 37.05, $n = 10$) was significantly weaker than the modulation strength of the same neurons to the polarization stimulus (89.81 ± 48.64, $n = 10$; $p = 0.02$, $t = 2.99$; paired t-test) and to the combination of the stimuli (98.90 ± 48.43, $n = 10$; $p = 0.002$, $t = -4.38$; paired t-test; Fig. 1F). The modulation strength did not differ between the response to the polarizer and to the combination of the stimuli ($p = 0.23$, $t = -1.28$; paired t-test). This indicates that the polarization input is weighted stronger than the sun-stimulus input and that the response to the combined celestial cues seems to be mainly shaped by the polarization input.

Weighting of celestial cues in TL neurons

To quantify whether polarized light truly dominates the response to the combined celestial cues and how they are weighted in TL neurons, we combined the responses to the isolated stimuli (Fig. 2A, upper plot) in a weighted linear model and calculated a predicted response to the combined stimuli. By varying the weight between the neuronal response to the polarizer and sun stimulus, we modeled different expected neuronal responses to the combined stimuli and correlated these modeled responses with the actual response to the combined stimuli (Fig. 2A, blue curve of lower plot). The modeled response with the highest similarity to the actual neuronal response (Fig. 2A, red curve of lower plot) was selected to determine the neuron-specific cue weighting. A weighting factor of 0 indicated that the combined response was

entirely characterized by the sun stimulus while a weighting of 1 represented a tuning that was purely described by the polarization input.

For all neurons, the correlation coefficients obtained through the comparison of the modeled and actual neuronal response were relatively high (Fig. 2B, inset in upper histogram, 0.86 ± 0.12, n = 10), suggesting that the response of TL neurons to the combined celestial stimuli can be well described by the weighted linear model. When presenting sun stimulus and polarized light simultaneously, most TL cells responded stronger to the polarization information (Fig. 2B, upper histogram), although the light intensity of the stimuli was set to the same photon flux. The bias towards the polarization stimulus may be induced by differences in the absolute sensitivity of the UV and green photoreceptors in the monarch butterfly eye. Thus, we assumed that the UV polarization stimulus may appear brighter to the butterflies than the green sun stimulus due to a higher sensitivity of the photoreceptors to UV light. To test whether this may explain the dominance of the polarization stimulus on the neuronal response to the combined stimuli, we repeated the experiments with a UV sun stimulus that had the same photon flux as the UV polarization stimulus (Fig. 2C). Again, except for one neuron, the weighted linear model described the actual neuronal response well (Fig. 2B, inset in lower histogram; 0.77 ± 0.28, n = 12), which further confirms that celestial information is linearly integrated in TL neurons. In contrast to the trials with the green sun stimulus and polarized light, the weighting to the combined UV stimuli shifted in favor of the UV sun stimulus (Fig. 2B, lower histogram). The observed weightings differed significantly between the experiments with the green sun stimulus and polarized light (0.65 ± 0.28, n = 10) and the UV sun stimulus and polarized light (0.30 ± 0.23, n = 12; $p < 0.001$, $F = 113.31$; ANOVA, Fig. 2B, boxplots). Taken together, our data show that TL neurons combine celestial cues linearly in monarch butterflies. However, the weighting between the sun and polarization input is highly affected by the spectral content and relative brightness of the presented stimuli.

TL neurons are tuned to a panoramic skyline

In addition to celestial cues, recent experiments in *Drosophila melanogaster* suggest that central-complex neurons encode the entire visual scenery around the animal (Seelig and Jayaraman, 2015; Kim et al., 2019). One salient cue in a visual scene that can be used by many insects for orientation is the profile of a panoramic skyline (Graham and Cheng, 2009; Reid et al., 2011; Legge et al., 2014; Franzke et al., 2020). In contrast to the sun and polarized skylight, coding a panoramic skyline neuronally is more complex as the neurons need to integrate information from different azimuths and elevations to precisely reproduce the silhouette of the

panoramic skyline (Dewar et al. 2017). To grasp how the monarch butterfly central complex encodes a panoramic skyline, we placed the butterflies at the center of an LED arena and recorded the neuronal activity of TL neurons while the animals were exposed to a panoramic skyline that was presented at the inner surface of the LED arena. We used the same panoramic skyline that has recently been used to study the monarch butterfly orientation behavior (Franzke et al., 2020; Fig. 3A). When we rotated the scene around the butterflies, we found that many TL neurons were modulated by the panoramic stimulus (Fig. 3B). To exclude that these modulations occurred spontaneously, we analyzed the inter-trial variability of the neuronal activity and correlated the neuronal activity in response to each trial (Fig. 3B, *grey curves*) with the averaged response (Fig. 3B, *orange curve*). As a control, the neuronal responses of the same TL neurons to a flat panorama (Fig. 3C) were correlated to the averaged response to the panoramic skyline. Neuronal responses to the panoramic skyline across trials were highly correlated with their averaged response (Fig. 3D, upper plot) indicating a low inter-trial variability and that the neuronal modulations occurred in response to the rotating panoramic skyline. In contrast, the neuronal activity in the presence of the flat panorama was poorly correlated with the averaged response to the panoramic skyline (Fig. 3D, lower plot). The correlation coefficients between inter-trial responses and the averaged response to the panoramic skyline were significantly higher (0.76 ± 0.07) than to the responses to the flat panorama and the averaged responses to the panoramic skyline (-0.02 ± 0.29; $p < 0.001$, sign rank = 120, Wilcoxon signed rank test, Fig. 3D). This demonstrates that monarch butterfly TL neurons encode, in addition to celestial cues, panoramic skylines.

Although it is not trivial to predict the TL response to the presented panoramic skyline, we noticed that the modulation of the spiking activity seemed to correlate negatively with the troughs of the profile (Fig. 3B), suggesting that they are tuned to changes in brightness during the stimulus rotation. To investigate this hypothesis, we modeled the neuronal responses for fictive TL cells whose neuronal tunings were based on changes in brightness during stimulus rotations. As the receptive fields of the TL neurons can cover patches of different elevations and azimuths (Seelig and Jayaraman, 2013; Takahashi et al., 2022), we varied both the azimuth and elevation (between -16.1° and +16.1°) of the center of the modeled neuron's receptive field (Fig. 3E). For each of the modeled responses (Figure 3F, *blue curves*), we calculated its cross correlations with the measured neuronal TL response (Figure 3F, *orange curves*). If TL neurons encoded changes in brightness associated with rotations of the panoramic skyline, we expected that one of the modeled neuronal responses will align well with the measured neuronal

response. Indeed, most measured neuronal responses correlated well with one of the modeled TL responses (Fig. 3G). Not surprising, they showed the highest correlation at elevation values between -10.75° and +10.75°. In addition, cross correlations allowed us to calculate the azimuthal panorama position that gave the strongest neuronal response. The angular shifts between the measured and modeled TL response leading to the highest correlation coefficient clustered in the anterior field of the animals ($p = 0.045$; $Z = 3.06$, $n = 19$, Rayleigh test; Fig. 3H).

Weighting of the sun and panoramic scene in TL neurons

We next wondered how TL neurons encode a visual scene that was composed of a simulated sun and the panoramic skyline. As demonstrated in the example TL neuron, the moving sun stimulus mainly dominated the neuronal response, irrespective of the absence/presence of the panoramic skyline (Fig. 4A, B), but the modulation of the panoramic profile was additionally encoded in the neuronal response of the TL neuron (arrow in Fig. 4B). To test whether the TL neurons combine both stimuli in a linear manner, as shown for the celestial cues, we also tested the same neurons' responses to the single stimuli. As expected, the TL neurons responded to the sun stimulus (Fig. 4C, *green curve*) and the panoramic scene (Fig. 4C, *orange curve*), when presented individually. Again, we used the neuronal tuning to the single stimuli to model the expected response of the TL neurons to a combined – sun and panorama – stimulus presentation. We then used the modeled neuronal response based on the weighted linear model (Fig. 4C, *red curve*) and correlated it with the measured neuronal response to both stimuli (Fig. 4C, *blue curve*). In contrast to the results for the combined celestial cues (Fig. 2), the weighted linear model did not always result in high correlation values with the measured responses (Fig. 4D, inset, 0.55 ± 0.29, $n = 13$). For five of the 13 TL neurons (correlation coefficient < 0.5; Fig. 4D, inset), the neuronal response to the combined celestial and terrestrial cue, i.e., panoramic skyline, could not be explained with a linear model. The predicted weighting factors were highly variable. While responses of some TL neurons were dominated by the sun stimulus (weight < 0.5; Fig. 4D), responses of other TL neurons were more dominated by the panoramic skyline (weight > 0.5; Fig. 4D). Taken together, we found a high variance of neuronal coding in cue hierarchy between the sun and the panoramic skyline. This stands in contrast to the results observed with the sun stimulus and the polarized light. Although we were not able to define from which TL subtype we obtained our recordings (see discussion), the results indicate that the cue hierarchy between celestial and terrestrial cues shows a high inter-individual flexibility in monarch butterflies.

Discussion

We show that the monarch butterfly CX integrates multiple visual cues, i.e., celestial and terrestrial panoramic skyline cues for orientation. While the sun stimulus and polarized light were integrated linearly, the coding of the sun stimulus and the panoramic skyline did not always match a linear summation of the neuronal response to the isolated stimuli. Moreover, while polarized light was usually weighted stronger than the green sun stimulus, the weighting of the sun versus the panorama stimulus was set in a variable manner across different TL neurons. This observation is in line with behavioral results on monarch butterflies tested within the same visual setting and might allow the butterflies to set the cue preference in a highly flexible manner between celestial and terrestrial cues (Franzke et al., 2020).

Celestial coding in the central complex

Monarch butterfly TL neurons are sensitive to polarized light (Heinze and Reppert, 2011; Nguyen et al. 2021, this work), similar to what has been reported for TL cells of a wide range of other insects, including desert locusts (Vitzthum et al., 2002, Heinze et al., 2009, Bockhorst et al., 2015, Pegel et al., 2018; Takahashi et al. 2022), field crickets (Sakura et al., 2008), dung beetles (el Jundi et al., 2015), sweat bees (Stone et al., 2019), and fruit flies (Hardcastle et al., 2021). In addition to polarized light, TL neurons in the present study were tuned to a green light spot – likely representing the sun. As we used the responsiveness to the polarization stimulus to physiologically identify the neurons, we might have missed TL neurons that were solely tuned to the sun stimulus. However, the here recorded TL neurons are suitable to combine information from the sun and the pattern of polarized light similar to what has been shown in TL-neurons in desert locusts (Pegel et al., 2018; Takahashi et al. 2022) and dung beetles (el Jundi et al., 2015), as well as in previous experiments in monarch butterflies (Heinze and Reppert, 2011; Nguyen et al., 2021). Thus, the TL neuron sensitivity to celestial cues is highly conserved and may play a crucial role for the heading coding in a variety of insects. How the TL neurons' gain to visual cues is further affected by an animal's locomotor state, as shown for the corresponding neurons in fruit flies (Seelig and Jayaraman, 2013) and as suggested by a recent study on monarch butterflies (Beetz et al. 2022), awaits to be explored.

We found a fixed spatial relationship between the preferred firing direction to the sun stimulus and the polarization stimulus. The clustering of the preferred sun-stimulus directions to the butterflies' right side is likely a result of a bias in recordings from the right brain hemisphere (at least six out of ten recordings were obtained from right TL neurons). Thus, these cells

receive likely visual input from the ipsilateral eye which is well in line with previous recordings from these compass neurons (Heinze and Reppert, 2011). Interestingly, we found that the preferred polarization directions of the same TL neurons were significantly aligned with the animals' longitudinal body axis which is at odds with a previous study (Heinze and Reppert, 2011). This resulted in an orthogonal relationship between the mean preferred sun and polarization directions, which parallels the 90°-relationship between the sun and polarization pattern in nature, an aspect that has also been reported in desert locust TL (Pegel et al., 2018) and optic lobe neurons (el Jundi et al., 2011). The bias in preferred polarization directions found in our TL neurons could thus be a consequence of a neuronal matched filter for celestial cues, allowing the butterflies to derive the same directional information from different celestial inputs.

Pegel et al. (2019) showed that the preferred directions to the sun stimulus differ between the three TL subtypes (TL2a, TL2b, TL3) in desert locusts. The monarch butterfly TL neurons can also be divided anatomically into three subtypes that innervate different layers in the lower division of the central body (Heinze et al., 2013). Unfortunately, we were not able to define from which subtype we performed our recordings as we often co-stained several TL subtypes in one experiment. As shown previously, monarch butterfly compass neurons show the same preferred firing direction, irrespective of the spectral information of the light stimulus (Heinze and Reppert, 2011; Nguyen et al., 2021). However, recordings from compass neurons in the desert locust suggest that the spectral influence on the preferred firing direction is strongly sensitive to the light intensity of the stimuli (Kinoshita et al., 2007; Pfeiffer and Homberg, 2007). It is therefore crucial to study the response characteristics of TL neurons to spectral cues at different light intensities in the future to shed light on how the monarch butterfly compass network may integrate different celestial cues into the central complex and how this represents the celestial cue hierarchy exhibited behaviorally.

Integration of the panoramic skyline in the central complex

In previous experiments, the sensitivity of TL cells has been studied with respect to vertical stripes (Omoto et al., 2017; Bockhorst and Homberg, 2017; Fisher et al., 2019), grating patterns (Rosner et al., 2019) or small light spots (Seelig and Jayaraman, 2013) in insects. We here found that TL neurons were sensitive to a simulated panoramic skyline by responding to changes in brightness while the panorama was rotated around the animal. As we only tested the response of the monarch TL neurons to one distinct panoramic scene, it has yet to be identified how modifying the frequency and amplitude of the panorama's profile will affect the

tuning of the TL neurons. We chose this specific panoramic skyline as a recent behavioral study showed that monarch butterflies are able to use this setting to sustain a directed flight course (Franzke et al., 2020). However, as their orientation performance was indistinguishable from a flight stabilization strategy, it was unclear whether the butterflies can employ compass orientation with respect to a panoramic scene. Although our data do not exclude the possibility that TL neurons transfer motion information to the central complex, our data indicate that the central complex receives visual compass information of the panoramic scene. This suggests that monarch butterflies can use a panoramic skyline as a compass cue to compute a heading with respect to it, which parallels behavioral results from Australian desert ants that can use a panorama to calculate a heading direction (Graham and Cheng, 2009). The structure and relative position of the receptive fields of the TL neurons studied with the panoramic scene are difficult to predict due to the complex nature of the stimulus. Exploring this requires to additionally map their receptive fields with respect to a small visual stimulus (Seelig and Jayaraman 2013), an aspect that was not feasible due to the short recording times of our intracellular recordings. Rather than encoding the current heading, the TL neurons seem to convey visual information into the insect compass, similar to the *Drosophila* ring neurons (Seelig and Jayaraman, 2013; Dewar et al., 2017). In both monarch butterflies and fruit flies, they synapse on a population of neurons termed CL1 neurons (Heinze et al., 2013), called EP-G cells in fruit flies, which likely represent a distinct heading direction within a visual scene based on multimodal information (Seelig and Jayaraman, 2015; Kim et al., 2019; Turner-Evans et al., 2020; Beetz et al., 2022). How monarch butterfly CL1 cells compute a heading based on terrestrial information from TL cells awaits to be answered through neuronal recordings during flight as the coding strongly depends on the animal's locomotory state (Beetz et al., 2022).

Flexible weighting between celestial and terrestrial information

When we presented the sun and polarization stimulus simultaneously to the butterflies, the TL neurons combined these cues in a linear manner. These results differ from the dung beetle TL neurons (el Jundi et al., 2015) but are in line with desert locust columnar CX-neurons (Pegel et al., 2019). The polarization UV stimulus was consistently ranked higher than the green sun stimulus in TL neurons in monarch butterflies when presented with a similar relative light intensity. When we presented a UV light spot instead of a green one, the unpolarized light stimulus dominated the neuronal tuning. This switch in cue preference was likely not a result of a change in wavelength but rather a consequence of a change in relative intensity of light, which is in line with the stronger response of TL neurons to UV light than to green light

(Nguyen et al., 2021). Thus, as the sun is several magnitudes brighter than the remaining sky in nature, it is likely the dominant cue being encoded in TL neurons under a real sky.

In general, the weighting between the simulated sun and polarized light was very similar across different TL neurons. This low variability in cue preference between TL neurons recorded in different monarch butterflies was similar to what has been found for TL neurons in dung beetles (el Jundi et al., 2015) and suggests that the weighting of celestial cues is determined at an early processing stage in the brain, such as at the level of the photoreceptors. In contrast, the simulated sun and the panoramic skyline were not always linearly integrated in the monarch butterfly central complex. Moreover, the cue preference was highly variable, which is well in line with the high inter-individual difference in the behavioral use of these cues for orientation in a flight simulator (Franzke et al., 2020). This high flexibility indicates that the weighting might not only be set based on the sensitivity of the inputs at the butterfly's eye but might additionally be adjusted at later stages in the brain network. This would allow a high inter-individual difference in weighting that is based on the animal's internal state, as well as its experience.

Author contributions

Study design: TATN, CM, KP, BeJ. Conducting experiments: TATN. Analysis of data: TATN. Interpretation of data: TATN, MJB, CM, KP, BeJ. Drafting of the manuscript: TATN, BeJ. Critical review of the manuscript: MJB, CM, KP. Acquired Funding: BeJ. All authors approved of the final version of the manuscript.

Competing interests

The authors declare no competing interests.

Funding

This work was supported by the Emmy Noether program of the Deutsche Forschungsgemeinschaft granted to BeJ (GZ: EL784/1-1) and a DFG Grant to KP (PF714/5-1).

Acknowledgments

We thank Dr. James Foster for fruitful comments on our analysis and Kolja Richter and Konrad Öchsner for their help in developing the LED arena. We thank Samantha Iiams, Aldrin Lugena, Guijun Wan and Ying Zhang for their help in capturing monarch butterflies and for checking them for *Ophryocystis elektroscirrha*. In addition, we would like to thank Sergio Siles and Marie Gerlinde Blaese (butterflyfarm.co.cr) for providing us with monarch butterfly pupae.

References

Beetz, M. J., Kraus, C., Franzke, M., Dreyer, D., Strube-Bloss, M. F., Roessler, W., Warrant, E. J., Merlin, C. and el Jundi, B. (2022). Flight-induced compass representation in the monarch butterfly heading network. *Curr. Biol.* 32, 338—349. doi: 10.1016/j.cub.2021.11.009

Berens, P. (2009). CircStat: A MATLAB toolbox for circular statistics. *J. Stat. Softw.* 31, 1—21. doi: 10.18637/jss.v031.i10

Bockhorst, T. and Homberg, U. (2015). Amplitude and dynamics of polarization-plane signaling in the central complex of the locust brain. *J. Neurophysiol.* 113, 3291—3311. doi: 10.1152/jn.00742.2014

Bockhorst, T. and Homberg, U. (2017). Interaction of compass sensing and object-motion detection in the locust central complex. *J. Neurophysiol.* 118, 496—506. doi: 10.1152/jn.00927.2016

Brines, M. L. and Gould, J. L. (1979). Bees have rules. *Science* 206, 571-3. doi: 10.1126/science.206.4418.571

Dacke, M., Baird, E., el Jundi, B., Warrant, E. J. and Byrne, M. (2021). How dung beetles steer straight. *Ann. Rev. Entomol.* 66, 243—256. doi: 10.1146/annurev-ento-042020-102149

Dewar, A. D. M., Wystrach, A., Phillippides, A. and Graham, P. (2017) Neural coding in the visual system of *Drosophila melanogaster*: How do small neural populations support visually guided behaviours? *PLoS Comput. Biol.* 13, e1005735. doi: 10.1371/journal.pcbi.1005735

Dreyer, D., el Jundi, B., Kishkinev, D., Suchentrunk, C., Campostrini, L., Frost, B. J., Zechmeister, T. and Warrant, E. J. (2018a). Evidence for a southward autumn migration of nocturnal noctuid moths in central Europe. *J. Exp. Biol.* 221, jeb179218. doi: 10.1242/jeb.179218

Dreyer, D., Frost, B., Mouritsen, H., Gunther, A., Green, K., Whitehouse, M., Johnsen, S., Heinze, S. and Warrant, E. (2018b). The Earth's magnetic field and visual landmarks steer migratory flight behavior in the nocturnal Australian bogong moth. *Curr. Biol.* 28, 2160—2166. doi: 10.1016/j.cub.2018.05.030

Edrich, W., Neumeyer, C. and von Heiversen, O. (1979). “Anti-sun orientation” of bees with regard to a field of ultraviolet light. *J. Comp. Physiol.* 134, 151—157. doi: 10.1007/BF00610473

el Jundi, B., Pfeiffer, K. and Homberg, U. (2011). A distinct layer of the medulla integrates sky compass signals in the brain of an insect. *PLoS One* 6, e27855. doi: 10.1371/journal.pone.0027855

el Jundi, B., Smolka, J., Baird, E., Byrne, M. J. and Dacke, M. (2014). Diurnal dung beetles use the intensity gradient and the polarization pattern of the sky for orientation. *J. Exp. Biol.* 217, 2422—2429. doi: 10.1242/jeb.101154

el Jundi, B., Warrant, E. J., Byrne, M. J., Khaldy, L., Baird, E., Smolka, J. and Dacke, M. (2015). Neural coding underlying the cue preference for celestial orientation. *Proc. Natl. Acad. Sci. U. S. A.* 112, 11395—11400. Doi: 10.1073/pnas.1501272112

el Jundi, B., Warrant, E. J., Pfeiffer, K. and Dacke, M. (2018). Neuroarchitecture of the dung beetle central complex. *J. Comp. Neurol.* 526, 2612—2630. doi: 10.1002/cne.24520

el Jundi, B., Baird, E., Byrne, M. J. and Dacke, M. (2019). The brain behind straight-line orientation in dung beetles. *J. Exp. Biol.* 222, jeb192450. doi: 10.1242/jeb.192450

Fisher, Y. E., Lu, J., D'Alessandro, I. and Wilson, R. I. (2019). Sensorimotor experience remaps visual input to a heading-direction network. *Nature* 576, 121—125. doi: 10.1038/s41586-019-1772-4

Franzke, M., Kraus, C., Dreyer, D., Pfeiffer, K., Beetz, M. J., Stöckl, A. L., Foster, J. J., Warrant, E. J. and el Jundi, B. (2020). Spatial orientation based on multiple visual cues in non-migratory monarch butterflies. *J. Exp. Biol.* 223, 1—12. doi: 10.1242/jeb.223800

Graham, P. and Cheng, K. (2009a). Ants use the panoramic skyline as a visual cue during navigation. *Curr. Biol.* 19, R935—R937. doi: 10.1016/j.cub.2009.08.015

Graham, P. and Cheng, K. (2009b). Which portion of the natural panorama is used for view-based navigation in the Australian desert ant? *J. Comp. Physiol. A* 195, 681—689. doi: 10.1007/s00359-009-0443-6

Green, J., Adachi, A., Shah, K. K., Hirokawa, J. D., Magani, P. S. and Maimon, G. (2017). A neural circuit architecture for angular integration in *Drosophila*. *Nature* 546, 101—106. doi: 10.1038/nature22343

Guerra, P. A., Merlin, C., Gegear, R. J. and Reppert, S. M. (2012). Discordant timing between antennae disrupts sun compass orientation in migratory monarch butterflies. *Nat. Comm.* 3, 958. doi: 10.1038/ncomms1965

Hardcastle, B. J., Omoto, J. J., Kandimalla, P., Nguyen, B. M., Keleş, M. F., Boyd, N. K., Hartenstein, V. and Frye, M. A. (2021). A visual pathway for skylight polarization processing in *Drosophila*. *Elife* 10, e63225. doi: 10.7554/eLife.63225

Heinze, S., Florman, J., Asokaraj, S., el Jundi, B. and Reppert, S. M. (2013). Anatomical basis of sun compass navigation II: the neuronal composition of the central complex of the monarch butterfly. *J. Comp. Neurol.* 521, 267—98. doi: 10.1002/cne.23214

Heinze, S., Gotthardt, S. and Homberg, U. (2009). Transformation of polarized light information in the central complex of the locust. *J. Neurosci.* 29, 11783—11793. doi: 10.1523/JNEUROSCI.1870-09.2009

Heinze, S. and Homberg, U. (2008). Neuroarchitecture of the central complex of the desert locust: Intrinsic and columnar neurons. *J. Comp. Neurol.* 511, 454—478. doi: 10.1002/cne.21842

Heinze, S. and Reppert, S. M. (2011). Sun compass integration of skylight cues in migratory monarch butterflies. *Neuron* 69, 345—358. doi: 10.1016/j.neuron.2010.12.025

Held, M., Berz, A., Hensgen, R., Muenz, T. S., Scholl, C., Roessler, W., Homberg, U. and Pfeiffer, K. (2016). Microglomerular synaptic complexes in the sky-compass network of the honeybee connect parallel pathways from the anterior optic tubercle to the central complex. *Front. Behav Neurosci.* 10, 91—105. doi: 10.3389/fnbeh.2016.00186

Hensgen, R., England, L., Homberg, U. and Pfeiffer, K. (2020). Neuroarchitecture of the central complex in the brain of the honeybee: Neuronal cell types. *J. Comp. Neurol.*, 1-28. doi: 10.1002/cne.24941

Homberg, U. (2015). Sky compass orientation in desert locusts—Evidence from field and laboratory studies. *Front. Behav. Neurosci.* 9, 346. doi: 10.3389/fnbeh.2015.00346

Hulse, B. K., Haberkern, H., Franconville, R., Turner-Evans, D. B., Takemura, S.-y., Wolff, T., Noorman, M., Dreher, M., Dan, C., Parekh, R. et al. (2021). A connectome of the Drosophila central complex reveals network motifs suitable for flexible navigation and context-dependent action selection. Elife 10, e66039.

Kim, S. S., Hermundstad, A. M., Romani, S., Abbott, L. F. and Jayaraman, V. (2019). Generation of stable heading representations in diverse visual scenes. *Nature* 576, 126—131. doi: 10.1038/s41586-019-1767-1

Kinoshita, M., Pfeiffer, K. and Homberg, U. (2007). Spectral properties of identified polarized-light sensitive interneurons in the brain of the desert locust *Schistocerca gregaria*. *J. Exp. Biol.* 210, 1350—1361. doi: 10.1242/jeb.02744

Labhart, T. (1996). How polarization-sensitive interneurones of crickets perform at low degrees of polarization. *J. Exp. Biol.* 199, 1467—1475. doi: 10.1242/jeb.199.7.1467

Lebhardt, F. and Ronacher, B. (2014). Interactions of the polarization and the sun compass in path integration of desert ants. *J. Comp. Physiol. A* 200, 711—720. doi: 10.1007/s00359-013-0871-1

Legge, E. L., Wystrach, A., Spetch, M. L. and Cheng, K. (2014). Combining sky and earth: desert ants (*Melophorus bagoti*) show weighted integration of celestial and terrestrial cues. *J. Exp. Biol.* 217, 4159—4166. doi: 10.1242/jeb.107862

Merlin, C., Gegear, R. J. and Reppert, S. M. (2009). Antennal circadian clocks coordinate sun compass orientation in migratory monarch butterflies. *Science* 325, 1700-4. doi: 10.1126/science.1176221

Merlin, C., Heinze, S. and Reppert, S. M. (2012). Unraveling navigational strategies in migratory insects. *Curr. Opin. Neurobiol.* 22, 353—361. doi: 10.1016/j.conb.2011.11.009

Merlin, C. and Liedvogel, M. (2019). The genetics and epigenetics of animal migration and orientation: birds, butterflies and beyond. *J. Exp. Biol.* 222, jeb191890. doi: 10.1242/jeb.191890

Nguyen, T. A. T., Beetz, M. J., Merlin, C. and el Jundi, B. (2021). Sun compass neurons are tuned to migratory orientation in monarch butterflies. *Proc. Biol. Sci.* 288, 20202988. doi: 10.1098/rspb.2020.2988

Okubo, T. S., Patella, P., D'Alessandro, I. and Wilson, R. I. (2020). A neural network for wind-guided compass navigation. *Neuron* 107, 924—940 e18. doi: 10.1016/j.neuron.2020.06.022

Pegel, U., Pfeiffer, K. and Homberg, U. (2018). Integration of celestial compass cues in the central complex of the locust brain. *J. Exp. Biol.* 221, jeb171207. doi: 10.1242/jeb.171207

Pegel, U., Pfeiffer, K., Zittrell, F., Scholtyssek, C. and Homberg, U. (2019). Two Compasses in the Central Complex of the Locust Brain. *J. Neurosci.* 39, 3070—3080. doi: 10.1523/JNEUROSCI.0940-18.2019

Pfeiffer, K. and Homberg, U. (2007). Coding of azimuthal directions via time-compensated combination of celestial compass cues. *Curr. Biol.* 17, 960—965. doi: 10.1016/j.cub.2007.04.059

Reid, S. F., Narendra, A., Hemmi, J. M. and Zeil, J. (2011). Polarised skylight and the landmark panorama provide night-active bull ants with compass information during route following. *J. Exp. Biol.* 214, 363—370. doi: 10.1242/jeb.049338

Reppert, S. M., Zhu, H. and White, R. H. (2004). Polarized light helps monarch butterflies navigate. *Curr. Biol.* 14, 155—158. doi: 10.1016/j.cub.2003.12.034

Rosner, R., Pegel, U. and Homberg, U. (2019). Responses of compass neurons in the locust brain to visual motion and leg motor activity. *J. Exp. Biol.* 222, jeb196261. doi: 10.1242/jeb.196261

Rossel, S. and Wehner, R. (1984). Celestial orientation in bees: the use of spectral cues. *J. Comp. Physiol. A* 155, 605—613. doi:10.1007/BF00610846

Rother, L., Kraft, N., Smith, D. B., el Jundi, B., Gill, R. J. and Pfeiffer, K. (2021). A micro-CT-based standard brain atlas of the bumblebee. *Cell. Tissue Res.* 386, 29—45. doi: 10.1007/s00441-021-03482-z

Sakura, M., Lambrinos, D. and Labhart, T. (2008). Polarized skylight navigation in insects: model and electrophysiology of e-vector coding by neurons in the central complex. *J. Neurophysiol.* 99, 667—682. doi: 10.1152/jn.00784.2007

Sauman, I., Briscoe, A. D., Zhu, H., Shi, D., Froy, O., Stalleicken, J., Yuan, Q., Casselman, A. and Reppert, S. M. (2005). Connecting the navigational clock to sun compass input in monarch butterfly brain. *Neuron* 46, 457—467. doi: 10.1016/j.neuron.2005.03.014

Seelig, J. D. and Jayaraman, V. (2013). Feature detection and orientation tuning in the *Drosophila* central complex. *Nature* 503, 262—266. doi: 10.1038/nature12601

Seelig, J. D. and Jayaraman, V. (2015). Neural dynamics for landmark orientation and angular path integration. *Nature* 521, 186—191. doi: 10.1038/nature14446

Stalleicken, J., Labhart, T. and Mouritsen, H. (2006). Physiological characterization of the compound eye in monarch butterflies with focus on the dorsal rim area. *J. Comp. Physiol. A* 192, 321—331. doi: 10.1007/s00359-005-0073-6

Stalleicken, J., Mukhida, M., Labhart, T., Wehner, R., Frost, B. and Mouritsen, H. (2005). Do monarch butterflies use polarized skylight for migratory orientation? *J. Exp. Biol.* 208, 2399—408. doi: 10.1242/jeb.01613

Stone, T., Webb, B., Adden, A., Weddig, N. B., Honkanen, A., Templin, R., Wcislo, W., Scimeca, L., Warrant, E. and Heinze, S. (2017). An anatomically constrained model for path integration in the bee brain. *Curr. Biol.* 27, 3069—3085. doi: 10.1016/j.cub.2017.08.052

Takahashi, N., Zittrell, F., Hensgen, R. and Homberg, U. (2022). Receptive field structure for two celestial compass cues at the input stage of the central complex in the locust brain. *J. Exp. Biol,* jeb.243858. doi: 10.1242/jeb.243858

Towne, W. F. and Moscrip, H. (2008). The connection between landscapes and the solar ephemeris in honeybees. *J. Exp. Biol.* 211, 3729—36. doi: 10.1242/jeb.022970

Towne, W. F., Ritrovato, A. E., Esposto, A. and Brown, D. F. (2017). Honeybees use the skyline in orientation. *J. Exp. Biol.* 220, 2476—2485. doi: 10.1242/jeb.160002

Turner-Evans, D., Wegener, S., Rouault, H., Franconville, R., Wolff, T., Seelig, J. D., Druckmann, S. and Jayaraman, V. (2017). Angular velocity integration in a fly heading circuit. *Elife* 6, e23496. doi: 10.7554/eLife.23496

Turner-Evans, D. B., Jensen, K. T., Ali, S., Paterson, T., Sheridan, A., Ray, R. P., Wolff, T., Lauritzen, J. S., Rubin, G. M., Bock, D. D. et al. (2020). The neuroanatomical ultrastructure and function of a biological ring attractor. *Neuron* 108, 145—163. doi: 10.1016/j.neuron.2020.08.006

Vitzthum, H., Müller, M. and Homberg, U. (2002). Neurons of the central complex of the locust *Schistocerca gregaria* are sensitive to polarized light. *J. Neurosci.* 22, 1114. doi: 10.1523/JNEUROSCI.22-03-01114.2002

Wehner, R. (2003). Desert ant navigation: how miniature brains solve complex tasks. *J. Comp. Physiol. A* 189, 579—588. doi: 10.1007/s00359-003-0431-1

Wehner, R. and Müller, M. (2006). The significance of direct sunlight and polarized skylight in the ant's celestial system of navigation. *Proc. Natl. Acad. Sci. U. S. A.* 103, 12575—9. doi: 10.1073/pnas.0604430103

Figures

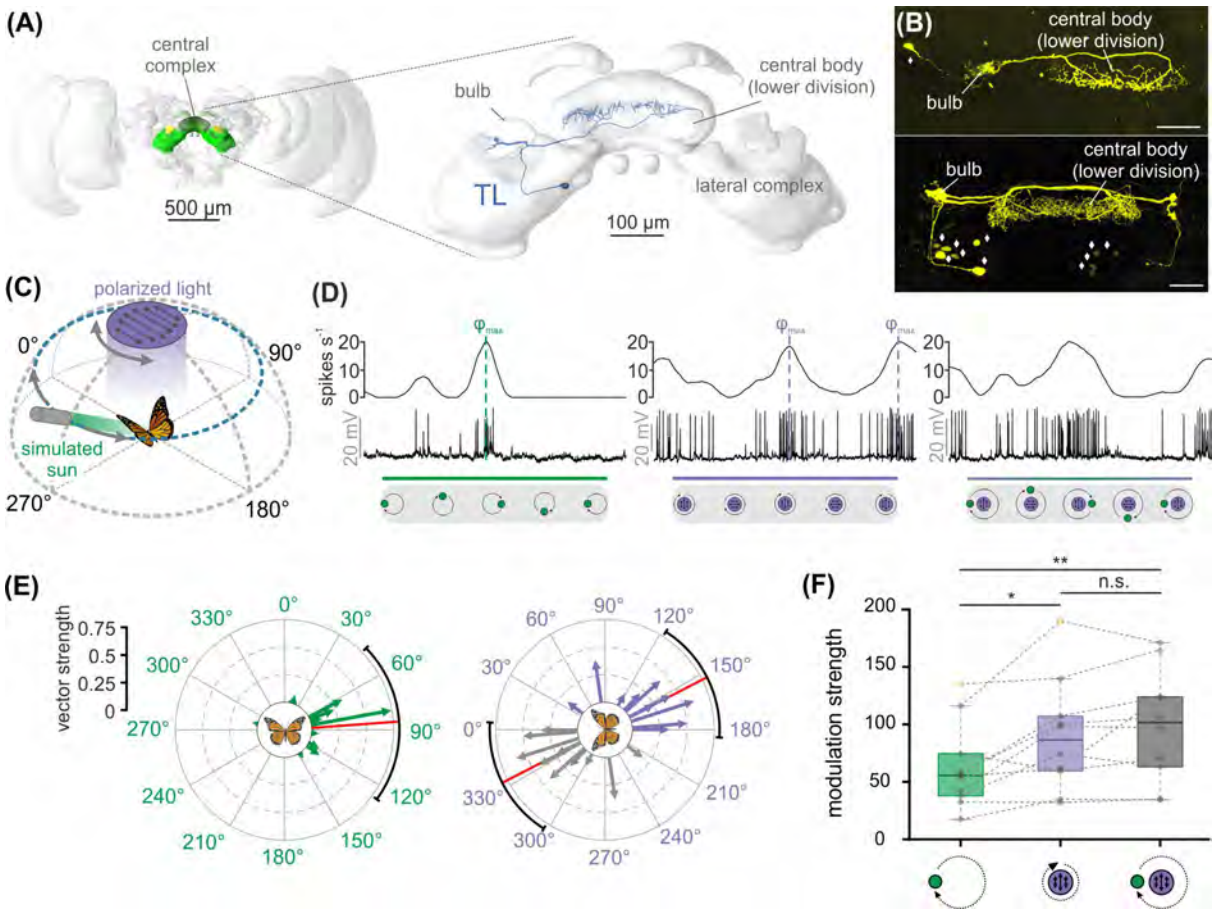

Fig. 1: TL neurons of the central complex encode simulated celestial cues. (A) Left: Frontal view of the monarch butterfly brain. Highlighted in green are the neuropils of the central complex and lateral complex. Right: The central complex and lateral complex. A reconstructed tangential neuron (TL) is shown in blue. Modified from Heinze et al. (2013). **(B)** Two examples of TL neuron tracings (anterior views) during electrophysiological recordings (maximum intensity projection views). While single cell tracings of one TL cell was possible (top, synaptic input in the right bulb), in most experiments, several TL neurons from both hemispheres were labeled (bottom). Diamonds indicate the position of TL neuron somata. Scale bars: 50 µm. **(C)** Schematic illustration of the presented simulated celestial cues. The polarization stimulus was positioned dorsally to the butterfly and was rotated by 360°. The angle of polarization was aligned with the antero-posterior axis of the animal at the beginning of the rotation. The sun stimulus (elevation: 30°) was moved on a circular path around the animal. The angle of polarized light was oriented perpendicular to the direction of the sun stimulus, simulating their spatial relationship in nature. **(D)** Neural tuning of the same TL neuron to a moving sun

stimulus (left), a rotating polarizer (middle) and when both stimuli were presented simultaneously (right). The upper curve of each plot shows the sliding window average of the action potential recordings (middle row). The lower grey boxes illustrate the position of the stimuli during a clockwise 360°-rotation indicated. Preferred firing directions (ϕ_{max}) to the sun (left) and polarized light (middle) are indicated by dashed vertical lines. **(E)** The preferred firing directions of the tested TL-neurons (n = 10) in response to the sun stimulus (left) and the polarization stimulus (right). Each arrow represents a single neuron. Arrow length indicates the vector strength (directedness) of the neural tuning. The circular plots are labeled in relation to the animals' body axis (see schematic at the plot's center), with 0° being anterior, 90° being right, and 270° being left to the animal. The mean preferred firing directions (sun stimulus: 85.88° ± 54.94°; polarized light: 152.96° ± 34.16°) are indicated by the red solid lines and the confidence intervals (95%) by the black arcs. **(F)** Modulation strength of neural activity (n = 10 TL neurons) in response to the sun stimulus (left), polarized light (middle), and the combination of both celestial cues (right). The neural modulation to the sun stimulus was significantly weaker than to polarized light ($p_{GREEN\ vs.\ POL} = 0.02$, t = 2.99, n = 10; paired t-test) and the combination of the stimuli ($p_{GREEN\ vs.\ COMBO} = 0.002$, t = -4.38, n = 10; paired t-test), while the modulation strength to polarized light and the combined stimuli did not differ from each other ($p_{POL\ vs.\ COMBO} = 0.23$, t = -1.28; paired t-test). Grey circles show individual data points. Outliers are indicated in yellow. Dashed grey lines connect individual data points from the same TL-neuron. Boxes indicate interquartile range. Whiskers extend to the 2.5th and 97.5th percentiles. Black horizontal lines show the median. n.s.: not significant, *: $p < 0.05$, **: $p < 0.01$.

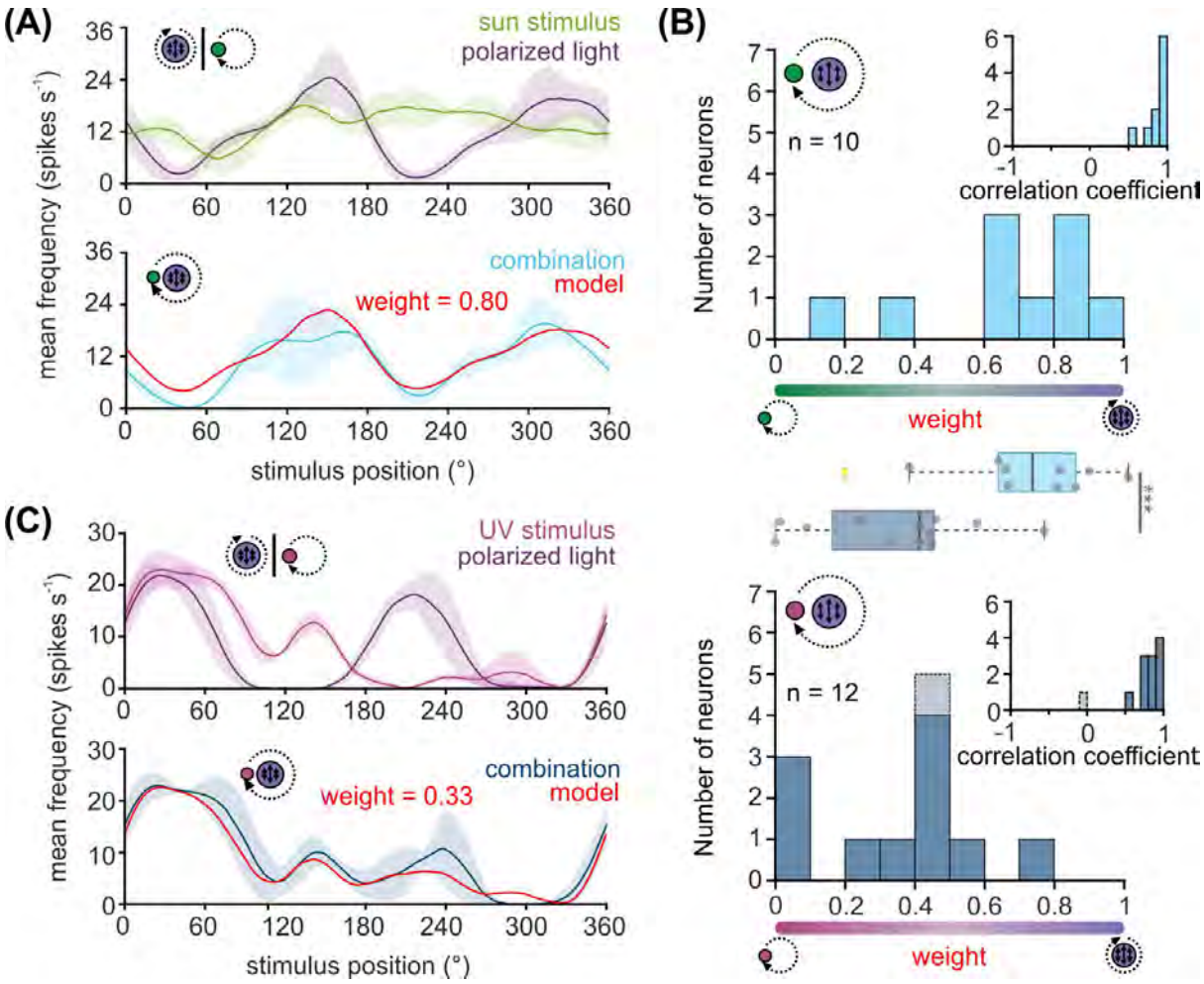

Fig. 2: Weighting of celestial cues in TL neurons. (A, C) Upper plot: sliding window averages of the action potential rates of two TL neurons to the green sun stimulus (A, green curve) or UV light spot (C, magenta) as well as to the polarization stimulus (A, C, violet curves) are shown. Lower plot: The response of the same neurons as shown in the corresponding upper plots when both stimuli were presented simultaneously (A, light blue; C, dark blue curve). Based on the response to the single cues, a weighted linear model was fitted to the data (red curve) and a weighting of the single cues was calculated. A weight between 0 and 0.5 suggests that the sun stimulus (A) or the UV light spot (C) dominated the combined response while a weight between 0.5 and 1 indicates that the polarization input dominates the combined response. The shaded areas show the standard deviation. **(B)** Histograms of the weighting factors obtained for the experiments with the green sun stimulus and polarized light (top, n = 10) and the UV light spot and polarized light (bottom, n = 12). Insets show the correlation coefficients which describe how well the weighted linear model explains the measured neural response to the combined stimulus. The weighting factor that was obtained from a low correlation coefficient is shown in grey. Box plots in the middle: While the weighting is shifted

to the polarization input when a green sun stimulus was combined with polarized light, the weighting is significantly shifted in favor of the light spot, when a UV light cue was combined with polarized light ($p < 0.001$, $F = 113.31$; linear mixed model ANOVA). Grey circles show individual data points (yellow circles indicate outliers). Boxes indicate interquartile range. Whiskers extend to the 2.5th and 97.5th percentiles. Black horizontal lines show the median. ***: $p < 0.001$.

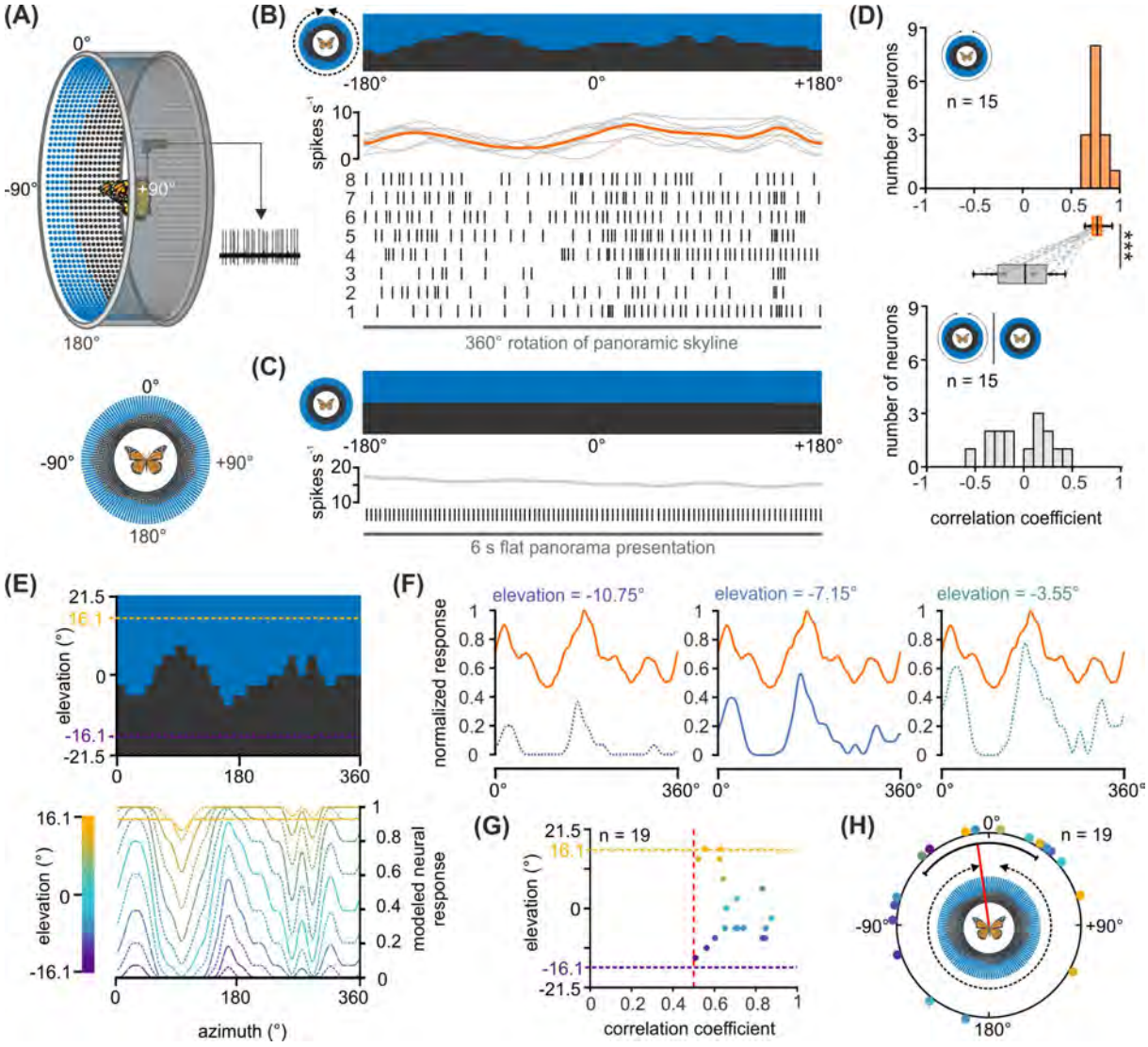

Fig. 3: Response of central-complex TL neurons to a panoramic skyline. (A) Schematic drawing of the LED arena (top) that was used to test the coding of a panoramic scene in TL neurons. 0° was defined as the direction anterior to the butterfly, before the panoramic scene was rotated by 360° around the animal (bottom). **(B)** The response of a TL neuron to eight 360°-rotations of the panoramic scene is shown as raster plot (middle). Each vertical line represents an action potential. The diagram on top shows the sliding window average of the action potentials for the eight rotations (grey curves) as well as their mean (orange curve). The

orientation of the panoramic scene prior to rotation is shown (top). **(C)** The TL neuron does not spontaneously modulate its action potential rate when a flat panorama is presented for 6s. **(D)** Distribution of correlation coefficients when comparing the neural response from each trial with the averaged response (orange, upper panel) and when comparing the neural response to the flat panorama with the averaged response to the panoramic skyline (grey, lower panel). Box plots: The neurons showed a higher inter-trial modulation to the panoramic scene compared to the modulation to the flat panorama ($p < 0.001$; sign rank = 120, Wilcoxon signed rank test). Paired data points across the tested groups are connected by dashed lines. Boxes indicate interquartile range. Whiskers extend to the 2.5^{th} and 97.5^{th} percentiles. Black horizontal lines show the median. ***: $p < 0.001$. **(E)** Modeled neuronal response curves to the panoramic skyline of fictive TL neurons that have visual fields centered at different elevations (lower panel). The center of the receptive fields were set for elevations within the panoramic scene (between -16.1° and 16.1°, dashed lines upper panel). **(F)** The measured neural response of one recorded TL neuron (orange curve) to the panoramic scene plotted against three modeled neural responses whose visual fields were centered at different elevations (see also lower panel in E). The measured neural response showed the best match to the modeled modulation at an elevation of -7.15 (middle plot; correlation coefficient = 0.84). **(G)** Elevations of the highest match between the measured TL neuron response and the modeled response plotted against the corresponding correlation coefficients. Each point represents an individual TL neuron (n = 19). Vertical, red dashed line indicates a correlation coefficient of 0.5. The vertical dashed lines represent the elevation range for the modeled receptive fields (between -16.1° and 16.1°). **(H)** Azimuthal shifts leading to the maximum correlation between the measured and modeled neural response are plotted for each neuron (n = 19). Shifts were clustered towards the frontal visual field ($p = 0.045$; $Z = 3.06$, n = 19, Rayleigh test). The mean is indicated by a red solid line and the confidence intervals (95%) by a black arc. The color code of the individual TL neurons in G and H corresponds to the color code of the heatmap in E.

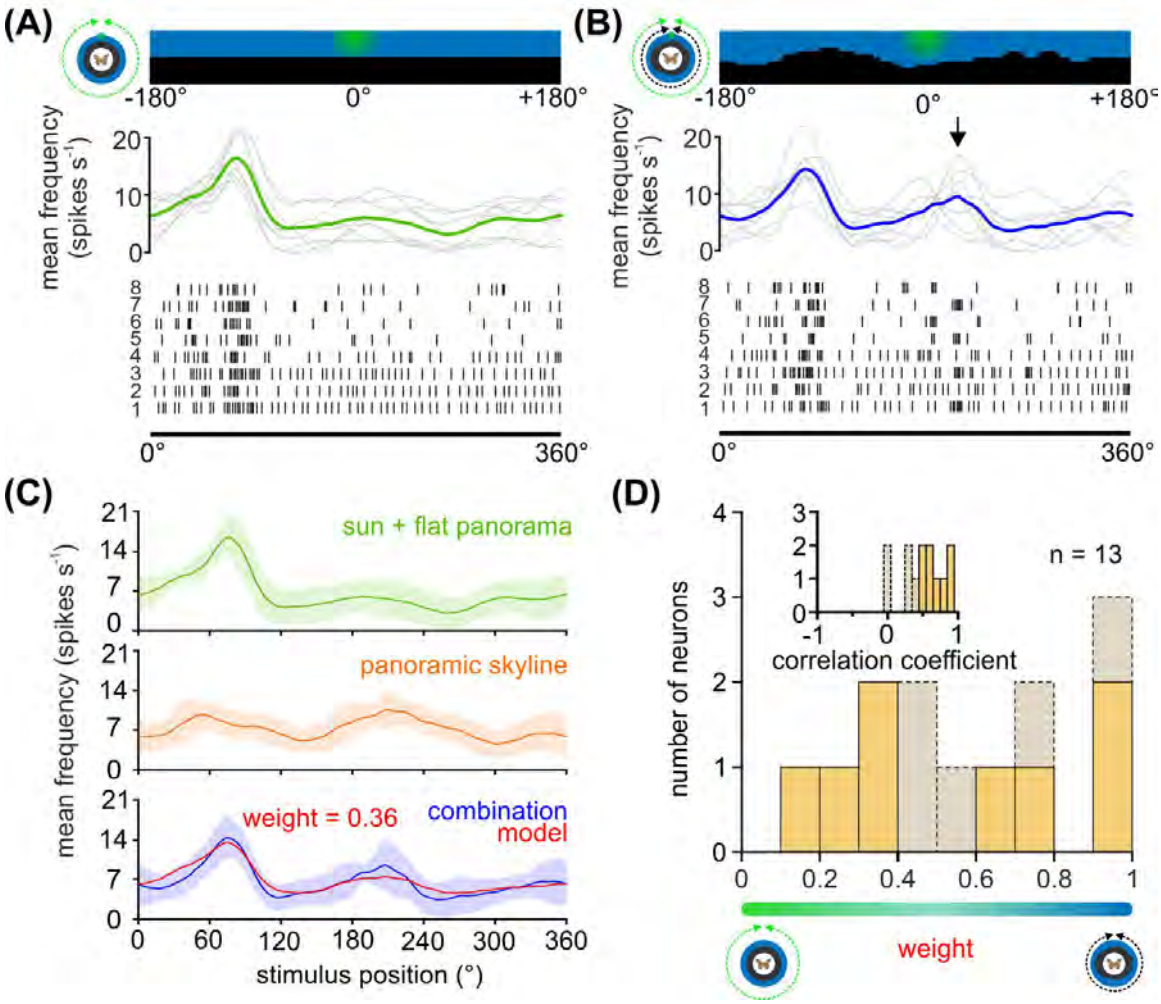

Fig. 4: Weighting the sun and panoramic skyline in TL neurons. (A, B) The response of a TL neuron to eight 360°-rotations of the sun stimulus (A), and when the sun stimulus and the panoramic scene were rotated simultaneously around the animal (B). The stimulus position prior to rotation is shown (top). The action potentials rates are shown as raster plots (bottom). Above the raster plots, the sliding window averages of the rotations are shown (middle plot, grey curves). The sliding window averages of the mean spiking frequency are color coded (A, moving sun stimulus in green; B moving sun stimulus and panorama in blue). Arrow indicates an increased spiking activity that was not observed when presenting the sun stimulus alone and thus can be attributed to the panoramic skyline **(C)** Sliding window averages of the same TL neuron as in (A) and (B) responding to a 360° rotation of different stimuli. From top to bottom: sun stimulus alone (green curve), panoramic skyline alone (orange curve), sun stimulus and panoramic skyline combined (blue curve). A weighted linear model (red curve, lower plot) was fitted to the observed neural activity to the combined stimulus. Shaded areas show the standard deviation. **(D)** The distribution of the weighting factors for experiments with the sun stimulus and panoramic skyline (n = 13). Low and high weighting values indicate that the sun stimulus

and the panorama dominated the combined response, respectively. The correlation coefficient distribution in the inset indicates how well the weighted linear model described the measured neural response to the combined stimulus. Weighting factors obtained from a low correlation coefficient (< 0.5), indicating that the neural response can be explained poorly with a linear model, are shown in grey.

4. Manuscript III: How is the time information transferred to the CX?

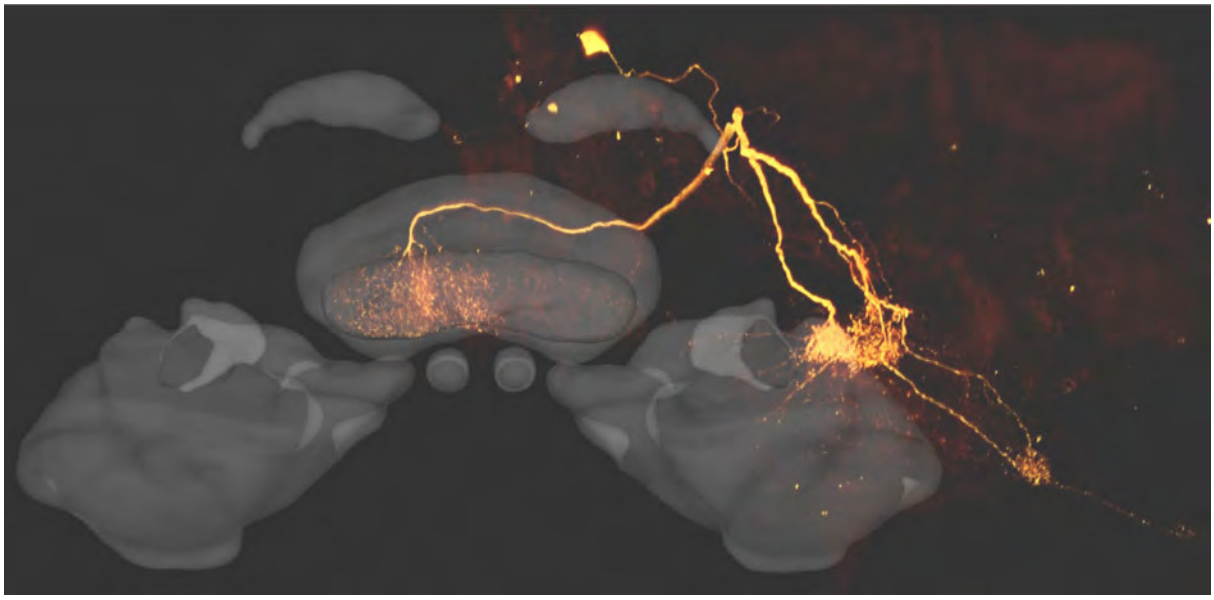

A novel type of compass neuron in the monarch butterfly central complex

Tu Anh Thi Nguyen[1], Basil el Jundi[1,2]*

Affiliations:

[1] University of Wuerzburg, Biocenter, Zoology II, Würzburg, Germany

[2]Department of Biology, Animal Physiology, Norwegian University of Science and Technology, Trondheim, Norway

*Corresponding author: basil.el.jundi@ntnu.no

Keywords: insect, central complex, navigation, orientation, landmark, migration, panorama, lepidoptera

Running Title:

A novel central-complex neuron

Abstract

Each fall, a new generation of monarch butterflies (*Danaus plexippus*) sets out for a long journey from Northern US and Canada to their overwintering habitat in Central Mexico. To maintain their flight direction during this long-distance navigational task, the butterflies use a time-compensated celestial compass for orientation. In addition to this, monarch butterflies can also use terrestrial cues to maintain a stable heading. Both, celestial cues, such as the sun and polarized light, and terrestrial cues are transferred to a brain region in the monarch butterfly central brain, termed the central complex. This brain region is believed to act as the main internal compass during the butterfly's annual migration. Recent results show that central-complex input neurons, termed tangential neurons, respond to simulated celestial cues as well as panoramic scenes in monarch butterflies. Here, we performed intracellular recordings from the central complex and discovered a novel type of tangential neuron in the monarch butterfly brain that is sensitive to simulated celestial cues but does not seem to encode terrestrial information. The new type of neuron, termed TPL, connects the posterior optic tubercle with the ellipsoid body of the central complex. While its role is unknown, our results indicate that the cell might have a modulatory function in the central complex network that could be crucial during dispersal and/or long-distance navigation in monarch butterflies.

Introduction

Spatial orientation has been well investigated in several insects ranging from foraging honeybees (Edrich et al., 1979; Brines and Gould, 1979) and desert ants (Graham and Cheng, 2009; Wehner, 2003), to straight-line orientating dung beetles (Dacke et al., 2021; el Jundi et al., 2019) and fruit flies (Giraldo et al., 2018), to migrating desert locusts (Homberg, 2015) and bogong moths (Dreyer et al., 2018). In all these insects, the insect's heading direction is determined by idiothetic, self-motion information (Müller and Wehner, 1988) and external cues such as celestial (Brines and Gould, 1979; el Jundi et al., 2019; Giraldo et al., 2018) and/or terrestrial information (Dreyer et al., 2018; Graham and Cheng, 2009; Towne et al., 2017). The monarch butterfly (*Danaus plexippus*) is undoubtedly the most famous long-distance migrating insects (Merlin and Liedvogel, 2019). Each fall, millions of these butterflies migrate from Northern US and Canada to certain trees in Central Mexico. To maintain a constant southerly flight direction during their migration, the butterflies rely on the sun as their main external orientation reference (Franzke et al., 2020; Stalleicken et al., 2005). To compensate for changes of the sun's azimuth over the course of a day, they adjust their sun-heading system by additionally integrating circadian clock information from the antennae (Guerra et al., 2012; Merlin et al. 2009) and brain (Sauman at al., 2005) into their migratory compass. In addition to the sun, the polarization pattern of the sky might also be integrated in the animal's migratory compass (Reppert et al., 2004). Recent studies also demonstrated that the butterflies could use the panoramic skyline for flight stabilization and/or orientation (Franzke et al., 2021; Franzke et al. 2020) but its role for migration is still not understood.

Both, unpolarized (sun, panoramic scenes) and polarized light are perceived by different regions of the butterfly's eye (Stalleicken et al., 2005) and are integrated in the medulla of the optic lobe in the brain. After passing the medulla and lobula, the visual information is transferred to the lower unit of the anterior optic tubercle, further to the bulb, and finally to the central complex (CX) (Heinze and Reppert, 2011; Heinze et al., 2013). The CX is a highly conserved insect brain region (Pfeiffer and Homberg, 2014) that can be divided into four neuropils: the central body lower and upper divisions, the paired noduli and the protocerebral bridge that are innervated by different types of CX neuron. These types of CX neuron can be divided into two main categories: Columnar neurons that interconnect different neuropils within the CX (Heinz and Homberg, 2008) and tangential neurons that transfer information from other regions of the insect brain to the CX (van Hadeln et al., 2019). The best physiological characterized tangential neurons in the monarch butterfly brain are the GABAergic TL neurons that have synaptic input

in the bulb (Homberg et al., 2018) and transfer information into the central body lower division. TL neurons are sensitive to celestial information (Heinze and Reppert, 2011; Nguyen et al., 2021) and respond to a simulated panoramic skyline (Nguyen et al., 2022). The information from the TL neurons is transferred to CL1 cells. Studies in the fruit fly have shown that these cells process the insect's current heading direction (Seelig and Jayaraman, 2015; Turner-Evans et al., 2017; Fisher et al., 2019; Kim et al., 2019). The CL1 heading-direction information is then transferred from the central body lower division to the protocerebral bridge (PB) where it is transferred to tangential neurons of the protocerebral bridge, termed TB neurons (Heinze et al. 2013). In addition to the branches in the PB, TB cells have synaptic input in the ipsilateral posterior optic tubercle (POTu) (Held et al. 2020. This irregular shaped neuropil is located within the posterior optic commissure and ventrolateral to the PB (Heinze and Reppert, 2012) and has been associated with circadian rhythm and time compensation in several insects (Homberg et al., 1991). While the anterior sky compass pathway via the anterior optic tubercle and bulb has been thoroughly investigated in many insects (Heinze and Reppert, 2011; el Jundi et al., 2015; Zeller et al. 2015; Hardcastle et al., 2021), a posterior polarization pathway though the POTu has been proposed to deliver time-of-day information to the CX in the desert locust brain (el Jundi and Homberg, 2010). If this pathway exists in other insects and what role the POTu play in the CX network is still not fully understood. We here recorded from a novel type of tangential neuron that connects the POTu with the central body lower division. The new cell type, termed TPL responded to simulated celestial (simulated sun and polarized light) but was insensitive to a panoramic scene. Taken together, the direct connection from the POTu to the central body lower division and the encoding of skylight cues in TPL neurons indicate that the POTu might also be critically involved in the heading-direction coding in monarch butterflies.

Materials and Methods

Experimental animals

Data acquisition on non-migratory monarch butterflies (*Danaus plexippus*) took place from April 2018 to September 2019 in Würzburg (Germany). Butterfly pupae from the Costa Rica Entomology Supply (butterflyfarm.co.cr) were kept in an incubator (HPP 110 and HPP 749, Memmert GmbH + Co. KG, Schwabach, Germany) at 25 °C, 70 % relative humidity and 12:12 light/dark-cycle. After eclosion, adult animals were moved to another incubator (I-30VL, Percival Scientific, Perry, IA, USA) at 12:12 light/dark condition, 25 °C and at 50 % relative humidity. The butterflies were provided with sponges soaked in 15 % sugar water solution as

ad libitum food source. Recordings from migratory animals were collected from October to November in 2018/2019 in College Station, (TX, USA). The migratory animals were kept in glassine envelops in an incubator (I-30VL, Percival Scientific, Perry, IA, USA) set to the abiotic autumn conditions (11:13 light-dark cycle, 23 °C set during light- and 12 °C during dark phases). Animals were fed manually every other day with a 20 % honey solution.

Preparation and electrophysiology

Experimental procedures were the same as described in Nguyen et al. (2021) and Nguyen et al. (2022) and were performed in two identical setups, one at the University of Würzburg (Germany) and one at the Texas A&M University (USA). To avoid introducing any artefacts generated by the animals' movements, legs and wings were clipped off prior to the recordings and the animals were fixed on a metal holder with dental wax (Omnident, Rodgau Nieder-Roden, Germany). The head was opened frontally using a thin blade and the neural sheath covering the brain tissue was removed using fine tweezers. One of the antennae remained intact to retain the circadian pacemaker for time compensation (Guerra et al., 2012; Merlin et al., 2009). During the entire recording, the brain was rinsed with monarch butterfly ringer (150 mM NaCl, 3 mM KCl, 10 mM TES, 25 mM sucrose, 3 mM $CaCl_2$). Electrodes were drawn from borosilicate glass (inner/outer diameter: 0.75/1.5 mm, diameter of inner filament: 0.2 mm; Hilgenberg, Malsfeld, Germany) with a Flaming/Brown horizontal puller P-97-puller (Sutter Instrument, Novato, CA, USA) and filled with 4% Neurobiotin (Vector Laboratories, Burlingame, UK, dissolved in 1M KCl) and 1M KCl. Two Ag-AgCl-wires were used during the recording: one was inserted into the sharp electrode (resistance of the electrodes was between 50-200MΩ), while another one was inserted into the head and served as reference electrode. The recording electrode was positioned in the central complex using a manual micromanipulator (Leica Microsystems, Wetzlar, Germany). The neural signals were amplified with a BA-03X Bridge Mode Amplifier (npi Elelctronic GmBH, Tamm, Germany) and digitized (Power1401, Cambridge Electronic Devices, Cambridge, UK) at a resolution of 1-20 kHz. The neural activity of the cells was recorded on a computer using the Spike2 software (version 9.00, Cambridge Electronic Devices, Cambridge, UK).

Visual stimuli

Celestial stimuli were presented as described in Nguyen et al. (2021). Because monarch butterflies are sensitive to polarized UV light (Sauman et al., 2005; Stalleicken et al., 2006), the animals were stimulated with a UV-LED (emission peak at 365 nm, LZ1-10UV00-0000, OSRAM Sylvania Inc., Wilmington, MA, US) that passed its light through a diffuser (quarter

white diffusion, LEE Filters, Hampshire, UK) and UV permeable polarization filter (Bolder Vision Optik Inc., Boulder, CO, USA). The polarization filter was mounted at the center of a rotation stage (DT-50, PI miCos GmbH, Karlsruhe, Germany), which allowed us to change the orientation of the angle of polarization during recording. Four arms extended from the center of the rotation stage. The head of two of these arms were equipped with an unpolarized green LED (emission peak at 520 nm LZ1-10G102-0000, OSRAM Sylvania Inc., Wilmington, MA, US) and an unpolarized UV LED. Both light spots were adjusted to an elevation of ~30° relative to the animals' position in the setup. By turning the rotation stage, the unpolarized light spots were moved on circular paths around the animal. The unpolarized light spots and the polarization stimulus were adjusted to the same photon flux of about 1.4×10^{14} photons/cm^2/s measured at the animal's position during recording. The angular extent of the polarization stimulus at the butterfly eye was 10.42° in non-migratory and 9.55° in migratory butterflies due to slight differences in the setups. The angular size of the unpolarized light spots were 1.44° in non-migratory and 1.32° in migratory butterflies. Before each experiment, the 0°-180° axis of the polarizer was aligned with the animal's longitudinal axis. The rotation stage was turned clockwise and anticlockwise while the tested stimulus (either the polarized *or* unpolarized light cue) was presented.

The panoramic stimuli were presented on an LED arena as described in Nguyen et al. (2022). The inner surface of the arena was equipped with 128x16 RGB-LED arrays (M160256CA3SA1, iPixel LED Light Co., Ltd, Baoan Shenzhen, China) and covered a visual field of 360° along the horizontal and 43° along the vertical plane around the animal. Each LED above the horizon was adjusted to a photon flux of about 6.68×10^{10} photons/cm^2/s in the blue range (emission peak: 458 nm). LEDs below the horizon were turned off. While searching for a central-complex cell, a panorama with a flat horizon was presented to the animals. After successfully targeting a compass neuron, a panoramic scenery with a variable height profile was presented and rotated by 360° around the animal in clock- and counterclockwise direction (at a constant velocity of 60°/s). We used the same panoramic scene during our recordings as presented to monarch butterflies in a behavioral experiment (Franzke et al., 2020). To test the neuron's responsiveness to a simulated sun, one LED above the horizon at an angular elevation of 18.9° was switched to a wavelength emission peak of about 516 nm and an intensity of about 6.14×10^{12} photons/cm^2/s. We combined the sun stimulus with the flat panorama while moving the sun stimulus around the animal and keeping the flat panorama stationary.

Histology and imaging

After presentation of the stimuli, Neurobiotin was iontophoretically (1 - 3.5 nA) injected into the neuron for about 3 - 5 min. After waiting for about 20 min, the brain was dissected and immersed in a fixative solution (4% paraformaldehyde, 1.3% picrinic acid, 10% glutaraldehyde in NaPi-buffer) for 18-24h. Samples were then rinsed in phosphate buffered saline (PBS) for 4x15 min and subsequently incubated in a solution containing either Alexa568-conjugated to streptavidin (Molecular Probes, Eugene, OR, USA, 1:1000) or Cy3-conjugated to streptavidin (*Thermo Fisher Scientific*, Waltham, MA USA, 1:1000), dissolved in 0.1M PBS with 0.3 % Triton X-100 detergent (PBT) for 3 days at 4 °C in the dark. Following several washing steps with PBT (2x20 minutes) and PBS (3x20 minutes), brain samples were dehydrated in an ascending ethanol series (30 %-100 %, 15min each). Brain tissues were then immersed with a 1:1 ethanol-methyl salicylate solution for 20 minutes, followed by clearing with 100 % methyl salicylate for about 1 hour at room temperature. Brains were then embedded in Permount (Fisher Scientific GmbH, Schwerte, Germany) between two cover slips kept apart by ten reinforcement rings (Avery, Toronto, Canada). The neurons were imaged using a confocal microscope (Leica TCS SP8, Wetzlar, Germany) with either a 10x air (HCX PL-Apo 10x/0.4 CS, Leica) or a 25x oil-immersion objective (HC PL-Apo CS2 10x/0.75 Imm Corr, Leica) to identify the cell's neuroanatomy. The brain samples were scanned with a resolution of 1024x1024 pixels and a distance of 1.5 µm in z-direction using a HeNa-laser. The images stacks were then imported in the 3D software Amira 5.3.3 (Thermo Fisher Scientific Inc., Waltham, MA, USA) where they were masked using the Arithmetic tool. For an intensity-based 3D visualization of the TPL neuron in the standard central complex (Heinze et al. 2013), we used the module Voltex.

Data analysis

Quality assessment of spike recordings were done as described previously (Nguyen et al., 2021; Nguyen et al. 2022). Subsequent data analysis was continued in MATLAB (version R2018a; MathWorks, Natick, MA, USA) using mostly custom-written scripts and by implementing externally provided functions like the CircStat toolbox (Berens, 2009) and the CircHist function (Zittrell et al., 2020). Action potentials within the spike recordings were counted using a threshold-based detection method. Within the recording, a 6 s section prior to light stimulation was selected to calculate the background activity and to determine the background variability after Kuebler and Thivierge (2014). Sliding averages of the responses were obtained by calculating the instantaneous frequencies of the action potentials and applying a low-pass filter. Preferred directions (φ_{max}) of a neuron for each light stimulus were calculated by pooling the

action potential counts of clockwise and counterclockwise rotations and testing if they deviated from a uniform distribution. Depending on the used stimulus, the action potential distribution followed a unimodal (unpolarized light) or bimodal (polarized light) distribution. To determine the modulation strengths, action potentials were divided into 18 bins with a bin size of 20° and normalized to the number of rotations. Then the modulation strength was calculated as described by Labhart (1996). A high modulation strength indicates a strong response, and a low modulation strength a weak response of a neuron to a visual stimulus. Tuning curves were obtained by shifting the gliding average curves for each trial with the preferred direction (φ_{max}) to 0° and by calculating the average. Tuning curves representing a certain neuron type were determined by normalizing the individual tuning curves by the area below the curve and then calculating the average curve shape. The tuning curves for polarized-light responses ranged from 0-180°, while the ones for the unpolarized light stimuli ranged from 0-360°. Tuning widths for each cell were defined as the curve full width at half maximum.

Statistics

To determine whether the distribution of spike rates in response to the celestial stimuli deviated from a uniform distribution, we employed the Rayleigh test (α=0.05). If the action potentials were non-uniformly distributed, the preferred firing direction of a neuron was calculated as the mean vector. Due to the uneven sample size for each neuron type, we applied the Wilcoxon signed rank test for unpaired mean values. Two neuron types were tested for differences in the background activity, background variability, modulation strengths and tuning widths in response to the celestial stimuli.

Results

Anatomy of the *Tangential Protocerebral*-central body *Lower* division (TPL) neuron

The CX receives information from other brain regions via tangential neurons (Heinze et al., 2013). Two well-investigated tangential neurons are (*i*) the TL neurons connecting the bulb and the central body lower division (CBL) (Fig. 1B, light blue) and (*ii*) the TB neurons arborizing in the protocerebral bridge (PB) and the posterior optic tubercle (POTu) (Fig. 1B, dark blue). Here, we found a yet uncharacterized tangential neuron type, termed TPL, in the monarch butterfly central complex (Fig. 1C). This neuron type was observed in five experiments. The striking similar morphology and physiology of the five neurons suggest that there is a single

TPL neuron per brain hemisphere. The soma of the TPL neuron is very large and localized superior and posterior to the PB in the pars intercerebralis. The primary neurite of the neuron runs anterior to the PB (Fig. 1C, inset) where it bifurcates into two main neurites: one neurite runs towards anteromedial, crosses the midline of the brain at the level of the central body upper (CBU), and enters the CBL, where it gives raise to varicose ramifications throughout all CBL columns (Fig. 1D). While the branches were strongly stained in the contralateral columns of the CBL, the ipsilateral columns were stained faintly (Fig. 1D). The second main neurite runs posteroventral behind the central complex and further bifurcates into two branches. They both extend towards the posterior commissure of the brain where they enter the POTu with both smooth and varicose arborizations (Fig. 1E). The neuron shows further branches anterior and lateroventral to the POTu, in a small, unknown brain region in the posterior lateral protocerebum. Similar to the branches in the POTu, the branches in the posterior lateral protocerebrum showed a mixed arbor morphology.

The novel TPL cell encodes celestial stimuli

In order to understand the possible role of the TPL cell in the monarch butterfly's sun compass, we recorded its action potential rate intracellularly (Fig. 2). We also obtained recordings from the remaining tangential neurons of the central complex (TL and TB neurons; Fig. 1B) and compared their physiological responses to the TPL neuron. We first investigated whether the TPL neuron differs from the "classical" tangential (TL and TB) neurons by comparing its background activity to the background activity of the TL/TB neurons (Fig. 2A, upper panel). The background activity of the TPL neurons ranged from 6 to 19.17 spikes/s (10.83 ± 7.25 spikes/s, mean ± std). This was not different from the background activity of the TB cells (6.33 ± 4.55 spikes/s; p = n.s., rank sum = 11; Wilcoxon rank sum test) or the TL neurons (10.50 ± 6.33 spikes/s; p = n.s., rank sum = 54.5; Wilcoxon rank sum test). We also compared the background variability of the three types of neuron (Fig. 2A, lower panel): the variability of the TPL neurons ranged from 0.68 to 0.86 (0.79 ± 0.10), which resembled the background variability of TB (0.72 ± 0.17, $p_{TPL\ vs.\ TB}$ = n.s., rank sum = 12; Wilcoxon rank sum test), and TL neurons (0.63 ± 0.23, $p_{TPL\ vs.\ TL}$ = n.s., rank sum = 79; Wilcoxon rank sum test). Taken together, the TPL spiking physiology in the dark was similar to the tangential CX-neurons of the monarch butterfly's sun compass.

We next wondered whether the TPL cells encode celestial cues and therefore presented the simulated skylight cues (simulated sun, polarized skylight, UV light spot, Nguyen et al., 2021) to the animals during recording. They were not only sensitive to changes in the sun stimulus

position (Fig. 2B) but also responded to the rotation of the polarized-light stimulus (Fig. 2C) and the UV light spot (Fig. 2D). The preferred sun stimulus (335.22° ± 32.71°) and the UV spot positions (10.31° ± 58.60°) of the TPL cells mostly clustered in the monarch butterflies' anterior visual field (Fig. 2E, left and right plot) while the preferred angle of polarizations (175.40° ± 22.47°) aligned with the animal's antero-posterior body axis (Fig. 2E, middle plot). Thus, similar to the TL and TB neurons (Heinze and Reppert, 2011; Nguyen et al., 2021; Nguyen et al., 2022), TPL neurons seem to carry celestial compass information into the central complex. We next analyzed the TPL cells' modulation strengths to the simulated celestial cues in detail and compared them to the modulation strengths of the responses of the TL and TB neurons (Fig. 2F). Modulation strengths of TPL cells were highly variable regardless of the tested stimuli (sun stimulus: 126.64 ± 54.64, polarized light: 148.59 ± 88.24, UV spot: 246.90 ± 114.84). For the simulated sun responses (Fig. 2F, left graph), the TL modulation strength (82.08 ± 37.17) was similar to the TPL cells' modulation strength (p = n.s., rank sum = 35; Wilcoxon rank sum test). In the presence of the polarized-light stimulus (Fig. 2F, middle graph), the TB (82.46 ± 28.76) and TL neurons (89.17 ± 43.60) showed a similar modulation strength as the TPL neuron (p = n.s., rank sum = 74; Wilcoxon rank sum test). This was not true for the modulation strength to the UV spot (Fig. 2F, right graph): while the TPL neurons (246.9 ± 114.8, n = 5) responded similarly strong as the TB neurons, they differed significantly form the TL neurons' response strength (105.7 ± 58.6, n =27, p = 0.01, rank sum = 131; Wilcoxon rank sum test). Taken together, the TPL neuron exhibited physiological properties that are typical for tangential compass neurons of the monarch butterfly central complex.

Comparison of tuning curves

In the next step, we analyzed the tuning curves of the TPL, TL and TB cells in response to the celestial stimuli. For each neuron type, we averaged the individual tuning curves in response to the celestial stimuli (Fig. 3A-C) and calculated a mean tuning curve (Fig 3A-C, red curves). In general, while the tuning curves to the polarization stimulus exhibited less variability between the neurons in all three types of tangential neurons (Fig. 3A-C, middle graphs), the responses to the sun stimulus (Fig. 3A-C, left graphs) and the UV light spot (Fig. 3A-C, right graphs) showed a high inter-individual variability. To compare the tuning curves statistically between the three types of neuron, we also measured the tuning widths of the neuron types (Fig. 3D). For the simulated sun, tuning widths of the TPL (52.77 ± 20.80°) and TL cells (148.63 ± 77.81°; Fig. 3D, right plot) did not differ from each other (p = n.s., rank sum = 13; Wilcoxon rank sum test). Furthermore, when presenting polarized light, tuning widths of TPL (87.24 ± 26.61°), TB (91.95 ± 13.69°91.95 ± 13.69°) and TL cells (84.14 ± 18.76°) were similar and did not differ

significantly from each other (Fig. 3D, middle plot). While the tuning widths in response to the UV spot were similar (Fig. 3D, left column) between TPL (73.81 ± 26.72°) and TB cells (82.18 ± 12.25°; p = n.s., rank sum = 24; Wilcoxon rank sum test), the TL neurons (144.85 ± 56.42°) exhibited significantly wider tuning curves compared to the former two neuron types ($p_{TPL\ vs.\ TL}$ = 0.006, rank sum = 29; $p_{TB\ vs.\ TL}$ = 0.02, rank sum = 25; Wilcoxon rank sum test). In summary, the tuning curves to the sun and polarization stimulus were similar between the tangential neurons but differed significantly in response to a UV light spot.

TPL neuron does not respond to the panoramic skyline

Since TL cells are responsive to a panoramic scene (Nguyen et al., 2022), we tested whether the TPL neurons are also sensitive to a simulated panorama that was moved by 360° around the animal (Fig. 4). We presented a profiled panorama while recording from TPL neurons in two animals (Fig. 4B). In addition, we presented as a control a flat panorama (Fig. 4A) as well as a flat panorama combined with a simulated sun (Fig. 4C) during our experiments. In contrast to the celestial stimuli tested previously (see above), both tested TPL cells were unresponsive to the presented stimuli, regardless of whether the panoramic stimulus was flat (Fig. 4A) or profiled (Fig. 4B). The two TPL neurons were also not tuned to the sun stimulus (Fig 4C). As the sun stimulus was presented at a lower elevation here than in Fig. 2, this indicates that the TPL neurons are only sensitive to unpolarized light stimuli at high elevations.

Discussion

We characterized a novel central-complex neuron type, named TPL, anatomically (Fig. 1) and physiologically (Fig. 2) in the monarch butterfly brain. The tested TPL neurons were sensitive to celestial stimuli (Fig. 2B-E) and their responses were similar to the classical tangential CX cells, such as TL and TB neurons (Fig 2F). Similarly, the TPL tuning widths in response to the sun stimulus and polarized light were similar to the corresponding tuning widths of TL and TB neurons, while the TPL tuning widths to the UV light spot was narrower that the one for the TL neurons (Fig. 3). In contrast to TL neurons that encode a panoramic scene (Nguyen et al., 2022), the two tested TPL neurons did not respond to a panoramic skyline (Fig. 4). Thus, our results open the possibility that the novel found central-complex TPL neuron is specifically tuned to celestial cues.

Comparison of the TPL neuron's general tuning characteristics

The TPL neuron shows strong physiological similarities to the remaining tangential CX neurons. The background activity and background variability were very similar in TPL, TB and TL cells. This contrasts with the observations made in desert locusts, where the spiking rate in the dark was higher in TB cells compared to TL cells (Heinze et al., 2009). Whether the background activity can predict how strong a TPL neuron responds to celestial cues, as shown for monarch butterfly TL neurons (Nguyen et al., 2021), is still unknown. We found that the TPL cells show preferred firing directions to the sun stimulus that are centered to the frontal visual field, similar to what has recently been reported for the TL cells (Nguyen et al., 2021). The preferred polarization angle of the recorded TPL neurons aligns with animal's antero-posterior axis, an observation that has also been made for the TL neurons (Nguyen et al., 2022). However, in contrast to the preferred firing directions of the TL neurons (Nguyen et al., 2022), we did not find any evidence for a matching of the natural, orthogonal relationship between the sun direction and the polarization angle in TPL neurons. Whether this is the case, or if the TPL neurons adjust their preferred firing directions in a time-of-day dependent manner, as shown for compass neurons of the anterior optic tubercle in desert locusts (Pfeiffer and Homberg, 2007) and monarch butterflies (Heinze and Reppert, 2011) requires additional recordings from TPL neurons throughout the course of the day. Like the tangential CX neurons in the desert locust (Heinze et al., 2009), the tuning widths in response to polarized light did not differ significantly between the tested tangential CX cells in monarch butterflies (Fig. 3D). Given the limited sample size of the recorded TPL neurons, we had to pool the tuning curve responses of both migratory and non-migratory animals in the present study. However, a recent study showed that TL neurons in migratory butterflies are tuned narrower to the sun than TL neurons in non-migratory monarch butterflies (Nguyen et al., 2021). Whether the tuning width of the TPL neurons in response to the simulated sun also depends on the monarch butterfly's lifestyle (non-migratory vs. non-migratory) has yet to be investigated.

The tested TPL neurons did not respond to the presented panoramic scene. Surprisingly, these two cells did also not respond to the sun stimulus (Fig. 4). Both findings differ from the results for the monarch TL cells in Nguyen et al (2022). Moreover, the insensitivity of the TPL neurons to the sun stimulus in Figure 4 contrasts the results shown in Figure 2. While the sun stimulus was adjusted to 30° in the experiments in Figure 2, the sun stimulus used in Figure 4 was adjusted to elevations below 18°. This indicates that the TPL cells have receptive fields for unpolarized light signals, such as the sun, centered at higher elevations. However, due to the

low sample size, further experiments into the coding of the panoramic scene and the processing of the sun at different elevations are needed to draw any solid conclusion.

TPL neuron may integrate time-compensated sun compass information

The neuroanatomy of the TPL neuron suggests that it receives synaptic input in the POTu and posterior lateral protocerebrum. This indicates that the TPL cells do not receive celestial information via the well-characterized anterior sky-compass pathway (Homberg et al., 2011). In desert locust, compass neurons in the POTu have been proposed to receive polarization information from the accessory medulla (aMe) of the optic lobe via a second, posterior polarization-vision pathway (el Jundi and Homberg, 2010). Indeed, the POTu in the desert locust has been demonstrated to contain presynaptic and postsynaptic profiles (Beetz et al., 2015; Held et al., 2020), making inputs from the aMe highly likely. In addition to polarized light information, neurons in the aMe encode also unpolarized light information, such as the sun position (el Jundi et al., 2011). Thus, if a similar pathway exists in monarch butterflies, TPL neurons could receive integrated skylight signals from the optic lobes via a posterior sky-compass pathway.

In addition to skylight cues, migrating monarch butterflies need to receive time information from the internal circadian clock to adjust their southerly migratory direction throughout the course of a day (Mouristen and Frost, 2002; Reppert et al., 2016; Sauman et al., 2005). Interestingly, the aMe houses clock neurons in the brain of many insect that are critically involved in the control of circadian rhythms (Helfrich-Förster and Homberg, 1993; Homberg et al., 1999; el Jundi and Homberg, 2010). Thus, it is an attractive theory to postulate that the TPL neuron might be involved in a posterior sky-compass pathway that carries time-compensated sun compass information to the central complex. This would allow the sun-compass network in the lower division of the central body to be compensated in a time-of-day dependent manner. But how the circadian clocks from the butterflies' antennae (Merlin et al., 2009) would interact with a brain clock in the aMe is a matter of speculation. Moreover, there is strong evidence that the aMe's function as circadian pacemaker does not seem to be conserved in monarch butterflies (Sauman et al., 2005). Taken together, by further investigating the hypothesized posterior innervation pathway in monarch butterflies and by studying the neurotransmitter immunoreactivity of the TPL cells in the future, as recently done for the TL cells in different insects (Homberg et al., 2018) and for the TB cells in desert locusts (Beetz et al., 2015), we may increase our understanding of the TPL neuron's role in the monarch butterfly compass system.

TPL cells as modulatory neurons

The only other animal in which a similar neuron as the TPL neuron has recently been anatomically characterized is the Bogong moths *Agrotis infusa*. In the moth brain, the neuron, termed TL (Ga-BU-POTu), also interconnects the POTu with the CBL but shows additional branches in the galls and bulbs (de Vries et al., 2017). Interestingly, like the monarch butterfly, these moths perform an annual long-distance migration (Dreyer et al., 2018; Warrant et al., 2016). Whether the TPL (monarch butterflies) and TL (Ga-BU-POTu, Bogong moth) cells are only found in these animals because they are involved in encoding the migratory behavior or because both insects are lepidopterans is unknown. As suggested by de Vries et al. (2017) for the TL (Ga-BU-POTu) neuron in Bogong moths, the monarch butterfly TPL cell might likely be modulatory and could alter the processing of compass cues in the CBL in e.g. a time-dependent (see previous section) or state-dependent manner (Beetz et al., 2022). Other candidates of modulatory CBL innervating neurons have been characterized in the desert locust CX (von Hadeln et al., 2019). The polarization sensitive TCX neurons are suggested to provide circadian information into the CX (Bockhorst and Homberg, 2015). A non-POTu innervating neuron, called ExR, was characterized in fruit flies (Hulse et al., 2021). This cell type was linked to processing of sleep and was also suggested to be modulatory. A possible output target of the monarch TPL cells are the CL neurons (Heinze et al., 2013), which have been demonstrated to encode the insect's heading direction in fruit flies (Kim et al., 2019; Seelig and Jayaraman, 2015). The TPL neuron could alternatively receive synaptic input from TB neurons in the POTu and, thus could be involved in transferring a feedback compass signals from the TB neurons of the protocerebral bridge to the CL heading network in the CBL. Taken together, while our data give physiological insights into a novel compass neuron of the CX, the function of this type of neuron in coding of sky compass information is still speculative and awaits to be shown.

Author contributions

Study design: TATN, BeJ. Conducting experiments: TATN. Analysis of data: TATN. Interpretation of data: TATN, BeJ. Drafting of the manuscript: TATN. Critical review of the manuscript: BeJ, Acquired Funding: BeJ. Both authors approved of the final version of the manuscript.

Competing interests

The authors declare no competing interests.

Funding

This work was supported by the Emmy Noether program of the Deutsche Forschungsgemeinschaft granted to BeJ (GZ: EL784/1-1) and a DFG Grant to KP (PF714/5-1).

Acknowledgments

We thank Dr. James Foster for fruitful comments on our analysis and Kolja Richter and Konrad Öchsner for their help in developing the LED arena. We thank Samantha Iiams, Aldrin Lugena, Guijun Wan and Ying Zhang for their help in capturing monarch butterflies and for checking them for *Ophryocystis elektroscirrha*. In addition, we would like to thank Sergio Siles and Marie Gerlinde Blaese (butterflyfarm.co.cr) for providing us with monarch butterfly pupae.

References

Beetz, M. J., el Jundi, B., Heinze, S. and Homberg, U. (2015). Topographic organization and possible function of the posterior optic tubercles in the brain of the desert locust Schistocerca gregaria. *J Comp Neurol.* 523, 1589-607.

Beetz, M. J., Kraus, C., Franzke, M., Dreyer, D., Strube-Bloss, M. F., Roessler, W., Warrant, E. J., Merlin, C. and el Jundi, B. (2022). Flight-induced compass representation in the monarch butterfly heading network. *Curr. Biol.* 32, 338—349.

Berens, P. (2009). CircStat: A MATLAB toolbox for circular statistics. *J.Stat Softw.* 31, 1—21.

Bockhorst, T. and Homberg, U. (2015). Amplitude and dynamics of polarization-plane signaling in the central complex of the locust brain. *J. Neurophysiol.* 113, 3291—3311. doi: 10.1152/jn.00742.2014

Brines, M. L. and Gould, J. L. (1979). Bees have rules. *Science* 206, 571—773.

Dacke, M., Baird, E., el Jundi, B., Warrant, E. J. and Byrne, M. (2021). How dung beetles steer straight. *Ann. Rev. Entomol.* 66, 243—256.

de Vries, L., Pfeiffer, K., Trebels, B., Adden, A. K., Green, K., Warrant, E. and Heinze, S. (2017). Comparison of Navigation-Related Brain Regions in Migratory versus Non-Migratory Noctuid Moths. *Front Behav Neurosci* 11, 158.

Dreyer, D., Frost, B., Mouritsen, H., Gunther, A., Green, K., Whitehouse, M., Johnsen, S., Heinze, S. and Warrant, E. (2018). The Earth's magnetic field and visual landmarks steer migratory flight behavior in the nocturnal Australian bogong moth. *Curr. Biol.* 28, 2160—2166.

Edrich, W., Neumeyer, C. and von Heiversen, O. (1979). “Anti-sun orientation” of bees with regard to a field of ultraviolet light. *J. Comp. Physiol.* 134, 151—157.

el Jundi, B. and Homberg, U. (2010). Evidence for the possible existence of a second polarization-vision pathway in the locust brain. *J. Insect Physiol.* 56, 971—979.

el Jundi, B., Pfeiffer, K. and Homberg, U. (2011). A distinct layer of the medulla integrates sky compass signals in the brain of an insect. *PLoS One* 6, e27855.

el Jundi, B., Warrant, E. J., Byrne, M. J., Khaldy, L., Baird, E., Smolka, J. and Dacke, M. (2015). Neural coding underlying the cue preference for celestial orientation. *Proc. Natl. Acad. Sci. U. S. A.* 112, 11395—11400.

el Jundi, B., Warrant, E. J., Pfeiffer, K. and Dacke, M. (2018). Neuroarchitecture of the dung beetle central complex. *J. Comp. Neurol.* 526, 2612—2630.

el Jundi, B., Baird, E., Byrne, M. and Dacke, M. (2019). The brain behind straight-line orientation in dung beetles. *J. Exp. Biol.* 222, jeb192450.

Fisher, Y. E., Lu, J., D'Alessandro, I. and Wilson, R. I. (2019). Sensorimotor experience remaps visual input to a heading-direction network. *Nature* 576, 121—125.

Franzke, M., Kraus, C., Dreyer, D., Pfeiffer, K., Beetz, M. J., Stöckl, A. L., Foster, J. J., Warrant, E. J. and el Jundi, B. (2020). Spatial orientation based on multiple visual cues in non-migratory monarch butterflies. *J. Exp. Biol.* 223, 1—12.

Franzke, M., Kraus, C., Gayler, M., Dreyer, D., Pfeiffer, K. and el Jundi, B. (2022). Stimulus-dependent orientation strategies in monarch butterflies. *J Exp Biol.* 225.

Giraldo, Y. M., Leitch, K. J., Ros, I. G., Warren, T. L., Weir, P. T. and Dickinson, M. H. (2018). Sun Navigation Requires Compass Neurons in *Drosophila*. *Curr. Biol.* 28, 2845—2852.

Graham, P. and Cheng, K. (2009). Ants use the panoramic skyline as a visual cue during navigation. *Curr. Biol.* 19, R935—R937.

Guerra, P. A., Merlin, C., Gegear, R. J. and Reppert, S. M. (2012). Discordant timing between antennae disrupts sun compass orientation in migratory monarch butterflies. *Nat. Comm.* 3, 958.

Hardcastle, B. J., Omoto, J. J., Kandimalla, P., Nguyen, B. M., Keleş, M. F., Boyd, N. K., Hartenstein, V. and Frye, M. A. (2021). A visual pathway for skylight polarization processing in *Drosophila*. *Elife* 10, e63225.

Heinze, S. and Homberg, U. (2008). Neuroarchitecture of the central complex of the desert locust: Intrinsic and columnar neurons. *J. Comp. Neurol.* 511, 454—478.

Heinze, S., Gotthardt, S. and Homberg, U. (2009). Transformation of polarized light information in the central complex of the locust. *J. Neurosci.* 29, 11783—11793.

Heinze, S. and Reppert, S. M. (2011). Sun compass integration of skylight cues in migratory monarch butterflies. *Neuron* 69, 345—358.

Heinze, S. and Reppert, S. M. (2012). Anatomical basis of sun compass navigation I: the general layout of the monarch butterfly brain. *J. Comp. Neurol.* 520, 1599—1628.

Heinze, S., Florman, J., Asokaraj, S., el Jundi, B. and Reppert, S. M. (2013). Anatomical basis of sun compass navigation II: the neuronal composition of the central complex of the monarch butterfly. *J. Comp. Neurol.* 521, 267—98.

Held, M., Le, K., Pegel, U., Dersch, F., Beetz, M. J., Pfeiffer, K. and Homberg, U. (2020). Anatomical and ultrastructural analysis of the posterior optic tubercle in the locust *Schistocerca gregaria*. *Arthropod Struct. Dev.* 58. 100971.

Helfrich-Förster, C. and Homberg, U. (1993). Pigment-dispersing hormone-immunoreactive neurons in the nervous system of wild-type *Drosophila melanogaster* and of several mutants with altered circadian rhythmicity. *J. Comp. Neurol.* 337, 177—190.

Homberg, U., Würden, S., Dircksen, H. and Rao, K. R. (1991). Comparative anatomy of pigment-dispersing hormone-immunoreactive neurons in the brain of orthopteroid insects. *Cell Tissue Res.* 266, 343—357.

Homberg, U., Heinze, S., Pfeiffer, K., Kinoshita, M. and el Jundi, B. (2011). Central neural coding of sky polarization in insects. *Philos. Trans. R. Soc. Lond. B, Biol. Sci.* 366, 680—687.

Homberg, U. (2015). Sky compass orientation in desert locusts—Evidence from field and laboratory studies. *Front. Behav. Neurosci.* 9, 346.

Homberg, U., Humberg, T. H., Seyfarth, J., Bode, K. and Perez, M. Q. (2018). GABA immunostaining in the central complex of dicondylian insects. *J. Comp. Neurol*. 526, 2301-2318.

Hulse, B. K., Haberkern, H., Franconville, R., Turner-Evans, D. B., Takemura, S.-y., Wolff, T., Noorman, M., Dreher, M., Dan, C., Parekh, R. et al. (2021). A connectome of the *Drosophila* central complex reveals network motifs suitable for flexible navigation and context-dependent action selection. *Elife* 10, e66039.

Kim, S. S., Hermundstad, A. M., Romani, S., Abbott, L. F. and Jayaraman, V. (2019). Generation of stable heading representations in diverse visual scenes. *Nature* 576, 126—131.

Labhart, T. (1996). How polarization-sensitive interneurones of crickets perform at low degrees of polarization. J. Exp. Biol. 199, 1467—75.

Merlin, C., Gegear, R. J. and Reppert, S. M. (2009). Antennal circadian clocks coordinate sun compass orientation in migratory monarch butterflies. *Science* 325, 1700—1704.

Merlin, C. and Liedvogel, M. (2019). The genetics and epigenetics of animal migration and orientation: birds, butterflies and beyond. *J. Exp. Biol.* 222, jeb191890.

Mouritsen, H. and Frost, B. J. (2002). Virtual migration in tethered flying monarch butterflies reveals their orientation mechanisms. *Proc. Natl. Acad. Sci. U.S.A.* 99, 10162-6.

Müller, M. and Wehner, R. (1988). Path integration in desert ants, *Cataglyphis fortis*. *Proc. Natl. Acad. Sci. U.S.A.* 85, 5287-90.

Nguyen, T. A. T., Beetz, M. J., Merlin, C. and el Jundi, B. (2021). Sun compass neurons are tuned to migratory orientation in monarch butterflies. *Proc. Biol. Sci.* 288, 20202988.

Nguyen, T. A. T., Beetz, M. J., Merlin, C., Pfeiffer, K. and el Jundi, B. (2022). Weighting of celestial and terrestrial cues in the monarch butterfly central complex. *Front Neural Circuits* 16, 862279.

Okubo, T. S., Patella, P., D'Alessandro, I. and Wilson, R. I. (2020). A neural network for wind-guided compass navigation. *Neuron* 107, 924—940 e18.

Pfeiffer, K. and Homberg, U. (2007). Coding of azimuthal directions via time-compensated combination of celestial compass cues. *Curr. Biol.* 17, 960—965.

Pfeiffer, K. and Homberg, U. (2014). Organization and functional roles of the central complex in the insect brain. *Ann. Rev. Entomol.* 59, 165—184.

Reppert, S. M., Zhu, H. and White, R. H. (2004). Polarized light helps monarch butterflies navigate. *Curr. Biol.* 14, 155—158.

Reppert S.M., Guerra, P.A. and Merlin, C. (2016). Neurobiology of Monarch Butterfly Migration. *Ann. Rev. Entomol.* 61, 25—42.

Sauman, I., Briscoe, A. D., Zhu, H., Shi, D., Froy, O., Stalleicken, J., Yuan, Q., Casselman, A. and Reppert, S. M. (2005). Connecting the navigational clock to sun compass input in monarch butterfly brain. *Neuron* 46, 457—467.

Seelig, J. D. and Jayaraman, V. (2015). Neural dynamics for landmark orientation and angular path integration. *Nature* 521, 186—191.

Stalleicken, J., Labhart, T. and Mouritsen, H. (2006). Physiological characterization of the compound eye in monarch butterflies with focus on the dorsal rim area. *J. Comp. Physiol. A* 192, 321—331.

Stalleicken, J., Mukhida, M., Labhart, T., Wehner, R., Frost, B. and Mouritsen, H. (2005). Do monarch butterflies use polarized skylight for migratory orientation? *J. Exp. Biol.* 208, 2399—408.

Towne, W. F., Ritrovato, A. E., Esposto, A. and Brown, D. F. (2017). Honeybees use the skyline in orientation. *J. Exp. Biol.* 220, 2476—2485.

Turner-Evans, D. B., Wegener, S., Rouaoult, H., Francoville, R., Wolff, T., Seelig, J. D., Druckmann, S. and Jayaraman, V. (2017). Angular velocity integration in a fly heading circuit. *ELife* 6, e23496.

von Hadeln, J., Hensgen, R., Bockhorst, T., Rosner, R., Heidasch, R., Pegel, U., Quintero Pérez, M. and Homberg, U. (2019). Neuroarchitecture of the central complex of the desert locust: Tangential neurons. *J. Comp. Neurol*. 528, 906-934.

Warrant, E., Frost, B., Green, K., Mouritsen, H., Dreyer, D., Adden, A., Brauburger, K. and Heinze, S. (2016). The Australian bogong moth *Agrotis infusa*: A long-distance nocturnal navigator. *Front. Behav. Neurosci.* 10, 77.

Wehner, R. (2003). Desert ant navigation: how miniature brains solve complex tasks. *J. Comp. Physiol. A* 189, 579—588.

Wolff, T. and Rubin, G. M. (2018). Neuroarchitecture of the *Drosophila* central complex: A catalog of nodulus and asymmetrical body neurons and a revision of the protocerebral bridge catalog. *J. Comp. Neurol.* 526, 2585-2611.

Zeller, M., Held, M., Bender, J., Berz, A., Heinloth, T., Hellfritz, T. and Pfeiffer, K. (2015). Transmedulla neurons in the sky compass network of the honeybee (*Apis mellifera*) are a possible site of circadian input. *PLoS ONE* 10, e0143244.

Figures

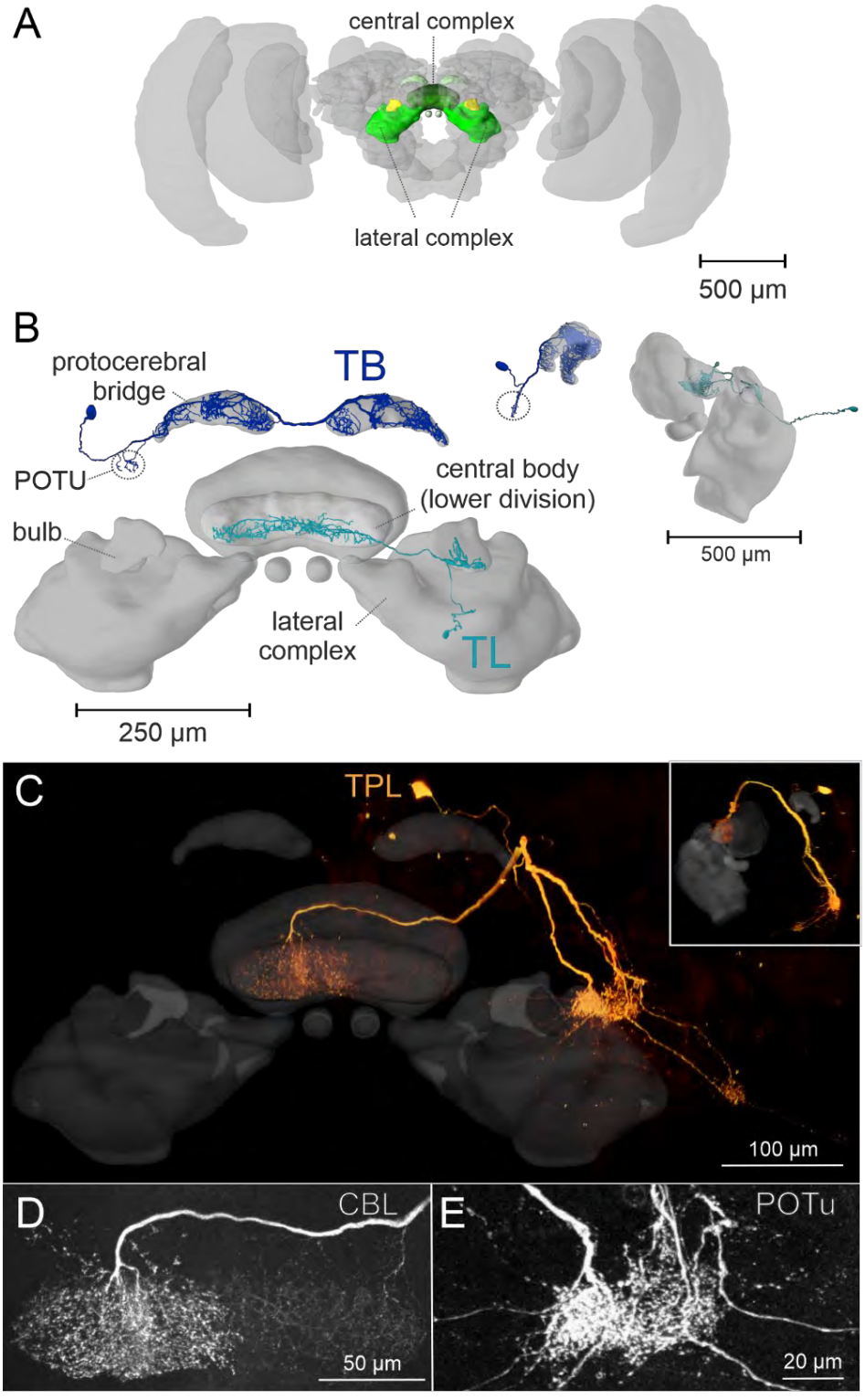

Fig. 1: Neuroanatomy of the TPL neuron. (A) Frontal view of the monarch butterfly brain. Highlighted in green are the neuropils of the central complex (CX) and lateral complex. Modified from Heinze et al. (2013). **(B)** 3D models of tangential CX neurons in the standard central complex of the monarch butterfly brain. TL neuron is shown in turquoise and TB neuron

is shown in dark blue. Left: frontal view. Right: lateral view. **(C)** Volume rendering visualization of a traced TPL neuron in combination with the CX standard atlas. Main picture: frontal view. Inset: lateral view. **(D, E)** Detailed view of the arborizations in the lower division of the central body (CBL,**D)** and the posterior optic tubercle **(**POTu, **E)**.

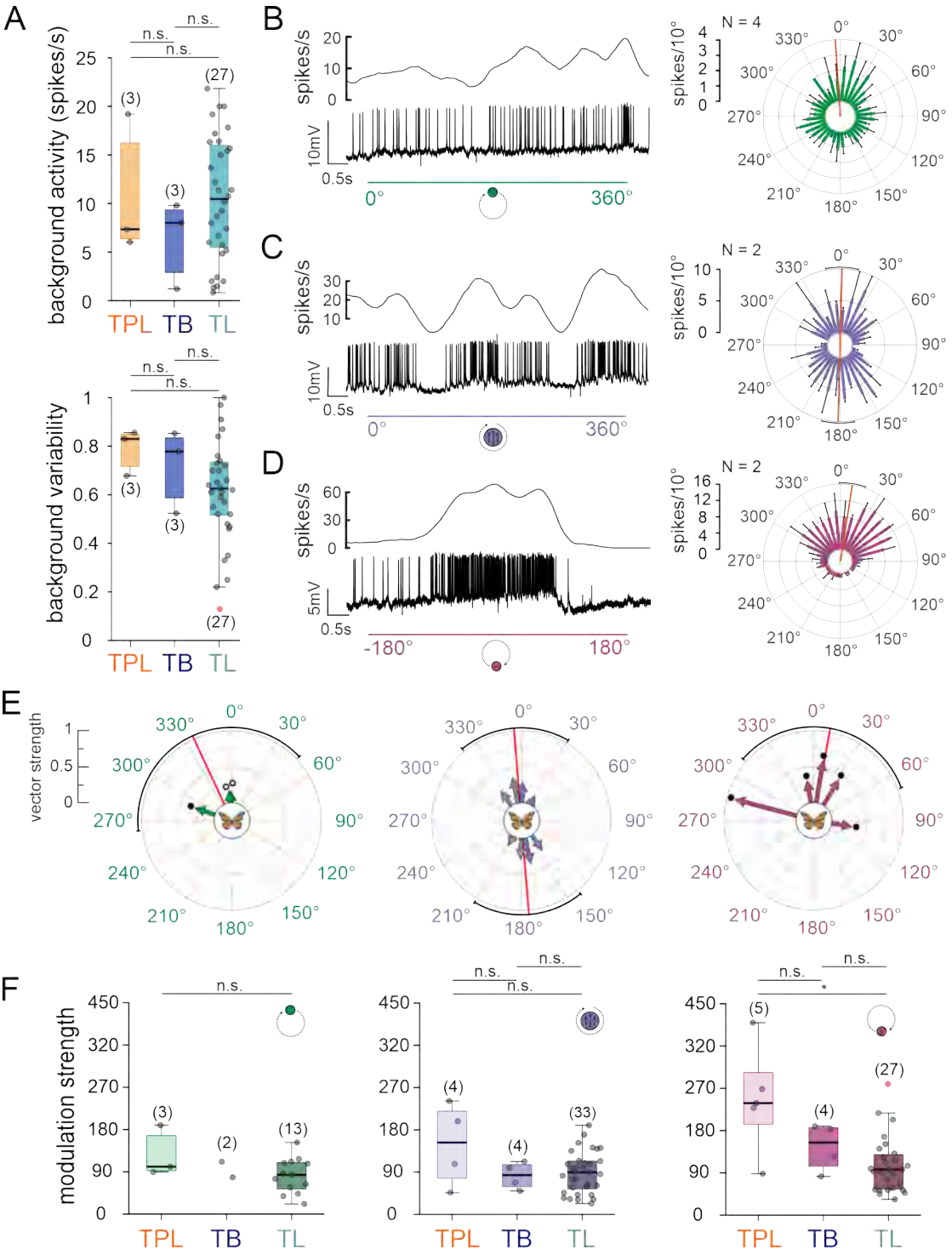

Fig. 2: TPL neurons are sensitive to celestial cues. (A) Background activity (upper plot) and background variability (lower plot) of TPL (n = 3), TB (n = 3), and TL (n = 27) neurons. The background activity of TPL cells (10.83 ± 7.25 spikes/s) did not differ significantly from the TB (p = n.s., rank sum = 11; Wilcoxon rank sum test) and TL cells (p = n.s., rank sum = 54.5; Wilcoxon rank sum test). Similarly, background variabilities from TPL cells (0.79 ± 0.10) resemble the observed TB (0.72 ± 0.17, $p_{TPL\ vs.\ TB}$ = n.s., rank sum = 12; Wilcoxon rank sum test) and TL neurons (0.63 ± 0.23, $p_{TPL\ vs.\ TL}$ = n.s., rank sum = 79; Wilcoxon rank sum test). In addition, TB and TL neurons did not differ in their background activity ($p_{TB\ vs.\ TL}$ = n.s.; rank sum = 34.5; Wilcoxon rank sum test) or background variability ($p_{TB\ vs.\ TL}$ = n.s; rank sum = 69; Wilcoxon rank sum test). Grey circles show individual data points with outliers shown in red. Boxes indicate interquartile range. Whiskers extend to the 2.5th and 97.5th percentiles. Black horizontal lines show the median. n.s.: not significant. **(B, C, D)** Neural response of the same TPL neuron to the sun stimulus (**B**, upper plot), dorsally presented polarized light (**C**, middle plot) and a UV light spot (**D**, lower plot). Left diagrams show the spike recording (middle) and the sliding window average (top). The stimulus duration/movement is shown as bar (bottom). Right circular plots show the action potential rate (10° bins) ± standard deviation of the same neuron averaged over several stimulus rotations (N-size). Red lines indicate the preferred direction to the unpolarized light stimuli (**B**: sun stimulus, 354.7° ± 107.9°; **D**: UV spot, 8.8° ± 59.1°) and the polarization stimulus (**C**: 1.7° ± 45.2°). Arcs represent the 95% confidence intervals. **(E)** The preferred firing directions of the tested TPL-neurons (n = 5) to the sun stimulus (left), the polarized light stimulus (middle) and the UV light spot (right). Each arrow represents a single neuron. Arrow length indicates the vector strength (directedness) of the neural tuning. The circular plots are labeled in relation to the animals' body axis (see schematic at the plot's center), with 0° being anterior to the animal. The mean preferred firing directions (sun stimulus: 335.2° ± 32.7°; polarized light: 175.4° ± 22.5°; UV spot: 10.3° ± 58.6°) are indicated by the red lines and the 95% confidence intervals by black arcs. For the unpolarized stimuli, unfilled dots mark neurons with their preferred direction ipsilateral to the soma and filled dots contralateral to the TPL soma. **(F)** Modulation strengths of TPL, TB and TL neurons in response to the sun stimulus (left), polarized light (middle) and the UV light spot (right). The modulation strength between the TPL (126.6 ± 54.6, n = 3) and TL (82.1 ± 37.2, n = 13) neurons to the sun stimulus did not differ significantly from each other (p = n.s., rank sum = 35; Wilcoxon rank sum test). The modulation strength of the TPL neurons to polarized light (148.6 ± 88.2, n = 4) did not differ from the TB (82.4 ± 28.8 n = 4) or TL (89.2 ± 43.6, n = 33) neuron response strength ($p_{TPL\ vs.\ TB}$ = n.s., rank sum = 21; $p_{TPL\ vs.\ TL}$ = n.s., rank sum = 107; Wilcoxon

rank sum test). Similarly, the UV light spot modulation strength of the TPL neurons (246.9 ± 114.8, n = 5) were similar to the TB (145.2 ± 50.9, n = 4), but differed significantly from the TL (105.7 ± 58.6, n =27) modulation strength. ($p_{TPL\ vs.\ TB}$ = n.s., rank sum = 21; $p_{TPL\ vs.\ TL}$ = 0.01, rank sum = 131; Wilcoxon rank sum test). Grey circles show individual data points with outliers shown in red. Boxes indicate interquartile range. Whiskers extend to the 2.5th and 97.5th percentiles. Black horizontal lines show the median. n.s.: not significant.

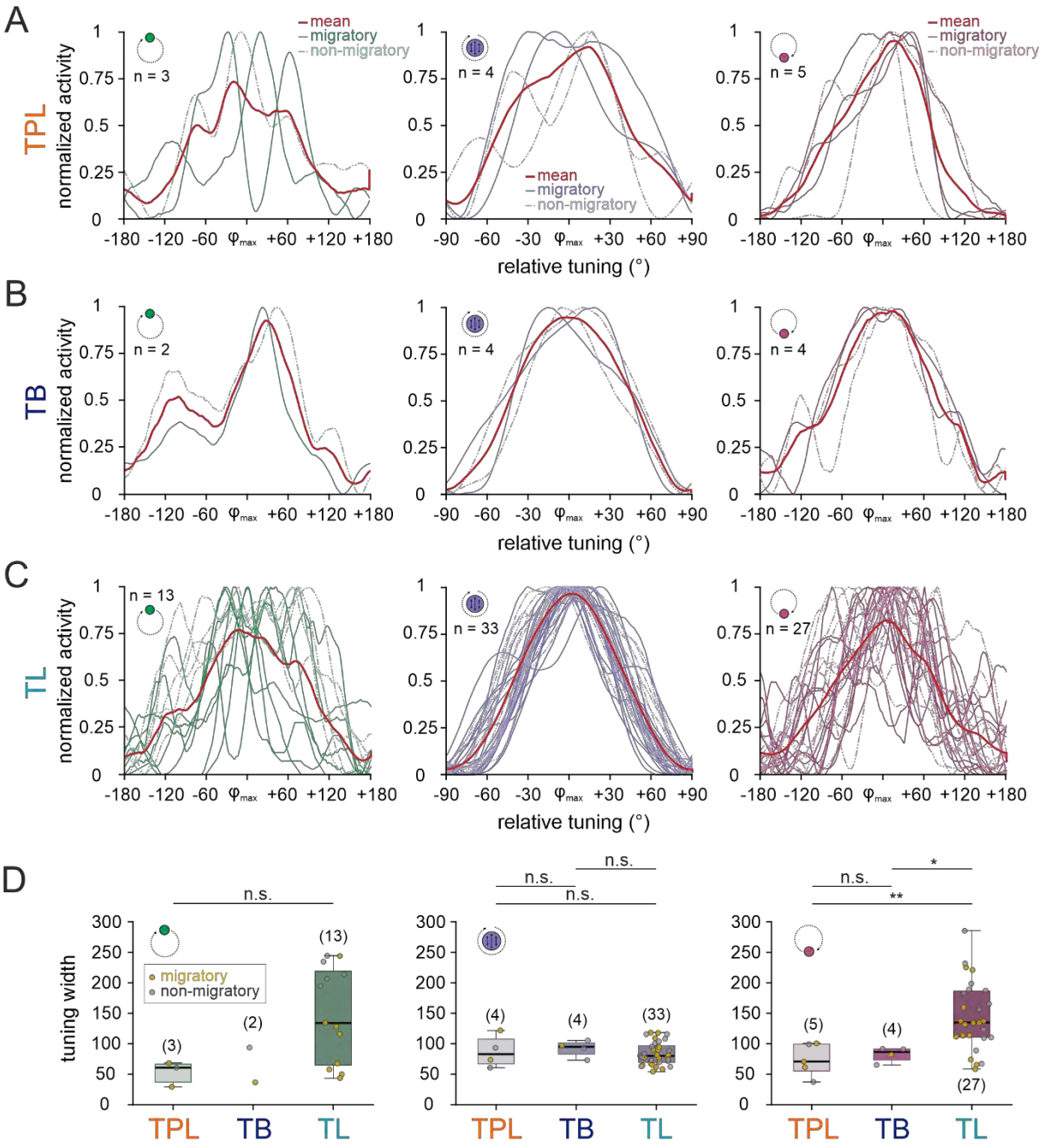

Fig. 3: Tuning curves of the tangential CX neurons. (A-C) Averaged tuning curves of the TPL **(A)**, TB **(B)** and TL neurons **(C)** responding to the sun stimulus (left), polarized light (middle) and the UV spot (right). Color-coding of single tuning curves indicates the animal's

state (migratory vs. non-migratory). The red curves show the averaged tuning curves. **(D)** Comparison the tuning widths (full width at half maximum) of the tangential neurons in response to the sun stimulus (left), polarized light (middle) and the UV light spot (right). The TPL (52.8° ± 20.8°, n = 3) and TL (148.6 ± 77.8°, n = 13) tuning width to the sun stimulus did not differ significantly from each other (p = n.s., rank sum = 13; Wilcoxon rank sum test). The TPL tuning width in response to the polarized light (87.2 ± 26.6°, n = 4) was similar to the one calculated for TB (92.0 ± 13.7°, n = 4; p = n.s., rank sum = 17; Wilcoxon rank sum test) and TL (84.1 ± 18.8°, n = 33; p = n.s., rank sum = 79; Wilcoxon rank sum test) neurons. For the UV spot, the TPL tuning width did not differ from the TB tuning width (p = n.s., rank sum = 24; Wilcoxon rank sum test). In contrast, TL cells (144.9 ± 56.4°, n = 27) showed a significantly broader tuning width than TPL (p = 0.006, rank sum = 29; Wilcoxon rank sum test) and TB (p = 0.02, rank sum = 25; Wilcoxon rank sum test) cells. Dots show individual data points. The state of the animals (migratory, yellow vs. non-migratory, black) are color coded. Boxes indicate interquartile range. Whiskers extend to the 2.5th and 97.5th percentiles. Black horizontal lines show the median. n.s.: not significant, *<0.05; **<0.01.

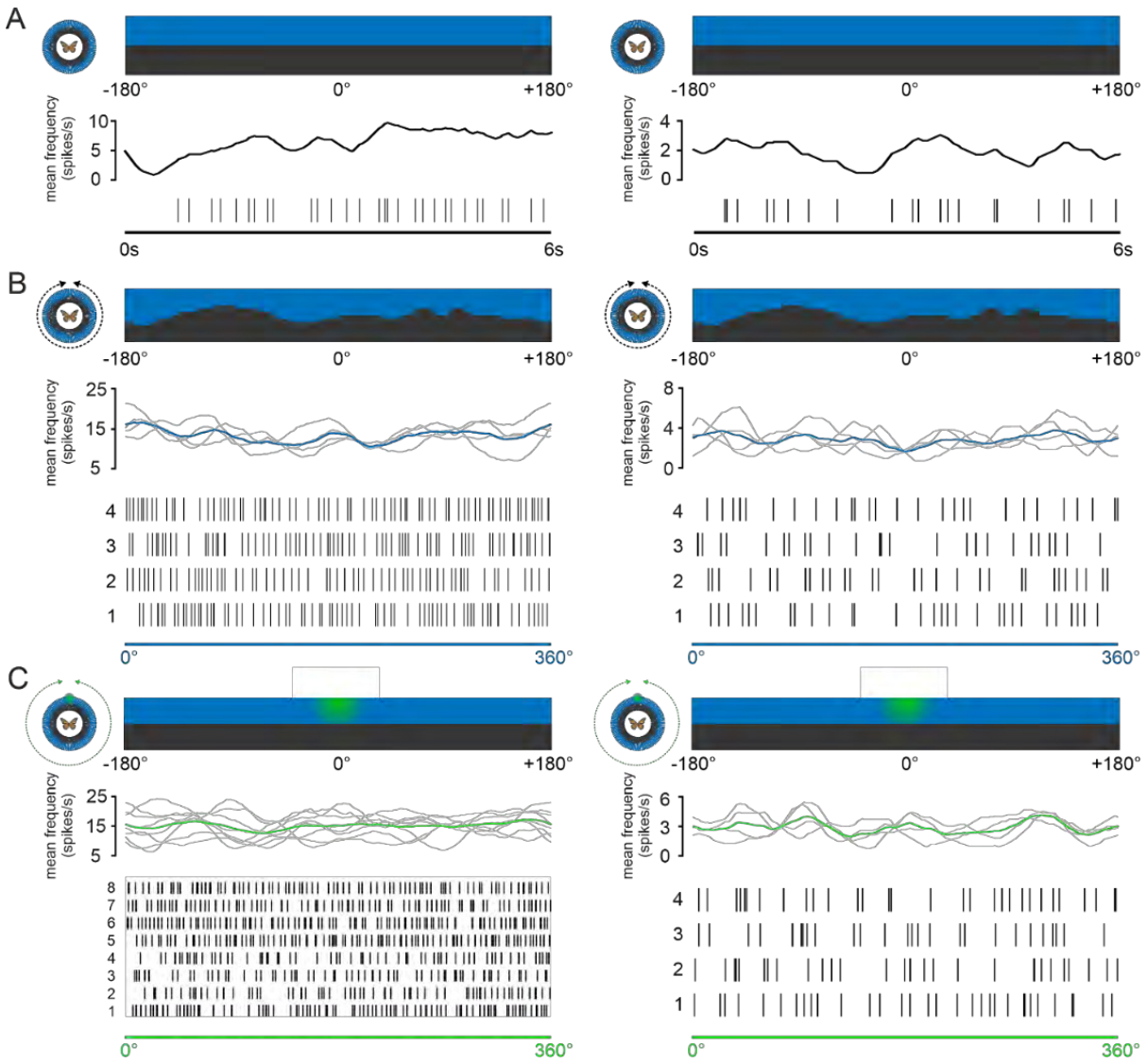

Fig. 4: TPL neuron response to a panoramic scene. Two TPL neurons (left and right column) were recorded in the presence of **(A)** a static flat panoramic stimulus **(B)** a profiled panorama an**d** a flat panorama in combination with the sun stimulus **(C)**. Both neurons did not respond to the presented stimuli. The upper panel in each figure shows the presented stimulus at the beginning of the experiments. The gliding averages (middle) in grey show the action potential rate of the cells to individual rotations, while the colored curves show the averaged sliding window averages [flat panorama, black, A), profiled panorama (blue, B), sun stimulus (green, C)]. The raster plots (below) show the neural activity, with each row showing the action potential distribution for one trial.

5. General Discussion

Past research has uncovered which orientation strategies insects employ and which internal and external cues they rely on to determine a heading direction (reviewed by Chapman et al., 2015; Grob et al., 2021 and Heinze et al., 2018). Furthermore, studies on the physiology and neural circuitry of the insect brain increased our understanding on how the orientation cue information is processed to determine a suitable heading direction (reviewed by Heinze, 2014 and Honkanen et al., 2018). Some insects can reliably return to their nest after a foraging trip (Fleischmann et al., 2018; Narendra et al., 2013). Migrating insects, however, leave their hatching grounds and need to cross unfamiliar territory to find a yet unknown destination (reviewed by Homberg et al., 2015 and Warrant et al., 2016). Monarch butterflies have been shown to be well adapted to the challenges presented to a long-distance migrator: They can consistently keep a heading direction by relying on a time-compensated sun compass (Merlin et al., 2009; Guerra and Reppert, 2013). As also done for other insects (reviewed by el Jundi et al., 2019 and Grob et al., 2019), compass orientation has been extensively studied in the monarch butterfly (reviewed by Reppert et al., 2018). Behavioral experiments investigated the monarch butterfly's internal cue hierarchy and their orientation strategy in response to simulated landmark and celestial cues (Franzke et al., 2020; Franzke et al, 2021; Stalleicken et al., 2005). Neurophysiological (Beetz et al., 2022; Heinze and Reppert, 2011) and neuroanatomical studies (Heinze et al., 2013) characterized the butterfly's internal sun compass located in the CX. The visual circuitry of the butterfly is the same in both migratory and non-migratory monarch butterflies (Heinze et al., 2013). However, the migratory state affects the neuropile volume of some regions in the CX, possibly influencing cue encoding in both animal groups. This dissertation aimed to understand the observations made in the behavioral experiments by identifying how monarch butterflies process celestial and terrestrial cues in the input stage of the CX. To observe the visual responses of neurons innervating the CX, single-cell recordings targeting the input neurons – known as TL cells – were collected while simulating different visual cues under controlled laboratory conditions.

5. 1 Role of the migratory state in shaping the monarch butterfly's internal sun compass

In the first project of my dissertation, I revealed differences in the coding of the sun between migratory and non-migratory butterflies (Nguyen et al., 2021). Studies in other insects investigated behavioral differences in the cue hierarchy for celestial orientation between closely

related species. Khaldy et al. (2020) revealed in behavioral experiments that dung beetles living in the woodlands weighted the polarized skylight higher than the sun. The compass system of dung beetles in the savanna, however, weighted the sun over the polarized light information (Khaldy et al., 2020). Furthermore, behavioral and electrophysiological experiments conducted by el Jundi et al. (2015) investigated, how compass coding differed between diurnal and nocturnal dung beetles in CX neurons. The compass neurons in the day-active beetles were adapted to bright light conditions and weighted the sun higher than the polarized light information. The same neurons in night-active animals were adapted to dim light cue conditions and were more strongly tuned to polarized light. Similarly, I showed that the internal sun compass system in monarch butterflies differs depending on the animal's lifestyle. To further understand how the monarch butterfly's migratory state influences compass coding, future studies may investigate the CX neurons downstream of the TL cells. How is the heading direction encoding in CL1 cells shaped by the TL visual input? Is it possible to predict the CL activity based on the TL response to the sun stimulus? However, contrastingly to TL neurons, the CL response depends on the insect's behavioral state, as demonstrated in the desert locust (Rosner et al., 2019) and in the monarch butterfly (Beetz et al., 2022). Thus, single cell recordings are not ideal to characterize CX neurons beyond the input stage, since this method requires the animal to be fully immobilized (Nguyen et al., 2021). Switching to tetrode recordings would likely be the best strategy to characterize CX cells in freely moving butterflies as done by Beetz et al. (2022). Furthermore, during intracellular recordings, the physiology of only one CX cell can be characterized. By using multichannel tetrode recordings, the neural activity of different CX neuropiles can be detected at the same time. Observing the simultaneous neural response of multiple CX may further increase our understanding of the internal compass system in the monarch butterfly.

The influence of the insect's behavioral state on the animal's neural tuning properties has also been observed in the desert locust. While not targeting any CX neurons, Rogers et al. (2010) compared the physiology of looming-sensitive neurons between the two different desert locust phases: solitarious animals avoiding other conspecifics and gregarious animals known for their migratory and swarming behavior (Homberg, 2015): Gregarious animals were more sensitive to looming objects in their anterior visual field compared to solitarious animals. In contrast, neurons in gregarious locusts seem to be adapted to avoid collisions with any conspecifics when flying in a swarm. However, comparative research on how different desert locust phases respond to sky compass cues did not reveal any differences in their visual cue processing. The polarized light sensitive photoreceptors in the DRA in both gregarious and solitarious desert

locusts did not differ in their physiology (Schmeling et al., 2015) and therefore possess similar receptive fields in response to polarized light. Additionally, compass neurons of the AOTu did not differ in their polarized-light coding between gregarious and solitarious locusts (el Jundi and Homberg 2012). However, even in monarch butterflies, The TL-cell physiology in response to polarized light was similar between migratory and non-migratory butterflies (Nguyen et al., 2021). Responses of compass cells to a sun stimulus have only been tested in gregarious desert locusts (Pegel et al., 2019; Pegel et al., 2018). Repeating the same experiments in solitarious desert locusts, may shed light on whether their sun compass system also differs from their gregarious counterpart.

My results also raise the question of whether there are anatomical differences in the neural substrate between migratory and non-migratory butterflies. While migratory state dependent brain volumes have been observed in the monarch butterfly (Heinze et al., 2013), past research on the CX in other insects did also investigate the influence of the behavioral state on neuropil volume: de Vries et al. (2019) compared the orientation behavior related brain volumes between a migratory and non-migratory nocturnal moth species and Ott and Rogers (2010) aimed to identify brain volume differences in gregarious and solitarious desert locusts. While the former study did not identify significant differences in CX size between the two tested groups (de Vries et al., 2019), the latter revealed that the CX volume is significantly increased in gregarious desert locusts compared to their solitarious conspecifics (Ott and Rogers, 2010). For the monarch butterfly, some brain regions differ in their volume depending on the animal's migratory state. However, only the PB volume is linked to changes in the butterfly's migratory state (Heinze et al., 2013). While the PB volume changes might be genetically or epigenetically modulated within migratory butterflies, it has yet to be determined whether the same is the case for the observed TL tuning differences. If not mediated by genetic or epigenetic factors, sun compass tuning differences might have developed due to experience gained during migration. To identify whether the sun compass tuning in TL cells is shaped by experience one promising target of investigation is the highly plastic input region of the TL cells, the bulb (Träger et al., 2008). Future projects may look into the synaptic connection in the bulb by comparing the TL connected microglomeruli counts in migratory and non-migratory butterflies. Another open question is how the TL subtype, as described in Heinze et al. (2013), affect bulb innervation and sun cue tuning.

5. 2 Integration of multiple visual cues in the central complex

While monarch butterflies can use both celestial and terrestrial information to determine a heading direction (Beetz et al., 2022; Franzke et al., 2022; Franzke et al., 2020; Stalleicken et al. 2005), not much is known about how the CX responds to multiple visual stimuli and how this affects heading direction encoding. In my second PhD project, I discovered that CX input cells integrate visual cues differently depending on the visual scenery they are exposed to (Nguyen et al., 2022). I found that celestial stimuli were combined linearly in monarch butterflies, which is also in line with the results from dung beetles (el Jundi et al., 2015) and desert locusts (Pegel et al., 2019). Exchanging the green sun stimulus with an unpolarized UV light spot, however, changed the TL weighting in favor of the unpolarized light cue (Nguyen et al., 2022). Similar to these results, the dung beetle's TL cells weighted the celestial stimuli differently depending on the animal's time of activity (el Jundi et al., 2015). To further investigate whether the celestial cue hierarchy in TL neurons can be explained by differences in the perceived intensities of the light stimuli, further projects may test the TL cell response to a combined stimulus (polarized light and sun stimulus) at different light intensities of, e.g. the sun stimulus.

As already demonstrated behaviorally by Franzke et al. (2020) in flight simulator experiments, the monarch butterfly is likely integrating panoramic skyline information with sun compass information. Since some of the monarch butterflies kept a flight direction in the presence of the panoramic skyline (Franzke et al., 2020), it was still unknown which features of the skyline the animals use to determine their heading. Future studies may investigate how the panoramic skyline, for instance the height or width of the higher segments of the panorama's profile or the elevation level of the horizon, is integrated by the butterfly's CL cells similarly to the experiments employed by Haberkern et al. (2022) in the fruit fly. But what happens if the monarch butterfly is exposed to both the sun stimulus and the panoramic skyline at the same time? While flight simulator experiments showed that monarch butterflies increase their flight performance if shown both stimuli (Franzke et al., 2020), TL cell recordings in the presence of the more naturalistic stimuli condition demonstrated that celestial and terrestrial cues are differently weighted depending on the tested TL neuron. Similar to the result shown in Kim et al. (2019) and Fisher et al. (2019) on the TL equivalent ring neurons in fruit flies, these neurons flexibly weight their cue response depending on the external visual scenery. One open question is if the weighting of visual cues depends on the TL subtype. In the fruit fly, visual processing differs between ring neurons subtypes (Hardcastle et al., 2021) and have been suggested to process either the wide field panoramic skyline or the narrow field sun cue (Shiozaki and

Kazama, 2017). Whether the TL subtypes also determine the visual cue weighting in monarch butterflies has yet to be determined. Furthermore, the migratory stage might influence how the butterflies perceive the visual scenery. Migratory monarch butterflies mostly spend their time in the sky at high elevations above the ground, with the sky covering most of the upper and the terrestrial silhouette a small part of the lower visual field. Contrastingly, non-migratory animals are mostly flying at lower elevations and across green vegetation, therefore the terrestrial silhouette dominates the animal's upper visual field. Differences in how both butterfly groups experience the visual scenery over a prolonged time may influence how the visual information is integrated in the butterfly's internal compass. Migratory monarch butterflies may weight the sun within the visual scenery more strongly, while the compass system in non-migratory monarch butterflies may also integrate terrestrial cues like landmarks or specific segments in the panoramic skyline. Furthermore, comparative electrophysiological recordings investigating the internal compass in monarch butterflies at different stages during their migratory flight, may shed light on whether the visual processing in TL neurons differs between migratory animals depending on their life span and the flight experience.

5. 3 Modulation of heading direction encoding in the monarch butterfly sun compass

Apart from visual (Heinze and Reppert, 2011; Nguyen et al. 2022; Nguyen et al. 2020; Seelig and Jayaraman, 2013) and mechanosensory information (Okubo et al., 2020), the internal compass system in insects might be modulated by "modulatory" neurons connecting the CX to other brain neuropiles. For instance, Sun et al. (2020) proposed a neural circuitry that is active during visual homing in ants. Whenever the ant receives novel visual stimuli, the CBU indirectly receives input information from the mushroom body (MB) via the superior medial protocerebrum (SMP). Furthermore, Matheson et al. (2022) demonstrated that the fruit fly's CBU equivalent known as the fan shaped body can integrate learned odor cue information from the MB. In the presence of an odor cue, the fly shifts from a wind-compass mediated directional movement to an odor guided upwind movement (Matheson et al., 2022). In my third PhD project, I characterized a compass neuron in the monarch butterfly that possibly modulates the heading direction encoding in the CX. The neuron, termed TPL, innervates the CBL and the POTu, for which the latter has been shown to process polarized light information from possible posterior polarization pathway in the desert locust (el Jundi and Homberg, 2010). Whether such a similar pathway also exists in the monarch butterfly has yet to be determined. Additional tracing experiments targeting the butterfly's medulla or other optic lobe neuropils may increase

our understanding of the butterfly's visual circuitry in the POTu. Furthermore, the TPL cell body lies in the pars intercerebralis, a region that houses a number of clock neurons (Sauman et al. 2005; Zhu et al., 2008). Future projects involving immunohistochemistry with antibodies against clock proteins in brain samples containing traced TPL cells may study whether these cells might be involved in time compensation. Furthermore, long-term recording from TPL cells may show how and if the TPL cell changes its coding in a time-of-day dependent manner, For such experiments, the first electrophysiological results on the TPL cells shown in my dissertation may form the basis for further experiments.

Apart from the monarch butterfly, a similar neuron like the TPL cell has also been anatomically described in the bogong moth (de Vries et al., 2017). Both animals have in common that they are capable of long-distance migration. Furthermore, apart from the bogong moth and the monarch butterfly, the POTu has also been confirmed in the desert locust (Held et al., 2020; Homberg et al., 1991), jewel wasp (Groothuis et al., 2019) and honeybee (Kaiser et al., 2022), while it does not exist in the fruit fly (Wolff et al., 2015) and the dung beetle (el Jundi et al., 2018) brain. This opens the possibility that insects that need to time-compensate their heading-direction behaviorally have evolved a pair of POTu in their brain. To determine whether the POTu is linked to migratory behavior or time compensation, neuroanatomical characterization of the migratory hoverflies (Massy et al., 2021) may uncover whether the POTu is typical for migratory/homing insects or not.

5. 4 Conclusion and outlook

While much is known on the CX circuitry and how it affects the monarch butterfly's capacity to determine and keep a heading direction (Beetz et al., 2022; Heinze and Reppert 2013), future research may focus on the CX circuitry beyond the input stage and compare their physiological responses to the experimental data derived from other insects (Hardcastle et al. 2021; Pegel et al., 2018; Pegel et al., 2019; Stone et al., 2018). Another open question is how the monarch butterfly includes non-visual information while encoding its heading direction. By investigating the multimodal integration of not only wind (Dacke et al., 2019; Omoto et al. 2020), but also olfactory information (reviewed by Steck 2012; Matheson et al. 2022) we increase or understanding on how these cues influence not only the response of the CX neurons, but also affect heading direction encoding in the monarch butterfly. As already mentioned by Franzke et al. (2022), the monarch butterfly employs different orientation strategies depending on the available cues. It is still unclear how the monarch butterfly switches from sun compass orientation to cues that pinpoint it to the overwintering site (Mouritsen, 2018). To approach this

question, future projects may identify the possible external triggers of the butterflies' overwintering site that guide the butterflies to the exact location of their overwintering site.

Taken together, my thesis increased our understanding of how the monarch butterfly integrates visual information in its internal compass system and how the migratory state affects sun compass coding. Furthermore, by investigating the TL response to more naturalistic cue conditions, I further increased our understanding of how multiple visual stimuli are interpreted in the input stage of the CX. Lastly a yet unfamiliar CX innervating neuron was physiologically characterized and opens up the possibility to investigate how the heading-direction system in the CX is modulated by, e.g. time of day information.

Abbreviations

AOTu	anterior optic tubercle
Bu	bulb
CBL	central body lower unit
CBU	central body upper unit
CL	columnar cells innervating the central body lower unit
CPU	columnar cells innervating the central body upper unit
CX	central complex
DRA	dorsal rim area
GABA	γ-aminobutyric acid
JH	juvenile hormone
LAL	lateral accessory lobe
Lo	lobula
Lx	lateral complex
MB	mushroom bodies
Me	medulla
NO	noduli
PB	protocerebral bridge
POTu	posterior optic tubercle
SMP	superior medial protocerebrum
TB	tangential neuron innervating the protocerebral bridge
TL	tangential neuron innervating the central body lower unit
TuBu	neuron innervating the anterior optic tubercle and bulb
TuLaL	see TuBu

Bibliography

Beall, G. (1948). The Fat Content of a Butterfly, *Danaus plexippus* Linn., As Affected by Migration. *Ecology* **29**, 80-94.

Beetz, M. J., Kraus, C., Franzke, M., Dreyer, D., Strube-Bloss, M. F., Rossler, W., Warrant, E. J., Merlin, C. and el Jundi, B. (2021). Flight-induced compass representation in the monarch butterfly heading network. *Current Biology* **32**, 338-349 e5.

Brines, M. L. and Gould, J. L. (1979). Bees have rules. *Science* **206**, 571-3.

Brower, L., Calvert, W. H., Hedrick, L. E. and Christian, J. (1977). Biological observations on an overwintering colony of monarch butterflies (*Danaus plexippus*, Danaidae) in Mexico. *Journal of the Lepidopterists' Society* **31**, 232-242.

Buehlmann, C., Mangan, M. and Graham, P. (2020). Multimodal interactions in insect navigation. *Animal Cognition* **23**, 1129-1141.

Calvert, W. H. (2001). Monarch butterfly (*Danaus plexippus* L., nymphalidae) fall migration: Flight behavior and direction in relation to celestial and physiographic cues. *Journal of the Lepidopterists' Society* **55**, 162-168.

Chapman, J. W., Reynolds, D. R. and Wilson, K. (2015). Long-range seasonal migration in insects: mechanisms, evolutionary drivers and ecological consequences. *Ecology Letters* **18**, 287-302.

Cheng, K., Shettleworth, S. J., Huttenlocher, J. and Rieser, J. J. (2007). Bayesian integration of spatial information. *Psychological Bulletin* **133**, 625-637.

Cheung, A., Zhang, S., Stricker, C. and Srinivasan, M. V. (2007). Animal navigation: the difficulty of moving in a straight line. *Biological Cybernetics* **97**, 47-61.

Ciofini, A., Mercatelli, L., Hariyama, T. and Ugolini, A. (2021). Sky radiance and spectral gradient are orienting cues for the sandhopper *Talitrus saltator* (Crustacea, Amphipoda). *Journal of Experimental Biology* **224**, jeb239574.

Coemans, M. A., Vos Hzn, J. J. and Nuboer, J. F. (1994). The relation between celestial colour gradients and the position of the sun, with regard to the sun compass. *Vision Research* **34**, 1461-70.

Collett, M., Collett, T. S., Bisch, S. and Wehner, R. (1998). Local and global vectors in desert ant navigation. *Nature* **394**, 269-272.

Collett, M., Harland, D. and Collett, T. S. (2002). The use of landmarks and panoramic context in the performance of local vectors by navigating honeybees. *Journal of Experimental Biology* **205**, 807-14.

Collett, T. (1996). Insect navigation en route to the goal: multiple strategies for the use of landmarks. *Journal of Experimental Biology* **199**, 227-35.

Collett, T. S. (1995). Making learning easy: the acquisition of visual information during the orientation flights of social wasps. *Journal of Comparative Physiology A* **177**, 737-747.

Coulson, K. L. (1959). Characteristics of the radiation emerging from the top of a Rayleigh atmosphere—I: Intensity and polarization. *Planetary and Space Science* **1**, 265-276.

Coyne, J. A., Bryant, S. H. and Turelli, M. (1987). Long-Distance Migration of *Drosophila*. 2. Presence in Desolate Sites and Dispersal Near a Desert Oasis. *The American Naturalist* **129**, 847-861.

Dacke, M., Baird, E., Byrne, M., Scholtz, C. H. and Warrant, E. J. (2013). Dung beetles use the Milky Way for orientation. *Current Biology* **23**, 298-300.

Dacke, M., Bell, A. T. A., Foster, J. J., Baird, E. J., Strube-Bloss, M. F., Byrne, M. J. and el Jundi, B. (2019). Multimodal cue integration in the dung beetle compass. *Proceedings of the National Academy of Sciences of the United States of America* **116**, 14248-14253.

Dacke, M., Byrne, M. J., Scholtz, C. H. and Warrant, E. J. (2004). Lunar orientation in a beetle. *Proceedings of the Royal Society - Biological Sciences (Series B)* **271**, 361-5.

Dacke, M., Nilsson, D.-E., Scholtz, C. H., Byrne, M. and Warrant, E. J. (2003). Insect orientation to polarized moonlight. *Nature* **424**, 33-33.

Dreyer, D., el Jundi, B., Kishkinev, D., Suchentrunk, C., Campostrini, L., Frost, B. J., Zechmeister, T. and Warrant, E. J. (2018). Evidence for a southward autumn migration of nocturnal noctuid moths in central Europe. *Journal of Experimental Biology* **221**. jeb179218.

Dreyer, D., Frost, B., Mouritsen, H., Gunther, A., Green, K., Whitehouse, M., Johnsen, S., Heinze, S. and Warrant, E. (2018). The Earth's Magnetic Field and Visual

Landmarks Steer Migratory Flight Behavior in the Nocturnal Australian Bogong Moth. *Current Biology* **28**, 2160-2166 e5.

Dyer, F. C. and Dickinson, J. A. (1994). Development of sun compensation by honeybees: how partially experienced bees estimate the sun's course. *Proceedings of the National Academy of Sciences* **91**, 4471-4474.

el Jundi, B. and Homberg, U. (2012). Receptive field properties and intensity-response functions of polarization-sensitive neurons of the optic tubercle in gregarious and solitarious locusts. *Journal of Neurophysiology* **108**, 1695-710.

el Jundi, B., Baird, E., Byrne, M. J. and Dacke, M. (2019). The brain behind straight-line orientation in dung beetles. *Journal of Experimental Biology* **222**. jeb192450.

el Jundi, B., Foster, J. J., Khaldy, L., Byrne, M. J., Dacke, M. and Baird, E. (2016). A Snapshot-Based Mechanism for Celestial Orientation. *Current Biology* **26**, 1456-62.

el Jundi, B., Smolka, J., Baird, E., Byrne, M. J. and Dacke, M. (2014). Diurnal dung beetles use the intensity gradient and the polarization pattern of the sky for orientation. *Journal of Experimental Biology* **217**, 2422-9.

el Jundi, B., Warrant, E. J., Byrne, M. J., Khaldy, L., Baird, E., Smolka, J. and Dacke, M. (2015). Neural coding underlying the cue preference for celestial orientation. *Proceedings of the National Academy of Sciences of the United States of America* **112**, 11395-400.

el Jundi, B., Warrant, E. J., Pfeiffer, K. and Dacke, M. (2018). Neuroarchitecture of the dung beetle central complex. *Journal of Comparative Neurology* **526**, 2612-2630.

Fisher, Y. E., Lu, J., D'Alessandro, I. and Wilson, R. I. (2019). Sensorimotor experience remaps visual input to a heading-direction network. *Nature* **576**, 121-125.

Fleischmann, P. N., Grob, R., Müller, V. L., Wehner, R. and Rössler, W. (2018). The Geomagnetic Field Is a Compass Cue in *Cataglyphis* Ant Navigation. *Current Biology* **28**, 1440-1444.e2.

Foster, J. J., el Jundi, B., Smolka, J., Khaldy, L., Nilsson, D. E., Byrne, M. J. and Dacke, M. (2017). Stellar performance: mechanisms underlying Milky Way orientation in dung beetles. *Philosophical Transactions of the Royal Society B: Biological Sciences* **372**.

Foster, J. J., Kirwan, J. D., el Jundi, B., Smolka, J., Khaldy, L., Baird, E., Byrne, M. J., Nilsson, D. E., Johnsen, S. and Dacke, M. (2019). Orienting to polarized light at night - matching lunar skylight to performance in a nocturnal beetle. *Journal of Experimental Biology* **222**. jeb188532.

Franzke, M., Kraus, C., Dreyer, D., Pfeiffer, K., Beetz, M. J., Stöckl, A. L., Foster, J. J., Warrant, E. J. and el Jundi, B. (2020). Spatial orientation based on multiple visual cues in non-migratory monarch butterflies. *Journal of Experimental Biology* **223**, jeb223800.

Franzke, M., Kraus, C., Gayler, M., Dreyer, D., Pfeiffer, K. and el Jundi, B. (2022). Stimulus-dependent orientation strategies in monarch butterflies. *Journal of Experimental Biology* **225**, jeb243687.

Gál, J., Horváth, G., Barta, A. and Wehner, R. (2001). Polarization of the moonlit clear night sky measured by full-sky imaging polarimetry at full Moon: Comparison of the polarization of moonlit and sunlit skies. *Journal of Geophysical Research: Atmospheres* **106**, 22647-22653.

Gibo, D. L. and Pallett, M. J. (1979). Soaring flight of monarch butterflies, *Danaus plexippus* (Lepidoptera: Danaidae), during the late summer migration in southern Ontario. *Canadian Journal of Zoology* **57**, 1393-1401.

Giraldo, Y. M., Leitch, K. J., Ros, I. G., Warren, T. L., Weir, P. T. and Dickinson, M. H. (2018). Sun Navigation Requires Compass Neurons in *Drosophila*. *Current Biology* **28**, 2845-2852.

Goehring, L. and Oberhauser, K. S. (2002). Effects of photoperiod, temperature, and host plant age on induction of reproductive diapause and development time in *Danaus plexippus*. *Ecological Entomology* **27**, 674-685.

Grob, R., el Jundi, B. and Fleischmann, P. N. (2021). Towards a common terminology for arthropod spatial orientation. *Ethology Ecology & Evolution* **33**, 338-358.

Guerra, P. A., Gegear, R. J. and Reppert, S. M. (2014). A magnetic compass aids monarch butterfly migration. *Nature Communications* **5**, 4164.

Guerra, Patrick A. and Reppert, Steven M. (2013). Coldness Triggers Northward Flight in Remigrant Monarch Butterflies. *Current Biology* **23**, 419-423.

Hanesch, U., Fischbach, K. F. and Heisenberg, M. (1989). Neuronal architecture of the central complex in *Drosophila melanogaster*. *Cell and Tissue Research* **257**, 343-366.

Hegedüs, R., Akesson, S. and Horvath, G. (2007). Polarization patterns of thick clouds: Overcast skies have distribution of the angle of polarization similar to that of clear skies. *Journal of the Optical Society of America. A, Optics, image science, and vision* **24**, 2347-56.

Heinze, S. (2014). Polarized-Light Processing in Insect Brains: Recent Insights from the Desert Locust, the Monarch Butterfly, the Cricket, and the Fruit Fly. In *Polarized Light and Polarization Vision in Animal Sciences*, (ed. G. Horváth), pp. 61-111. Berlin, Heidelberg: Springer Berlin Heidelberg.

Heinze, S. and Homberg, U. (2007). Maplike Representation of Celestial E-Vector Orientations in the Brain of an Insect. *Science* **315**, 995.

Heinze, S. and Homberg, U. (2009). Linking the Input to the Output: New Sets of Neurons Complement the Polarization Vision Network in the Locust Central Complex. *The Journal of Neuroscience* **29**, 4911.

Heinze, S. and Reppert, S. M. (2011). Sun compass integration of skylight cues in migratory monarch butterflies. *Neuron* **69**, 345-58.

Heinze, S. and Reppert, S. M. (2012). Anatomical basis of sun compass navigation I: the general layout of the monarch butterfly brain. *Journal of Comparative Neurology* **520**, 1599-628.

Heinze, S., Florman, J., Asokaraj, S., el Jundi, B. and Reppert, S. M. (2013). Anatomical basis of sun compass navigation II: the neuronal composition of the central complex of the monarch butterfly. *Journal of Comparative Neurology* **521**, 267-98.

Heinze, S., Narendra, A. and Cheung, A. (2018). Principles of Insect Path Integration. *Current Biology* **28**, R1043-R1058.

Held, M., Berz, A., Hensgen, R., Muenz, T. S., Scholl, C., Rossler, W., Homberg, U. and Pfeiffer, K. (2016). Microglomerular Synaptic Complexes in the Sky-Compass Network of the Honeybee Connect Parallel Pathways from the Anterior Optic Tubercle to the Central Complex. *Frontiers in Behavioral Neuroscience* **10**, 91-105.

Herman, W. S. (1981). Studies on the Adult Reproductive Diapause of the Monarch Butterfly, *Danaus plexippus*. *Biological Bulletin* **160**, 89-106.

Herman, W. S. and Tatar, M. (2001). Juvenile hormone regulation of longevity in the migratory monarch butterfly. *Proceedings of the Royal Society B: Biological Sciences* **268**, 2509-14.

Homberg, U. (2008). Evolution of the central complex in the arthropod brain with respect to the visual system. *Arthropod Structure & Development* **37**, 347-362.

Homberg, U., Humberg, T. H., Seyfarth, J., Bode, K. and Perez, M. Q. (2018). GABA immunostaining in the central complex of dicondylian insects. *Journal of Comparative Neurology* **526**, 2301-2318.

Honkanen, A., Adden, A., da Silva Freitas, J. and Heinze, S. (2019). The insect central complex and the neural basis of navigational strategies. *Journal of Experimental Biology* **222**, jeb188854.

Johnsen, S., Lohmann, K. J. and Warrant, E. J. (2020). Animal navigation: a noisy magnetic sense? *Journal of Experimental Biology* **223**.

Kaiser, A., Hensgen, R., Tschirner, K., Beetz, E., Wüstenberg, H., Pfaff, M., Mota, T. and Pfeiffer, K. (2022). A three-dimensional atlas of the honeybee central complex, associated neuropils and peptidergic layers of the central body. *Journal of Comparative Neurology* **530**, 2416-2438.

Kennedy, J. S. and Wigglesworth, V. B. (1951). The migration of the Desert Locust (*Schistocerca gregaria* Forsk.) I. The behaviour of swarms. II. A theory of long-range migrations. *Philosophical Transactions of the Royal Society of London. Series B, Biological Sciences* **235**, 163-290.

Kheradmand, B. and Nieh, J. C. (2019). The Role of Landscapes and Landmarks in Bee Navigation: A Review. *Insects* **10**.

Kim, S. S., Hermundstad, A. M., Romani, S., Abbott, L. F. and Jayaraman, V. (2019). Generation of stable heading representations in diverse visual scenes. *Nature* **576**, 126-131.

Klotz, J. H. and Reid, B. L. (1993). Nocturnal orientation in the black carpenter ant *Camponotus pennsylvanicus* (DeGeer) (Hymenoptera: Formicidae). *Insectes Sociaux* **40**, 95-106.

Kurylas, A. E., Rohlfing, T., Krofczik, S., Jenett, A. and Homberg, U. (2008). Standardized atlas of the brain of the desert locust, *Schistocerca gregaria*. *Cell Tissue Res* **333**, 125-45.

Labhart, T., Baumann, F. and Bernard, G. D. (2009). Specialized ommatidia of the polarization-sensitive dorsal rim area in the eye of monarch butterflies have non-functional reflecting tapeta. *Cell Tissue Res* **338**, 391-400.

Labhart, T., Hodel, B. and Valenzuela, I. (1984). The physiology of the cricket's compound eye with particular reference to the anatomically specialized dorsal rim area. *Journal of Comparative Physiology A* **155**, 289-296.

Lebhardt, F. and Ronacher, B. (2014). Interactions of the polarization and the sun compass in path integration of desert ants. *Journal of Comparative Physiology A* **200**, 711-720.

Legge, E. L., Wystrach, A., Spetch, M. L. and Cheng, K. (2014). Combining sky and earth: desert ants (*Melophorus bagoti*) show weighted integration of celestial and terrestrial cues. *Journal of Experimental Biology* **217**, 4159-66.

Lohmann, K. and Lohmann, C. (1996). Orientation and open-sea navigation in sea turtles. *Journal of Experimental Biology* **199**, 73-81.

Malcolm, S., Cockrell, B. J. and Brower, L. (1993). Spring recolonization of eastern North America by the monarch butterfly: successive brood or single sweep migration? , 253-267.

Masters, A., Malcolm, S. and Brower, L. (1988). Monarch Butterfly (*Danaus plexippus*) Thermoregulatory Behavior and Adaptations for Overwintering in Mexico. *Ecology* **69**, 458.

Matheson, A. M. M., Lanz, A. J., Medina, A. M., Licata, A. M., Currier, T. A., Syed, M. H. and Nagel, K. I. (2022). A neural circuit for wind-guided olfactory navigation. *Nature Communications* **13**, 4613.

Merlin, C. and Liedvogel, M. (2019). The genetics and epigenetics of animal migration and orientation: birds, butterflies and beyond. *The Journal of Experimental Biology* **222**, jeb191890.

Merlin, C., Gegear, R. J. and Reppert, S. M. (2009). Antennal circadian clocks coordinate sun compass orientation in migratory monarch butterflies. *Science* **325**, 1700-4.

Merlin, C., Heinze, S. and Reppert, S. M. (2012). Unraveling navigational strategies in migratory insects. *Current Opinion in Neurobiology* **22**, 353-361.

Mouritsen, H. (2018). Long-distance navigation and magnetoreception in migratory animals. *Nature* **558**, 50-59.

Mouritsen, H., Derbyshire, R., Stalleicken, J., Mouritsen, O. Ø., Frost, B. J. and Norris, D. R. (2013). An experimental displacement and over 50 years of tag-recoveries show that monarch butterflies are not true navigators. *Proceedings of the National Academy of Sciences of the United States of America* **110**, 7348.

Müller, M. and Wehner, R. (2007). Wind and sky as compass cues in desert ant navigation. *Naturwissenschaften* **94**, 589-594.

Narendra, A. (2007). Homing strategies of the Australian desert ant *Melophorus bagoti* II. Interaction of the path integrator with visual cue information. *Journal of Experimental Biology* **210**, 1804-1812.

Narendra, A., Gourmaud, S. and Zeil, J. (2013). Mapping the navigational knowledge of individually foraging ants, *Myrmecia croslandi*. *Proceedings of the Royal Society B: Biological Sciences* **280**, 20130683.

Nesbit, R. L., Hill, J. K., Woiwod, I. P., Sivell, D., Bensusan, K. J. and Chapman, J. W. (2009). Seasonally adaptive migratory headings mediated by a sun compass in the painted lady butterfly, *Vanessa cardui*. *Animal Behaviour* **78**, 1119-1125.

Nguyen, T. A. T., Beetz, M. J., Merlin, C. and el Jundi, B. (2021). Sun compass neurons are tuned to migratory orientation in monarch butterflies. *Proceedings of the Royal Society B: Biological Sciences* **288**, 20202988.

Nguyen, T. A. T., Beetz, M. J., Merlin, C., Pfeiffer, K. and el Jundi, B. (2022). Weighting of Celestial and Terrestrial Cues in the Monarch Butterfly Central Complex. *Frontiers in Neural Circuits* **16**.

Obara, Y. (1979). Bombyx mori mating dance: an essential in locating the female. *Applied Entomology and Zoology* **14**, 130-132.

Okubo, T. S., Patella, P., D'Alessandro, I. and Wilson, R. I. (2020). A Neural Network for Wind-Guided Compass Navigation. *Neuron* **107**, 924-940 e18.

Ott, S. and Rogers, S. (2010). Gregarious desert locusts have substantially larger brains with altered proportions compared with the solitarious phase. *Proceedings of the Royal Society B: Biological Sciences* **277**, 3087-96.

Phillips-Portillo, J. and Strausfeld, N. J. (2012). Representation of the brain's superior protocerebrum of the flesh fly, *Neobellieria bullata*, in the central body. *Journal of Comparative Neurology* **520**, 3070-87.

Pomozi, I., Horvath, G. and Wehner, R. (2001). How the clear-sky angle of polarization pattern continues underneath clouds: full-sky measurements and implications for animal orientation. *Journal of Experimental Biology* **204**, 2933-42.

Reppert, S. M. and de Roode, J. C. (2018). Demystifying Monarch Butterfly Migration. *Current Biology* **28**, R1009-R1022.

Reppert, S. M., Guerra, P. A. and Merlin, C. (2016). Neurobiology of Monarch Butterfly Migration. *Annual Review of Entomology* **61**, 25-42.

Reppert, S. M., Zhu, H. and White, R. H. (2004). Polarized Light Helps Monarch Butterflies Navigate. *Current Biology* **14**, 155-158.

Riffell, J. A., Abrell, L. and Hildebrand, J. G. (2008). Physical Processes and Real-Time Chemical Measurement of the Insect Olfactory Environment. *Journal of Chemical Ecology* **34**, 837-853.

Rogers, S. M., Harston, G. W., Kilburn-Toppin, F., Matheson, T., Burrows, M., Gabbiani, F. and Krapp, H. G. (2010). Spatiotemporal receptive field properties of a looming-sensitive neuron in solitarious and gregarious phases of the desert locust. *J Neurophysiol* **103**, 779-92.

Rosner, R., Pegel, U. and Homberg, U. (2019). Responses of compass neurons in the locust brain to visual motion and leg motor activity. *Journal of Experimental Biology* **222**.

Rossel, S. and Wehner, R. (1984). Celestial orientation in bees: the use of spectral cues. *Journal of Comparative Physiology A* **155**, 605-613.

Rother, L., Kraft, N., Smith, D. B., el Jundi, B., Gill, R. J. and Pfeiffer, K. (2021). A micro-CT-based standard brain atlas of the bumblebee. *Cell Tissue Res* **386**, 29-45.

Sauman, I., Briscoe, A. D., Zhu, H., Shi, D., Froy, O., Stalleicken, J., Yuan, Q., Casselman, A. and Reppert, S. M. (2005). Connecting the navigational clock to sun compass input in monarch butterfly brain. *Neuron* **46**, 457-67.

Schmeling, F., Tegtmeier, J., Kinoshita, M. and Homberg, U. (2015). Photoreceptor projections and receptive fields in the dorsal rim area and main retina of the locust eye. *Journal of Comparative Physiology A* **201**, 427-40.

Schmeling, F., Wakakuwa, M., Tegtmeier, J., Kinoshita, M., Bockhorst, T., Arikawa, K. and Homberg, U. (2014). Opsin expression, physiological characterization and identification of photoreceptor cells in the dorsal rim area and main retina of the desert locust, *Schistocerca gregaria*. *Journal of Experimental Biology* **217**, 3557-3568.

Schmitt, F., Stieb, S. M., Wehner, R. and Rossler, W. (2016). Experience-related reorganization of giant synapses in the lateral complex: Potential role in plasticity of the sky-compass pathway in the desert ant *Cataglyphis fortis*. *Developmental Neurobiology* **76**, 390-404.

Schroeder, H., Majewska, A. and Altizer, S. (2019). Monarch butterflies reared under autumn-like conditions have more efficient flight and lower post-flight metabolism. *Ecological Entomology* **45**, 562-572.

Schultheiss, P., Stannard, T., Pereira, S., Reynolds, A. M., Wehner, R. and Cheng, K. (2016). Similarities and differences in path integration and search in two species of desert ants inhabiting a visually rich and a visually barren habitat. *Behavioral Ecology and Sociobiology* **70**, 1319-1329.

Schwarz, S., Mangan, M., Zeil, J., Webb, B. and Wystrach, A. (2017). How Ants Use Vision When Homing Backward. *Current Biology* **27**, 401-407.

Seelig, J. D. and Jayaraman, V. (2013). Feature detection and orientation tuning in the *Drosophila* central complex. *Nature* **503**, 262-6.

Seelig, J. D. and Jayaraman, V. (2015). Neural dynamics for landmark orientation and angular path integration. *Nature* **521**, 186-91.

Shiozaki, H. M. and Kazama, H. (2017). Parallel encoding of recent visual experience and self-motion during navigation in *Drosophila*. *Nature Neuroscience* **20**, 1395.

Srinivasan, M. V., Zhang, S., Altwein, M. and Tautz, J. (2000). Honeybee navigation: nature and calibration of the "odometer". *Science* **287**, 851-3.

Stalleicken, J., Labhart, T. and Mouritsen, H. (2006). Physiological characterization of the compound eye in monarch butterflies with focus on the dorsal rim area. *Journal of Comparative Physiology A* **192**, 321-331.

Stalleicken, J., Mukhida, M., Labhart, T., Wehner, R., Frost, B. and Mouritsen, H. (2005). Do monarch butterflies use polarized skylight for migratory orientation? *Journal of Experimental Biology* **208**, 2399-408.

Steinbeck, F., Adden, A. and Graham, P. (2020). Connecting brain to behaviour: a role for general purpose steering circuits in insect orientation? *Journal of Experimental Biology* **223**.

Stone, T., Mangan, M., Wystrach, A. and Webb, B. (2018). Rotation invariant visual processing for spatial memory in insects. *Interface Focus* **8**, 20180010.

Stone, T., Webb, B., Adden, A., Weddig, N. B., Honkanen, A., Templin, R., Wcislo, W., Scimeca, L., Warrant, E. and Heinze, S. (2017). An Anatomically Constrained Model for Path Integration in the Bee Brain. *Current Biology* **27**, 3069-3085 e11.

Stuchlik, A. and Bures, J. (2002). Relative contribution of allothetic and idiothetic navigation to place avoidance on stable and rotating arenas in darkness. *Behavioural Brain Research* **128**, 179-188.

Towne, W. F. and Moscrip, H. (2008). The connection between landscapes and the solar ephemeris in honeybees. *Journal of Experimental Biology* **211**, 3729-36.

Träger, U., Wagner, R., Bausenwein, B. and Homberg, U. (2008). A novel type of microglomerular synaptic complex in the polarization vision pathway of the locust brain. *Journal of Comparative Neurology* **506**, 288-300.

Ugolini, A. and Chiussi, R. (1996). Astronomical orientation and learning in the earwig *Labidura riparia*. *Behavioural Processes* **36**, 151-161.

Ugolini, A., Melis, C. and Innocenti, R. (1999). Moon orientation in adult and young sandhoppers. *Journal of Comparative Physiology A* **184**, 9-12.

Ugolini, A., Melis, C., Innocenti, R., Tiribilli, B. and Castellini, C. (1999). Moon and sun compasses in sandhoppers rely on two separate chronometric mechanisms. *Proceedings of the Royal Society of London. Series B: Biological Sciences* **266**, 749-752.

Ugolini, A., Tiribilli, B. and Boddi, V. (2002). The sun compass of the sandhopper *Talitrus saltator*: The speed of the chronometric mechanism depends on the hours of light. *The Journal of Experimental Biology* **205**, 3225-30.

Urquhart, F. A. and Urquhart, N. R. (1977). Overwintering Areas and Migratory Routes of the Monarch Butterfly (*Danaus P. Plexippus*, Lepidoptera: Danaidae) in North America, with Special Reference to the Western Population. *The Canadian Entomologist* **109**, 1583-1589.

Urquhart, F. A. and Urquhart, N. R. (1978). Autumnal migration routes of the eastern population of the monarch butterfly (*Danaus p. plexippus* L.; Danaidae; Lepidoptera) in North America to the overwintering site in the Neovolcanic Plateau of Mexico. *Canadian Journal of Zoology* **56**, 1759-1764.

Urquhart, F. A. and Urquhart, N. R. (1979). Vernal Migration of the Monarch Butterfly (*Danaus P. plexippus*, Lepidoptera: Danaidae) in North-America from the Overwintering Site in the Neo-Volcanic Plateau of Mexico. *Canadian Entomologist* **111**, 15-18.

Varga, A. G. and Ritzmann, R. E. (2016). Cellular Basis of Head Direction and Contextual Cues in the Insect Brain. *Current Biology* **26**, 1816-28.

Warrant, E., Frost, B., Green, K., Mouritsen, H., Dreyer, D., Adden, A., Brauburger, K. and Heinze, S. (2016). The Australian Bogong Moth Agrotis infusa: A Long-Distance Nocturnal Navigator. *Frontiers in Behavioral Neuroscience* **10**, 77.

Wehner, R. and Müller, M. (2006). The significance of direct sunlight and polarized skylight in the ant's celestial system of navigation. *Proceedings of the National Academy of Sciences of the United States of America* **103**, 12575-9.

Wiltschko, W. and Wiltschko, R. (1972). Magnetic Compass of European Robins. *Science* **176**, 62-64.

Wittlinger, M., Wehner, R. and Wolf, H. (2006). The ant odometer: stepping on stilts and stumps. *Science* **312**, 1965-7.

Zhan, S., Zhang, W., Niitepõld, K., Hsu, J., Haeger, J. F., Zalucki, M. P., Altizer, S., de Roode, J. C., Reppert, S. M. and Kronforst, M. R. (2014). The genetics of monarch butterfly migration and warning colouration. *Nature* **514**, 317-321.

Zhu, H., Gegear, R. J., Casselman, A., Kanginakudru, S. and Reppert, S. M. (2009). Defining behavioral and molecular differences between summer and migratory monarch butterflies. *BMC Biology* **7**, 1-14.

Zhu, H., Sauman, I., Yuan, Q., Casselman, A., Emery-Le, M., Emery, P. and Reppert, S. M. (2008). Cryptochromes define a novel circadian clock mechanism in monarch butterflies that may underlie sun compass navigation. *PLoS Biology* **6**, e4.

Danksagungen

Während meiner Doktorarbeit habe ich viele Erfolge erzielen können. Es gab jedoch Momente, die mich vor großen Herausforderungen gestellt haben. Zudem war meine Arbeit geprägt durch die COVID-19-Pandemie, welche sich sowohl auf meinen privaten als auch auf meinen Laboralltag ausgewirkt haben. Viele Herausforderungen konnte ich jedoch bewältigen, weil ich meine Probleme nie alleine stemmen musste. Daher möchte ich die Personen würdigen, welche mir in diesem Lebensabschnitt begegnet sind und mir maßgeblich geholfen haben.

An erster Stelle danke ich meinem Doktorvater **Prof. Dr. Basil el Jundi**. Vielen Dank für dein Vertrauen, als du mich in deine Arbeitsgruppe aufgenommen hattest. Ich schätze nicht nur deine Fachexpertise, sondern auch deine Geduld. Du warst der Ansprechpartner für jegliche Fragen. Deine konstruktive Kritik und förderlichen Ratschläge trugen maßgeblich zu meiner persönlichen Entwicklung bei. Vielen Dank, dass du mich über sämtliche Phasen der Doktorarbeit begleitet hast und das Motto „Dran bleiben!“ werde ich auch in Zukunft in positiver Erinnerung behalten.

Prof. Dr. Eric Warrant, thank you for being part of my PhD-committee and providing helpful feedback on my research project during the annual progress reports.

Mit der **AG el Jundi** hatte ich während meiner Doktorarbeit die meiste Zeit verbracht. Die Labortreffen und gemeinsam verlebte Zeit sowohl im Labor als auch in den Pausenräumen prägten meinen Alltag. **My**, als Mitdoktorandin in der AG el Jundi kannst du wahrscheinlich am besten in unserer Gruppe verstehen, welche Herausforderungen einem die Doktorarbeit stellt. Vielen Dank sowohl für den fachlicher Austausch, als auch für die mentale und emotionale Unterstützung. Du hast maßgeblich zur Organisation des Labors und der Forschungsreisen beigetragen. **Jerome**, vielen Dank für deine wertvollen Beiträge zur Analyse und Auswertung der experimentellen Ergebnisse. **Christian**, du wurdest mit der Zeit zu einem festen Bestandteil unserer Gruppe. Ich schätze an dir deine Gewissenhaftigkeit und Disziplin. Außerdem konnte man im Labor mit dir Witze machen. **Marco** und **Lea**, vielen Dank, dass ihr in euren Abschlussarbeiten Teilaspekte meines Forschungsprojektes bearbeitet habt.

Die Zusammenarbeit mit der **AG Pfeiffer** und **AG Stöckl** war sehr fruchtbar gewesen für meine Doktorarbeit. Ich konnte nicht nur von eurem Fachwissen und eurer Erfahrung als Wissenschaftler profitieren, sondern habe viel aus den Diskussionen während unserer Journal

Clubs mitnehmen können. **Keram**, vielen Dank für deine Literaturempfehlungen und Unterstützung bei der Umsetzung meiner Datenanalyse mit MATLAB. Des Weiteren bedanke ich mich für die Bereitstellung der Barrel-Arena, welche ich für meine Elektrophysiologe-Experimente nutzen konnte. **Anna and James**, thank you for your feedback on my research project, for providing critical remarks related to any experimental designs or answering any MATLAB-related questions. **Lisa und Bianca**, der Erfahrungsaustausch mit euch half mir bei Problemen im Elektrophysiologie-Setup. Ihr wart eine mentale und emotionale Stütze bei experimentellen Rückschlägen. **Martina und Ronja**, danke für eure Gesellschaft im Büro-Alltag. **Evelyn und Katja**, danke für eure Hilfe bei der Organisationsarbeit im Labor und euren ermutigenden Worten. Ich werde unsere gemeinsamen Pausen positiv in Erinnerung behalten. **Kolja**, auch wenn ich dich vergleichweise nur kurz kennenlernen konnte: Vielen Dank für die Beantwortung meiner Fragen zur Arena-Bedienung.

Prof. Dr. Wolfgang Rössler, als Leiter der Zoologie II bedanke ich mich, dass du die Räumlichkeiten der Uni Würzburg bereitgestellt hast. Die gute Infrastruktur und das positive Arbeitsumfeld waren eine maßgebliche Grundlage zum Gelingen meiner Doktorarbeit.

Die **Zoologie II** lebt von ihren Mitarbeitern. Während den wöchentlichen Seminaren konnten wir uns über unsere Forschungsarbeit austauschen. Des Weiteren boten die Mittagszeit im Seminarraum oder am Teich eine Pause von den Experimenten und eine Gelegenheit, um mit anderen Mitdoktoranden in Kontakt zu kommen. Vielen Dank für eure Gesellschaft! An dieser Stelle möchte ich namentlich erwähnen: **Nadine, Robin, Valerie, Fabian, Sarah, Jens, Sinan und Felix**. **Conny und Karin**, vielen Dank für eure Hilfsbereitschaft, der Bereitstellung der Materialien für die Immunohistochemie und Aufrechterhaltung der Labor-Infrastruktur in der Zoologie II. **Daniela**, als meine Büronachbarin möchte ich mich für deine Gesellschaft bedanken, welche meinen Arbeitsalltag positiv beeinflusst hat.

Während meiner Arbeit als Doktorand konnte ich von den Einrichung der Universität Würzburg profitieren. Die **Wissenschaftlichen Werkstätten auf dem Hubland-Campus** bauten größere und kleinere Geräte, welche zur Effizenz meiner experimentielle Arbeit beigetragen haben. Ich danke für eure Ausführung meiner Aufträge. Namentlich möchte ich auch **Konrad Öchsner** erwähnen: Vielen Dank für Ihre kompetente und zeitnahe Hilfe bei der Wartung der Arena. Des Weiteren möchte ich mich bei der **Imaging Core Facility am Hubland** für die Bereitstellung ihrer Räumlichkeiten und bei Fragen zur Nutzung der Konfokalmikroskope bedanken.

During our field trips in Texas we worked closely with our collaborators at **Texas A&M University at College Station**. Dear **Prof. Dr. Christine Merlin**, thank you for your hospitality, providing the infrastructure during our research stays and sharing your knowledge on handling the migratory monarch butterflies. Furthermore, I want to mention **Samantha, Aldrin, Guijun and Ying**. Thank you for your kindness, lending a helpful hand during any issues and doing the tedious work of screening the migratory butterflies for any OE parasites.

Sergio Siles and **Marie Gerlinde Blaese** from **Costa Rica Entomolgy Supply**, thank you for providing the monarch butterflies for my PhD project and making sure that they found their way from Costa Rica to Würzburg!

Mein privates Umfeld hat mich über die Zeit als Doktorand begleitet und war besonders während der harten Endphase eine wichtige emotional Stütze für mich. **Riccarda** und **Martin**, vielen Dank für die gemeinsamen Telefonate und euren aufmunternden Worte. **Flo**, vielen Dank für die gemeinsamen virtuellen und realen Treffen und dein Verständnis für meine Lebensituation. Du hattest stets ein offenes Ohr für mich. Deine kontinuierliche mentale und emotionale Unterstützung haben mir über die Tiefs während der Arbeit an der Dissertation hinweggeholfen. **Mai und Basti**, danke für eure konstruktiven Hinweise in meiner Schreibphase. Die gemeinsame Zeit mit euch bot eine willkommene Abwechslung von der Schreibarbeit.

Con cảm ơn **bố và mẹ** vì đã luôn bên con. Bố và mẹ đã chịu bao vất vả để nuôi con khôn lớn lên người. Cám ơn vì đã tiếp tục giúp đỡ con!

Curriculum vitae with list of publications

[Page intentionally left blank]

[Page intentionally left blank]

[Page intentionally left blank]

Appendix

Affidavit

I hereby confirm that my thesis entitled “Neural coding of different visual cues in the monarch butterfly sun compass” is the result of my own work. I did not receive any help or support from commercial consultants. All sources and / or materials applied are listed and specified in the thesis.

Furthermore, I confirm that this thesis has not yet been submitted as part of another examination process neither in identical nor in similar form.

Würzburg, 2.11.2022

Place, Date Signature

Eidesstattliche Erklärung

Hiermit erkläre ich an Eides statt, die Dissertation „Neuronale Kodierung verschiedener visueller Signale im Sonnenkompass des Monarchfalters“ eigenständig, d.h. insbesondere selbständig und ohne Hilfe eines kommerziellen Promotionsberaters, angefertigt und keine anderen als die von mir angegebenen Quellen und Hilfsmittel verwendet zu haben.

Ich erkläre außerdem, dass die Dissertation weder in gleicher noch in ähnlicher Form bereits in einem anderen Prüfungsverfahren vorgelegen hat.

Würzburg, 2.11.2022

Ort, Datum Unterschrift

"Dissertation Based on Several Published Manuscripts": Statement of individual author contributions and of legal second publication rights

(If required please use more than one sheet)

Publication (complete reference):					
Nguyen TAT, Beetz MJ, Merlin C and el Jundi B (2021). Sun compass neurons are tuned to migratory orientation in monarch butterflies. *Proceedings of the Royal Society B: Biological Sciences* 288, 20202988.					
Participated in	**Author Initials,** Responsibility decreasing from left to right				
Study Design Methods Development	TATN	BeJ	CM		
Data Collection	TATN				
Data Analysis and Interpretation	TATN	BeJ	MJB		
Manuscript Writing Writing of Introduction Writing of Materials & Methods Writing of Discussion Writing of First Draft	 TATN TATN TATN TATN	 BeJ BeJ BeJ	 MJB MJB MJB	 CM CM CM	

Explanations (if applicable):

Publication (complete reference):					
Nguyen TAT, Beetz MJ, Merlin C, Pfeiffer K and el Jundi B (2022). Weighting of celestial and terrestrial cues in the monarch butterfly central complex. Submitted to *Frontiers in Neural Circuits.*					
Participated in	**Author Initials,** Responsibility decreasing from left to right				
Study Design Methods Development	TATN	BeJ	KP	CM	
Data Collection	TATN				
Data Analysis and Interpretation	TATN	BeJ	MJB		
Manuscript Writing Writing of Introduction Writing of Materials & Methods Writing of Discussion Writing of First Draft	 TATN TANT TANT TATN	 BeJ BeJ BeJ	 KP KP KP	 MJB MJB MJB	

Explanations (if applicable):

Publication (complete reference): Nguyen TAT and el Jundi B. Characterization of a new type of compass neuron in the monarch butterfly central complex. *In preparation*					
Participated in	**Author Initials,** Responsibility decreasing from left to right				
Study Design Methods Development	TATN	BeJ			
Data Collection	TATN				
Data Analysis and Interpretation	TATN	BeJ			
Manuscript Writing Writing of Introduction Writing of Materials & Methods Writing of Discussion Writing of First Draft	 TATN TATN TATN TATN	 BeJ BeJ BeJ			

Explanations (if applicable):

The doctoral researcher confirms that she/he has obtained permission from both the publishers and the co-authors for legal second publication.

The doctoral researcher and the primary supervisor confirm the correctness of the above mentioned assessment.

Tu Anh Thi Nguyen	2/11/2022	Würzburg	
Doctoral Researcher's Name	Date	Place	Signature

Basil el Jundi	2/11/2022	Würzburg	
Primary Supervisor's Name	Date	Place	Signature _____

"Dissertation Based on Several Published Manuscripts": Statement of individual author contributions to figures/tables/chapters included in the manuscripts

(If required please use more than one sheet)

Publication (complete reference): Nguyen TAT, Beetz MJ, Merlin C and el Jundi B (2021). Sun compass neurons are tuned to migratory orientation in monarch butterflies. *Proceedings of the Royal Society B: Biological Sciences* 288, 20202988.

Figure	**Author Initials,** Responsibility decreasing from left to right				
1	TATN	BeJ			
2	TATN	BeJ			
3	TATN	BeJ			
4	TATN	BeJ			
S1	TATN	BeJ			
S2	TATN	BeJ			
S3	TATN	BeJ			
S4	TATN	BeJ			
S5	TATN	BeJ			

Explanations (if applicable):

Publication (complete reference): Nguyen TAT, Beetz MJ, Merlin C, Pfeiffer K and el Jundi B (2022). Weighting of celestial and terrestrial cues in the monarch butterfly central complex. Submitted to *Frontiers in Neural Circuits.*

Figure	**Author Initials,** Responsibility decreasing from left to right				
1	TATN	BeJ			
2	TATN	BeJ			
3	TATN	BeJ			
4	TATN	BeJ			

Explanations (if applicable):

Publication (complete reference):

Nguyen TAT and el Jundi B. Characterization of a new type of compass neuron in the monarch butterfly central complex. *In preparation*

Figure	**Author Initials,** Responsibility decreasing from left to right				
1	TATN	BeJ			
2	TATN	BeJ			
3	TATN	BeJ			
4	TATN	BeJ			

Explanations (if applicable):

I also confirm my primary supervisor's acceptance.

Tu Anh Thi Nguyen Würzburg

_____

Doctoral Researcher's Name Date Place Signature